NTNU

Norwegian University of
Science and Technology

Advanced small-scale characterization of hydrogen embrittlement

Roar Andre Fagerkind

Materials Technology
Submission date: June 2016
Supervisor: Afrooz Barnoush, IPM
Co-supervisor: Tarlan Hajilou, IPM

Norwegian University of Science and Technology
Department of Engineering Design and Materials

Problem Text

NTNU - NORWEGIAN UNIVERSITY
OF SCIENCE AND TECHNOLOGY
DEPARTMENT OF ENGINEERING DESIGN
AND MATERIALS

MASTER THESIS SPRING 2016
FOR
STUD.TECHN. Roar André Fagerkind

Advanced small-scale characterization of hydrogen embrittlement

Avansert små-skala karakterisering av hydrogensprøhet

The candidate is supposed to continue with the cutting and preparation of micro-cantilever samples as he did within the project work. Different geometry and sizes as well as the inclusion of a notch will be explored. In addition to preparation of cantilevers the candidate is responsible for cyclic loading of the cantilevers to form a controlled sharp crack in the cantilevers. This will be a novel approach.

Formal requirements:

Three weeks after start of the thesis work, an A3 sheet illustrating the work is to be handed in. A template for this presentation is available on the IPM's web site under the menu "Masteroppgave" (https://www.ntnu.edu/web/ipm/master-thesis). This sheet should be updated one week before the master's thesis is submitted.

Risk assessment of experimental activities shall always be performed. Experimental work defined in the problem description shall be planed and risk assessed up-front and within 3 weeks after receiving the problem text. Any specific experimental activities which are not properly covered by the general risk assessment shall be particularly assessed before performing the experimental work. Risk assessments should be signed by the supervisor and copies shall be included in the appendix of the thesis.

The thesis should include the signed problem text, and be written as a research report with summary both in English and Norwegian, conclusion, literature references, table of contents, etc. During preparation of the text, the candidate should make efforts to create a well arranged and well written report. To ease the evaluation of the thesis, it is important to cross-reference text, tables and figures. For evaluation of the work a thorough discussion of results is appreciated.

The thesis shall be submitted electronically via DAIM, NTNU's system for Digital Archiving and Submission of Master's theses.

Torgeir Welo
Head of Division

Afrooz Barnoush
Professor/Supervisor

Preface

This report is written as a partial requirement for a Master's degree in Material Science and Technology at the Norwegian University of Science and Technology (NTNU). This report is a continuation of the project work done during Autumn 2015.

Extensive work has been put into the fabrication and fracture testing of micro-cantilevers in order to study the hydrogen effects on the grain boundary of FeSi steels. This report has been in close collaboration with Ph.D. student Tarlan Hajilou, where the cantilevers fabricated have been used for her fracture tests at the nanomechanical lab at NTNU.
The focus of this report will be on the production process of micro-cantilevers.

A risk assessment and two A3-posters presenting the experimental work and its results can be found in appendix A, B and C, as required by the Department of Engineering Design and Materials (IPM) at NTNU. Pictures of the cantilevers made can be viewed in appendix D.

Abstract

Large amounts of micro-cantilevers were made using a focused ion beam (FIB) microscope. The cantilevers were made to be tested under cyclic loading in a triboindenter to determine the hydrogen effect on the grain boundaries of a FeSi-alloy (3wt% Si and 0,02wt% C). The hydrogen effect was determined by analyzing load-displacement curves where the displacement were from 3 to 5 μm vertically, under atmospheric and acidic conditions (introduction of hydrogen). The focus of this report has been on the fabrication of the micro-cantilevers.

A machining procedure for making cantilevers of good quality is presented in this report. It is made for cantilevers of the dimensions: 14,5 μm length, 4 μm width, 2,6 μm height, and an elevation of 5 μm from the cantilever to the sample floor, but has been used to make cantilevers of varying dimensions. The hydrogen effect on one of the samples has been determined, where it was found that the introduction of hydrogen on the grain boundary lowered the needed force to bend the cantilever by 80 μN.

Sammendrag

En stor mengde mikrobjelker ble fabrikert ved bruk av fokusert ionestråle (FIB) mikroskop. Bjelkene ble lagd for å testes under syklisk lasting i en triboindenter for å bestemme hydrogeneffekten på korngrensene til en type FeSi legering (3wt% Si og 0,02wt% C). Hydrogeneffekten ble fastslått ved å analysere belastnings-forflytningskurver hvor forflytningen var fra 3 til 5 μm vertikalt, under atmosfæriske og syrlige betingelser (introduksjon av hydrogen). Fokuset for denne rapporten har vært på fabrikeringsprosessen for mikrobjelkene.

En maskineringsprosedyre for å lage bjelker av god kvalitet er presentert i denne rapporten. Prosedyren er laget for bjelker av dimensjonene: 14,5 μm lengde, 4 μm bredde, 2,6 μm høyde, og en elevasjon på 5 μm fra bjelken til prøvegulvet, men har blitt brukt til å lage bjelker av varierende dimensjoner. Hydrogeneffekten på en av prøvene har blitt funnet. Det ble fastslått at introduksjonen av hydrogen på korngrensen senket den nødvendige kraften for å bøye bjelken med 80 μN.

Acknowledgements

Great efforts have been taken in the completion of this project. It would not have been possible without the kind help and support from many individuals and organizations. I would like to extend my sincere thanks to all of them.

I am highly indebted to my supervisor, Professor Afrooz Barnoush, for providing me the opportunity for this novel approach to the study of hydrogen embrittlement.

I extend my gratitude to my co-supervisor, Ph.D. student Tarlan Hajilou, for their guidance and constant supervision, as well as for providing the necessary information regarding this project.

The Fine Mechanical Lab at NTNU is highly appreciated for their production of samples and sample holders used in this report.

I am thankful to Senior Engineer Nousha Kheradmand for providing access and training for the usage of the NTNU metallography lab.

The Research Council of Norway is acknowledged for the support to the Norwegian Micro- and Nano-Fabrication Facility, NorFab.

I would like to express my special gratitude to my friends and family for their love and support throughout this project.

Table of Contents

Introduction

Hydrogen embrittlement is a huge and costly technical difficulty a wide arrange of industries face every day. Although researchers worldwide have researched the topic tirelessly, the mechanisms concerning hydrogen embrittlement are still largely debated. A multitude of mechanisms have been proposed, some seen as more valid than others, but still more research is required to fully understand the multitude of processes which occur from the introduction of hydrogen to the given metal and to its brittle fracture. How does the hydrogen accumulate in the metal? By what mechanics does it influence metals mechanical properties? These are the questions that have been given and answered, though with varying degrees of satisfaction.

One way to learn more about the effects of hydrogen on affected metals are through the microscale study of its effect on the grain boundary. A set of micro-cantilevers designed to be bent in a triboindenter can then be fabricated on the grain boundary and introduced to an environment of concentrated hydrogen to instill a high hydrogen concentration on the grain boundary. By then bending these micro-cantilevers, both in environments containing hydrogen and without, one can determine the differences in the force required to bend the cantilever to a certain depth, and thus determine hydrogens reduction of the material's toughness.

The micro-cantilevers can be machined by utilizing the focused ion beam (FIB) microscope. By bombarding the metal sample with charged ion particles, material can be removed to design cantilevers on the microscale, which would be impossible to do accurately with macroscale tools.

It is a requirement before testing that the cantilevers are uniform and of good quality with minimum damage and oddities before testing. This report therefore focuses on determining a process which will make sure that those who follow the given procedure will obtain micro-cantilevers that are of pristine quality in a short amount of time, so the focus of further research can be directed towards the understanding of the many micromechanics concerning the introduction of hydrogen on the grain boundary of metals.

1. Theory

1.1 Hydrogen embrittlement

Hydrogen embrittlement is understood as the reduction of toughness in iron and other affected metals, turning them brittle (hence its name) due to the introduction of hydrogen. It is a huge technical problem that has been thoroughly researched, albeit mostly on the macroscale. Yet, more experiments are needed to fully understand the mechanisms that govern hydrogen embrittlement and prove the validity of already established theories. Temporal in nature, by effectively removing the hydrogen from the affected metal, its original strength and toughness may be restored completely.

The field study of hydrogen embrittlement was effectively started by Johnson in 1875 when he published his papers on the subject. He studied the change in mechanical properties of a piece of iron after being immersed in different acids. After 30-60 minutes of immersion in strong hydrochloric or dilute sulfuric acid, he bent the iron piece to study the macroscale effects of this immersion. The iron piece was found to break after being bent once on itself, while it would be able to be bent two or three times before fracture without the introduction of hydrogen. Johnson also found that, with enough time, the original mechanical properties of the submerged iron piece would return. This raised the need for determining the mechanisms under which the hydrogen embrittlement operates. [5]

1.1.1 Hydrogen-enhanced local plasticity (HELP)

A large amount of mechanisms to account for hydrogen embrittlement have been proposed through the years. Unfortunately, only a few remain valid to date. One of these mechanisms are the hydrogen-enhanced plasticity theory., which was introduced by Birnbaum and Sofronis.

The phenomenon became evident through the experiments of Bechem in 1972. Bechem theorized that the increased material ductility by introduction to hydrogen were an indicative of hydrogen enhancing plasticity processes. He also suggested that the hydrogen-induced fracture stresses were connected with the microstructural state of the material. This contradicted previous beliefs that the ductility was a direct effect caused by the embrittlement process and was thus not considered important to the understanding of the underlying mechanics of hydrogen embrittlement. It was later revealed through experiments performed by the «Illinois group» led by Robertson Birnbaum, that the introduction of hydrogen gas increased the velocity of dislocation motion in the material. When removing the hydrogen gas from the sample, the dislocation motion ceased. It was then apparent that hydrogen enhanced the dislocation motion in affected materials. These observations were initially challenged, and it was postulated that this stemmed from the pressure difference created by the introduced gas environment into the objective pole-piece of the electron microscope, or just simply a thin foil effect. However, it was found that the time required to calibrate the microscope for the introduced gas pressure was a few seconds, while the observed effect lingered for a significantly longer period. The final nail in the coffin to the superstition came when macroscale experiments such as stress relaxation and strain rate change tests were conducted. They showed that the presence of hydrogen decreased the activation area for dislocation motion and their activation energy. In situ experiments in a transmission electron microscope (TEM) has also been conducted to further iron the theory. The sample was cracked under the presence of hydrogen gas or water-saturated inert gas. It was found that before the crack evolution, the sample would experience extensive thinning ahead of the crack, observed in the microscope as a set of parallel lines. The crack also widened considerably. The cracking mechanism was also found to change, as under the influence of hydrogen it changed from transgrannular to intergrannular.

To summarize, hydrogen increases the production and mobility of dislocations irrespective of the type of dislocation and crystal structure. The hydrogen segregates to dislocation stress fields and other elastic obstacles, increasing the intensity of them in preferred directions and reducing them in others. In the reduced directions, the interaction energy of the dislocation which impedes its motion will be reduced, thus allowing increased mobility of the dislocation in that direction. [5]

1.2 Focused Ion Beam Microscopy

The Focused Ion Beam (FIB) microscope is a highly versatile instrument that has been used extensively in the semiconductor industry and material science. Highly resembling the Scanning Electron Microscope (SEM), it differs in its source of imaging, utilizing a focused beam of ions rather than electrons. [1] [2] [3] The ions are extracted from an ion-source and then propelled towards the sample by an accelerating voltage. The kinetic interactions between the ions and the sample produces the emission of secondary-electrons (SE-electrons), which can be collected by a compatible detector, giving topographic information of the sample surface. This information can in turn be fed to a computer, which produces an image. [1] The FIB's forte is however its ability to precisely «cut» into the sample surface (milling) through ion-solid interactions, and to perform local chemical vapor deposition (CVD) with a gas injection needle. As the bombardment of ions from the FIB causes damage to the sample surface, it is often seen in conjunction with a SEM, creating a highly versatile «dual-beam» microscope. The FIB and SEM column are then tilted at a certain angle in relation to each other, so that their beams intersect at a shared point on the sample surface at a given working distance. [1] [2] [3] The SEM is then used primarily as an imaging column, while the FIB column is used for the milling and CVD. [1] An schematic example of a FIB-SEM dual beam microscope is given in Figure 1.

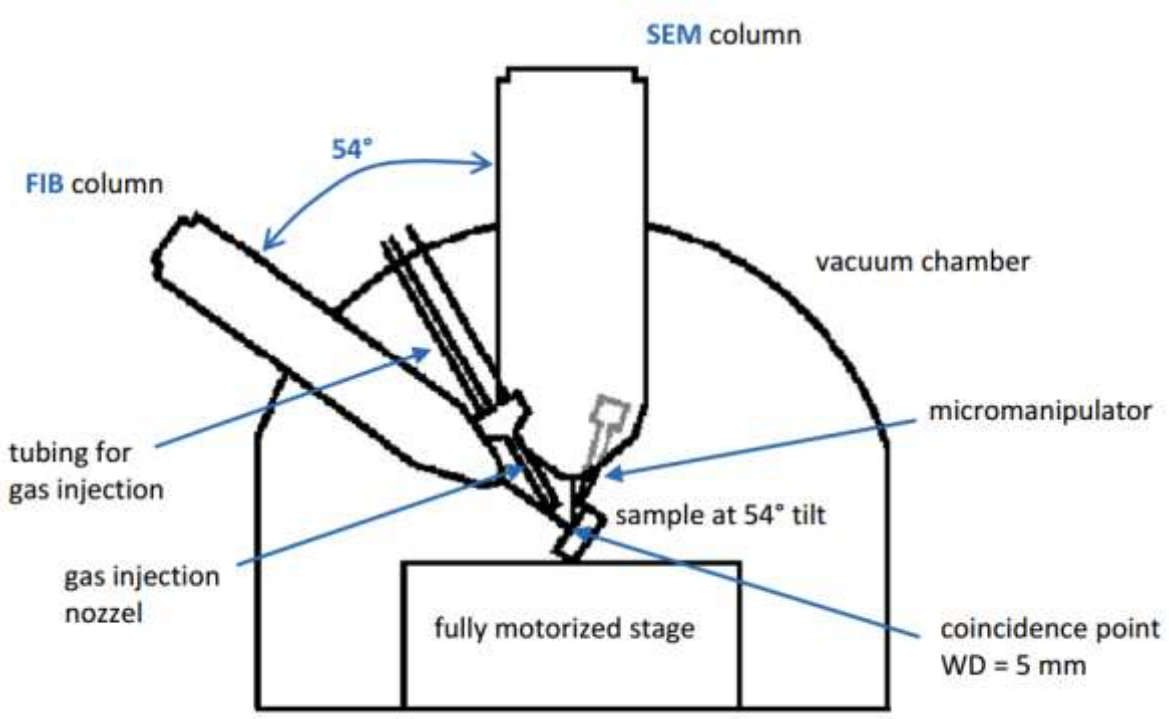

Figure 1 –Representation of a FIB-SEM dual-beam microscope [4]

1.3 Microscope structure

The FIB and the SEM microscope are rather structurally similar. Both consist of a chamber with a vacuum system, a sample stage, various detectors (e.g. Everhart Thornley Detector), focal lenses, a source of imaging, and a connected computer to control the microscope and display the imaged sample. An illustration of the FIB column is given in Figure 2. [1] [2] [3] What distinguishes the two microscopes from each other is the source of imaging. The FIB microscope utilizes a source consisting of ions rather than electrons. Typically, the source is a liquid metal ion source (LMIS), as it provides a brighter and more focused beam when the appropriate lenses are used. The most widely used LMIS is the gallium ion source (Ga^+), although bismuth, gold, indium, and tin are also applicable. The reasons gallium is chosen in favor of the others, is due to its advantages in comparison to the other LMIS. [1] [3] Gallium has a low melting temperature (30 °C), which makes the design and operation of the source simple, low vapor pressure, low volatility (due to negligible evaporation), usually more stable than other LMIS, and it does not react with the material defining the needle (typically wolfram). [1]

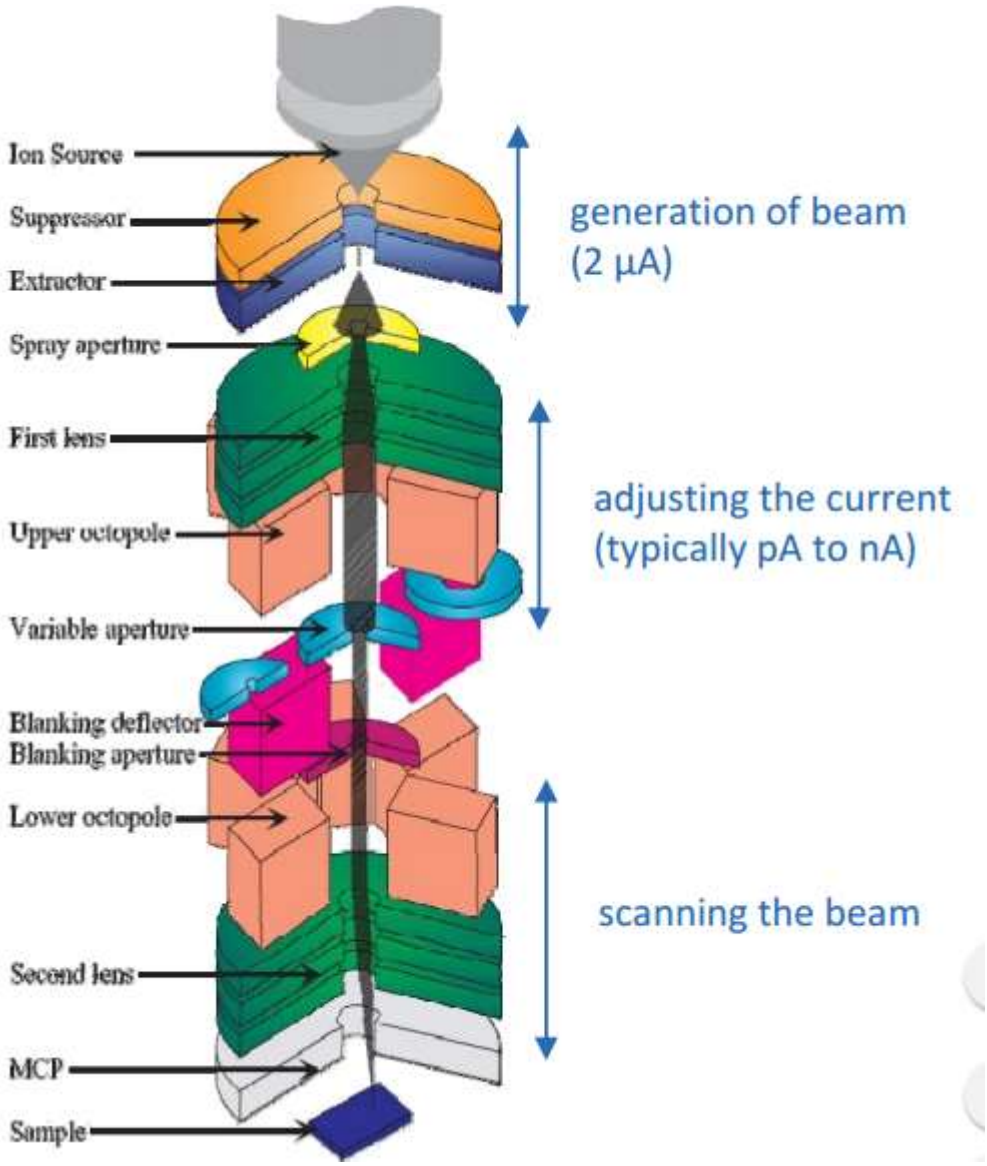

Figure 2 - An schematic respresentation of the FIB column and its major components [4]

The ion-beam column generally consist of a Ga-blunt needle, which is responsible for extracting the ions from the LMIS and propelling them towards the sample surface. The extraction of the ions are

carried out by field emission, where the extracted ions form a Taylor-cone at the end of the needle. The cone is formed as a direct effect from the electrostatic forces and the ion surface tension on the needle geometry. A large negative potential between the needle and an extraction electrode generates the electric field (typically with a magnitude of 10^{10} V/m) which propels the ions towards the sample surface. To help focus the beam on the sample for increased resolution (smaller spot size) a wide array of apertures and lenses are utilized. In the most basic ion beam columns, a condensor and objective lens are used to define and focus the beam. Beam-defining apertures are used to select the beam current and spot diameter, deflection plates to raster the beam over the sample surface, stigmation poles to ensure a spherical beam profile, a high speed beam blanker to deflect the beam off the sample and onto a beam stop, and a Faraday cup to act as said beam stop. The reason electrostatic lenses are used, rather than electromagnetic lenses as in SEM, is due to the correlation between the electromagnetic lenses' strength as a function of their size (charge/mass ratio). An electromagnetic lens for a FIB would simply weigh a ludicrous amount (on the scale of thousands of kilograms). [1]

1.4 Ion-solid interactions

The FIB microscope's usage of an ion source rather than an electron source causes some concern. The main concern is the ions' effect on the sample material. When the Ga^+-ion hits the surface of the sample, it transfers a lot of kinetic energy to the affected atoms. This energy is proportional to the voltage used on the FIB-microscope. The energy can sometimes be of such a magnitude, that the ion can cause irreparable damage to the imaged area of the sample. The damage can be atomic sputtering, ion emission, heating of the sample, or implantation of ions in the sample surface. An illustration of the possible outcomes of the ion-solid interactions is shown in Figure 3. [1] [2] [3]

The transfer of an ion's kinetic energy to the surface can happen through two mechanisms: inelastic and elastic collision. In the first case, the ion's energy is wholly transferred to the electrons of the sample trough the ion's momentum. This is called electronic energy loss, and results in ionization and the emission of electrons and electromagnetic radiation from the sample surface. The emitted electrons from this process are necessary to provide an image of the sample surface. The second case, elastic collision, is called nuclear energy loss, and can result in the displacement of sample atoms from their original position in the lattice and the emission of the surface atoms of the sample (sputtering). [1] [2] [3] Here, the energy is transferred as translational energy to screened target atoms. [1] For the FIB microscope, the dominant process for energy loss is considered to be electronic energy loss. [2]. In some cases, the emitted atom due to inelastic collision might have enough energy to displace other atoms in the sample and thus cause a large amount of atoms to have excess kinetic energy. [1] This generally leads to defects in the lattice parameters of the sample through interstitial-vacancy and incorporation of Ga, however, nuclear energy loss is also what is used to be able to mill the sample with FIB. [1] [2]

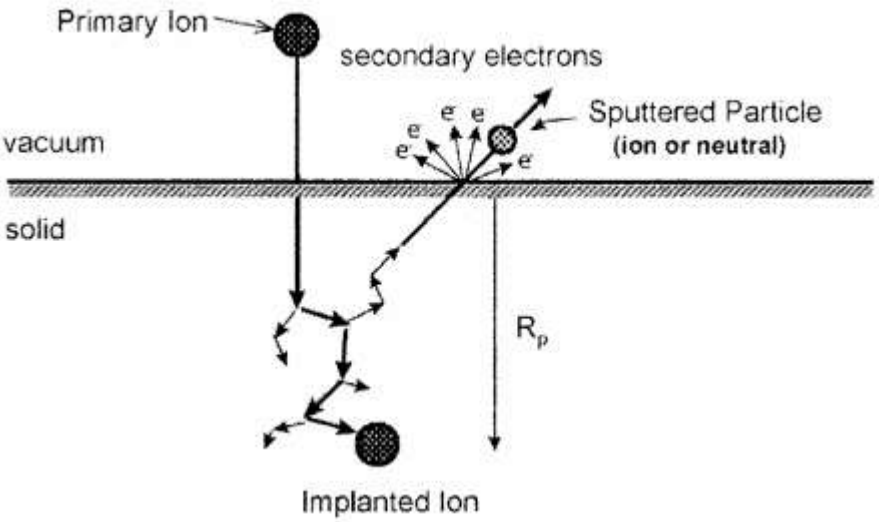

Figure 3 –Schematic illustration of the implementation of a 30 keV Ga-ion in a crystal lattice. The ion causes the emission of electrons, but also atoms in the crystal lattice [3]

By utilizing the nuclear energy loss mechanism, material can be selectively removed from the sample by the FIB. [1] This mechanism is referred to as «knock-on sputtering». Emitted surface particles during milling generally have an energy of 2-5 eV. The path of the emitted particles has a cosine distribution for normal incidence ion bombardment (see Figure 4). [2]

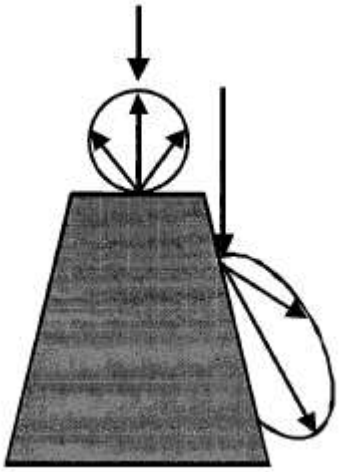

Figure 4 - Representation of the mean path of the emitted sample particles related to the incident angle [2]

2. Experimental procedure

2.1 Sample material

The samples used were FeSi-alloys (0,02 wt% C and 3 wt% Si) of different heights with a diameter of 11,5 mm. They were cut to the correct dimensions by the Fine Mechanical Lab at NTNU to ensure they would fit into the FIB sample holders provided. An iron alloy containing Si was used as the dual beam FIB/SEM microscope provided had a well calibrated/tested Si-profile for milling.

2.2 Sample preparation

The samples were ground with silicon carbide grinding paper and then etched with acetone in a Struers LectroPol-5.

The samples were marked with indents in a 3x3 grid with a macro indenter. The markings were evenly spaced and on the same line. Two indents were made in a corner to be able to distinguish which direction the sample were in the microscope. Figure 5 gives an illustration of how the indent placement in the sample. Some of the samples had the indents situated in the middle, and not spread out across the sample as seen in the illustration. Others also had a different indent grid than shown below, though the principle remains the same.

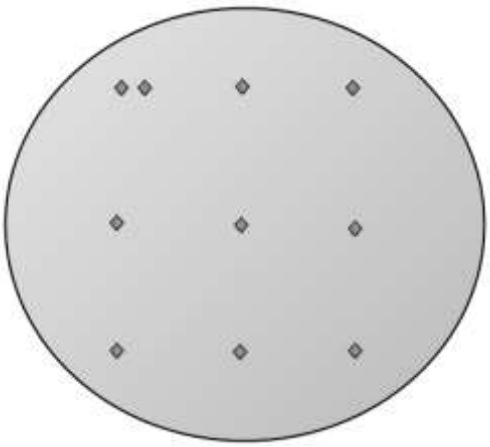

Figure 5 - Simple illustration of the placement of the macro-indents on the samples

The samples were mounted in a brass FIB sample holder which fastened the sample mechanically by 3 screws with a square profiled screwdriver as shown in Figure 6. Mechanical fastening was chosen as carbon tape showed drift during tilting/rotation of the stage.

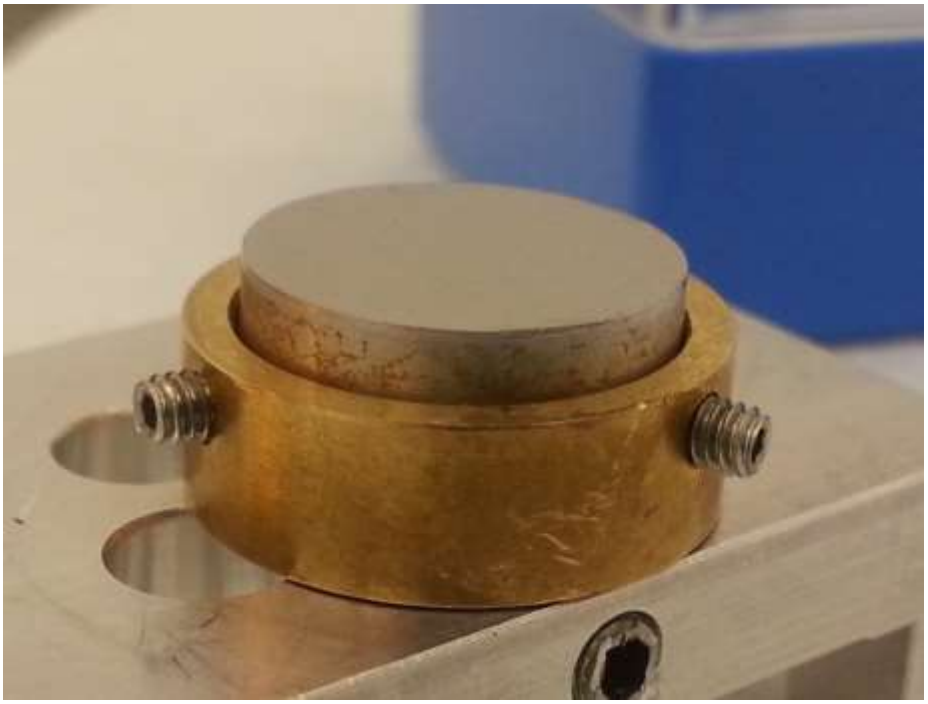

Figure 6 –Image of the FIB sample holder mounted in the stage's sample holder

When the sample was not in use, the sample was stored in a plastic container in the NTNU nanolab cleanroom, containing a bag of silica gel to reduce oxidation.

2.3 Milling procedure

The final procedure for the milling of the cantilevers can be found in Table 1. The tilts given are in relation to the stage unless specified. A revision of the original parameters were necessary due to the need for bending the cantilevers to a further depth (5 μm) during fracture testing and an increased need for swiftness in the machining process. This called for the inclusion of a new step to remove material from under the cantilever. All the milling were done with regular cross-sections with a 4 passes multiscan. The multiscan was used to reduce the time needed for milling.

The pictures given in Table 1 were taken with a FEI Helios nanolab 400s dual beam microscope, at an accelerating voltage of 5 kV and a current of 0,69 nA with a dwell time of 5 μm, while the FIB pictures had a voltage of 30 kV, a current of 0,93 pA and a dwell time of 5 μm.

Approximately, it took 1 hour and 12 minutes to finish a cantilever while also imaging the cantilever as in step 11 below (see Table 2 for approximate times). This does not include the time needed to pump/vent the chamber, mounting and removal of sample, correcting microscope parameters, initial focusing and adjustment of FIB/SEM beam shift.

A multitude of pictures from different angles were taken of the finished cantilever to give needed information about the cantilever quality to the co-supervisor. The pictures were taken from different angles to make sure one would be able to spot if there was any redeposition or symmetry errors.

Table 1 – Final milling parameters

	FIB	SEM
Step 1: Coarse milling of cantilever base shape Tilt: 52° Current: 2,8 nA Voltage: 30 kV Depth: 10 µm Time: 20 min.		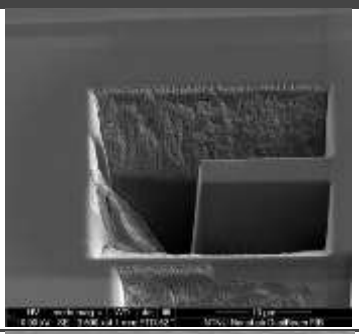
Step 2: Coarse milling of cantilever profile Tilt: 52° Current: 2,8 nA Voltage: 30 kV Depth: 6 + 10 µm Time: 5 min. 30 sec.	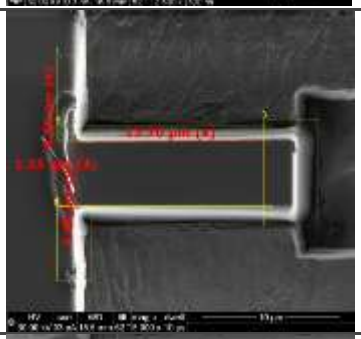	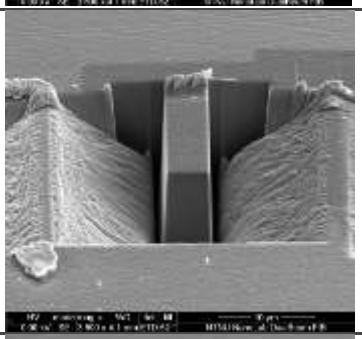
Step 3: Coarse milling of cross-section Tilt: -9 ° Current: 9,3 nA Voltage: 30 kV Depth: 10 µm Time: 2 x 1 min. 30 sec.		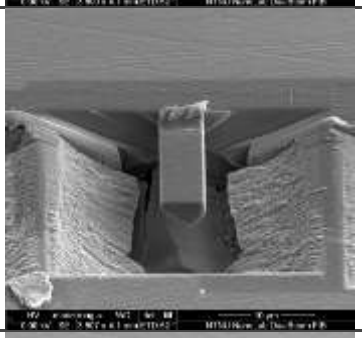
Step 4: Removal of redeposition under cantilever Tilt: 7 ° Current: 9,3 nA Voltage: 30 kV Depth: 10 µm + 10 µm Time: 2 x 2 min. + 2 x 2 min.	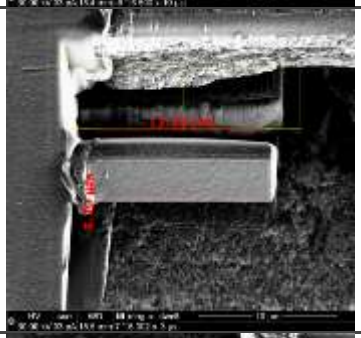	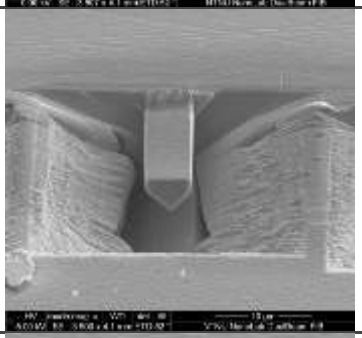
Step 5: Removal of redeposition on cross-section Tilt: -9 ° Current: 9,3 nA Voltage: 30 kV Depth: 6 µm Time: 2 x 30 sec.	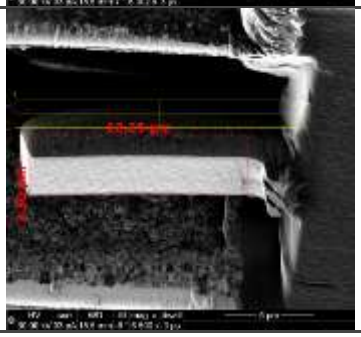	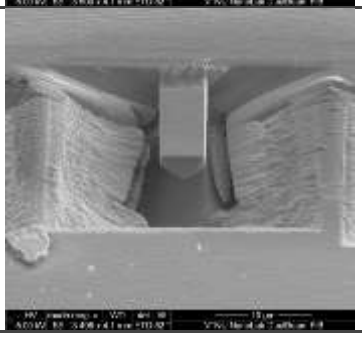

Step 6: Fine milling of final cantilever profile Tilt: 52 ° Current: 0,92 nA Voltage: 30 kV Depth: 10 µm + 6 µm Time: 7 min.	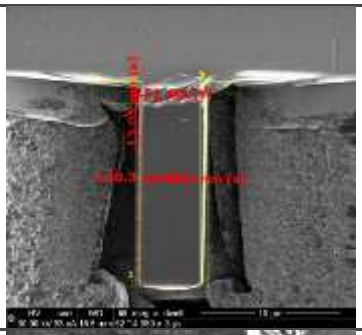	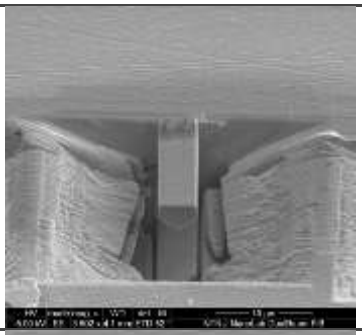
Step 7: Fine milling of final cantilever cross-section Tilt: -9 ° Current: 0,92 nA Voltage: 30 kV Depth: 6 µm Time: 2 x 2 min. 30 sec.	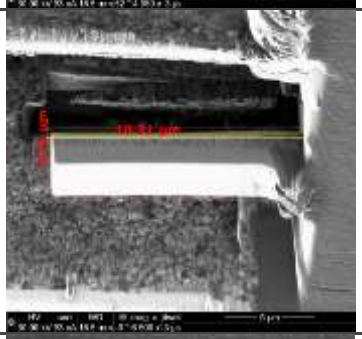	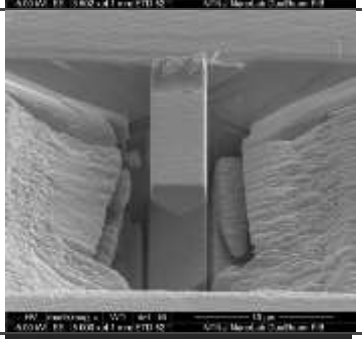
Step 8: Milling of hole for bending Tilt: 52° Current: 93 pA Voltage: 30 kV Depth: 0,05 Time: 2 sec.	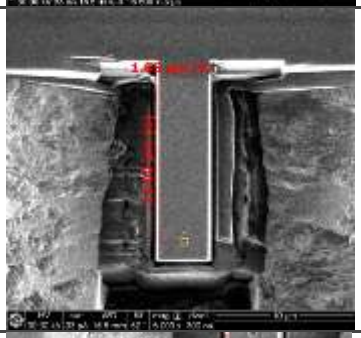	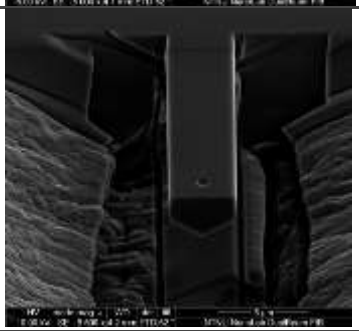
Step 9: Milling of roman numeral Tilt: 52° Current: 93 pA Voltage: 30 kV Depth: 1 **µm** Time: 1 min.	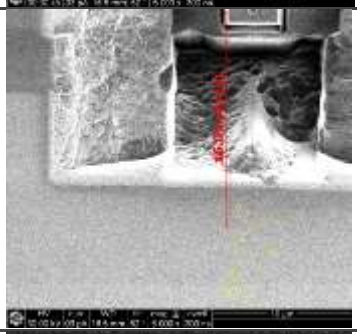	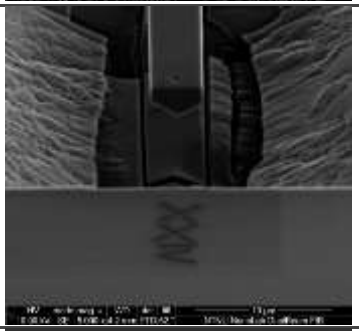
Step 10: Milling of notch on grain-boundary Tilt: 52° Current: 9.7 pA Depth: 1 **µm** Time: 1 min.	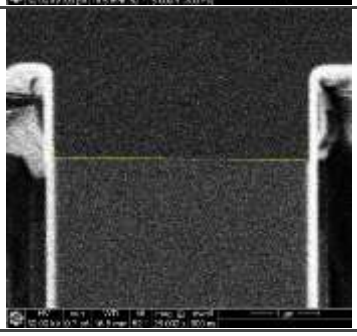	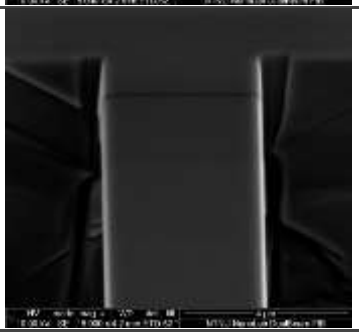
Step 11: Imaging of cantilever		**SEM**

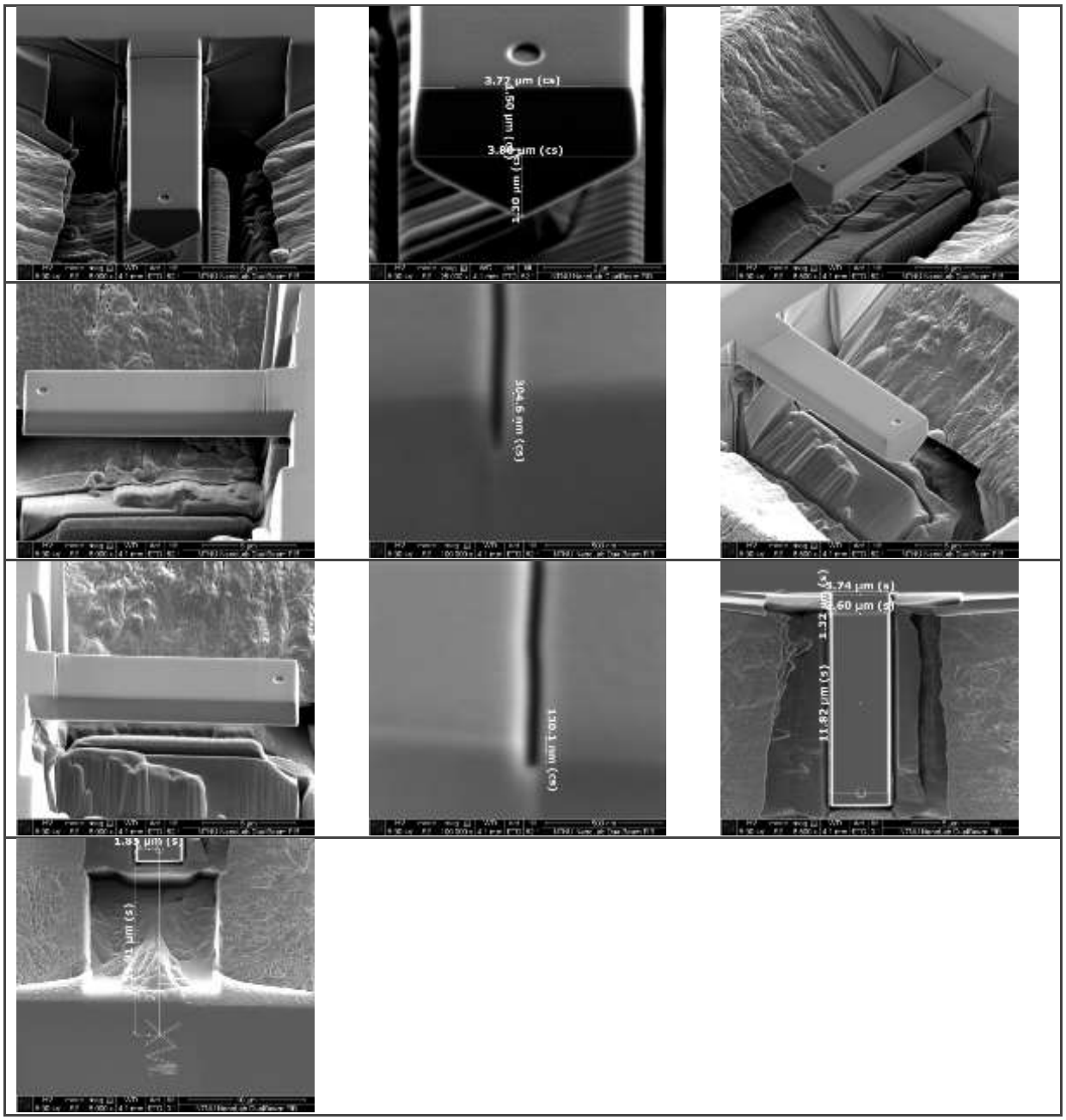

Table 2 – Approximate time spent in the making of 1 cantilever

Task	Time
Milling	52 min
Placement/adjusting/focusing	10 min
Imaging	10 min
Total	**1h 12 min**

2.3.2 Theoretical dimensions of the cantilever

Presented in Figure 7 are the theoretical ideal dimensions of the cantilevers made in this report. Note that not all of the cantilevers were of these dimensions. The resulting dimensions were the product of repeated experiments. The most important part of the dimensions of the cantilevers, are that the batch made for cyclic loading is of similar size. As long as the lengths and widths are of close magnitude (< 10 µm difference) the cantilevers are valid for testing.

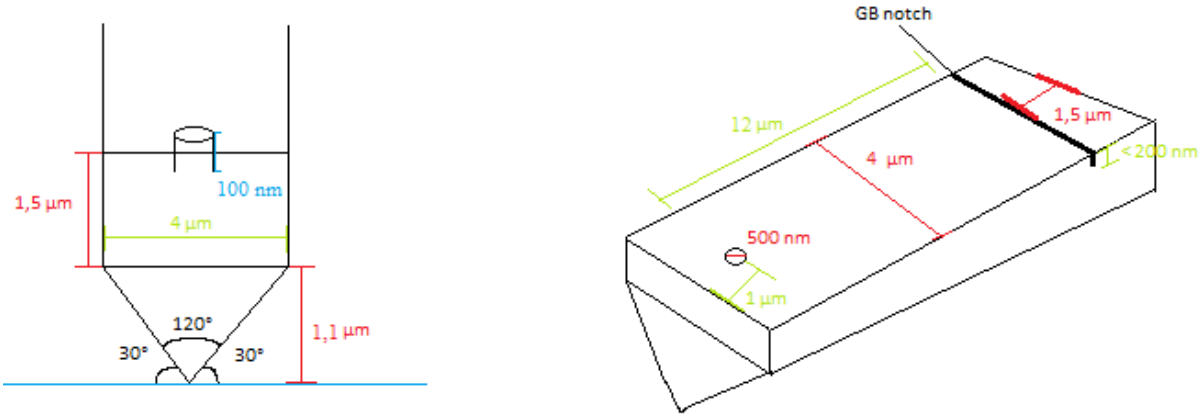

Figure 7 – Schematic of the theoretical dimensions of the cantilevers

2.3.3 Determining safe distance to mill at -9° and 7°

As the need for bending the cantilevers to a further depth became apparent, a revised milling procedure was necessary. A sufficient depth of 5 µm was achieved through the inclusion of an additional milling step at 7°. It was necessary to calculate the distance from the edge of the cantilever one could mill from without damaging the cross-section in the process. The trigonometric calculations used to determine the distance for both the tilt at -9° and 7° are given below.

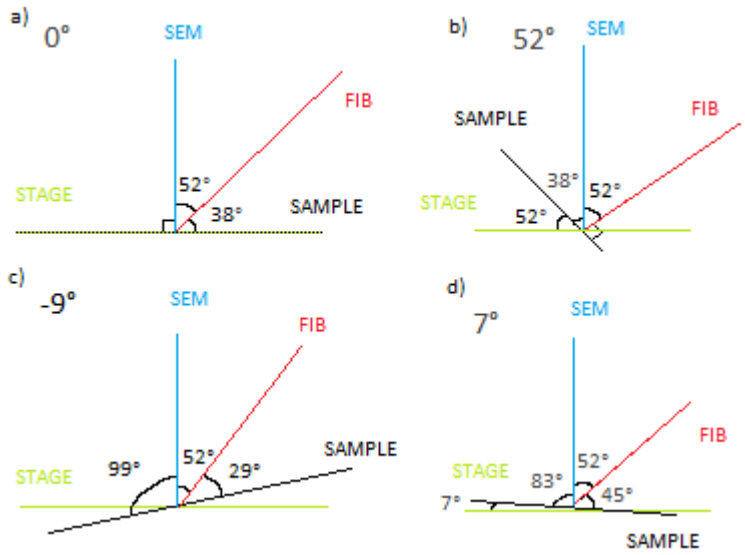

Figure 8 – Overview of the various tilts used during the experimentation and the sample's relative angles with respect to the stage/FIB/SEM

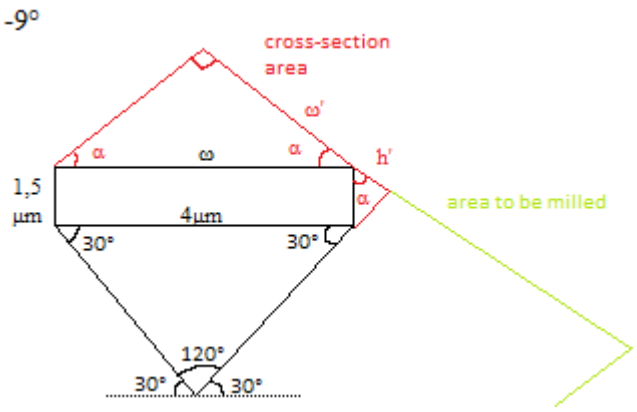

Figure 9 –Illustration of the trigonometric calculations for an angle of -9° with respect to the stage

Safe distance at-9°:

$$\omega' + h' = \omega \cdot \sin(\alpha) + h \cdot \cos(\alpha)$$

$$\omega' + h' = 4\ \mu m \cdot \sin(29°) + 1{,}5\ \mu m \cdot \cos(29°)$$

$$\omega' + h' = \underline{3{,}25\ \mu m}$$

Although the calculation is for 29° instead of 30° (as shown in Figure 9), in reality, milling at a 29° angle in relation to the FIB produced an angle of 30° in the final cross-section. A measurement of the cross-section angles can be seen in Figure 10.

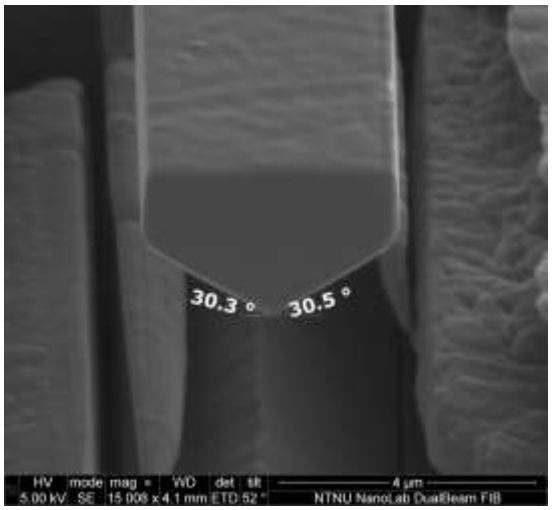

Figure 10 – SEM angle meassurement of the cross-section profile

Total height of cross-section.

$$1{,}5\ \mu m + 2{,}286 \ldots * \sin(29°) = (1{,}5 + 1{,}1)\ \mu m = \underline{2{,}6\ \mu m}$$

Safe distance at 7°:

At 7° the incident beam angle will be sharper than at -9 ° (see Figure 11). It is therefore required to calculate a new safe distance to make sure the cross-section is not affected.

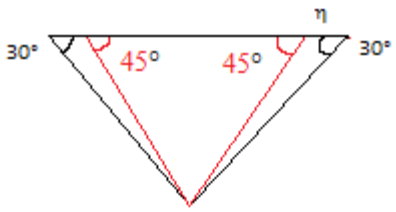

Figure 11 – Schematic showing how the change in angle impacts the cross-section

$$\eta = \frac{1{,}1\ \mu m}{\sin(45°)} = 1{,}56\ \mu m$$

$$\theta = 1{,}56\ \mu m * \cos(45°) = 1{,}1\ \mu m$$

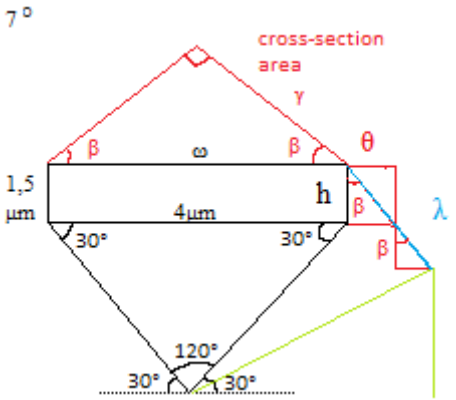

Figure 12 - Illustration of the trigonometric calculations for an angle of 7° with respect to the stage

$$\gamma + \lambda = 4\ \mu m \cdot \sin(\beta) + 2 * h \cdot \cos(\beta)$$

$$4\ \mu m \cdot \sin(45°) + 2 * 1{,}5 * \cos(45°) = \underline{\underline{4{,}9\ \mu m}}$$

A distance of 5,25 µm was chosen in order to be absolutely certain that the milling at 7° would not interfere with the cross-section. Through measuring in SEM, it has been shown that milling at 5,25 µm gives satisfactory results (see Figure 13).

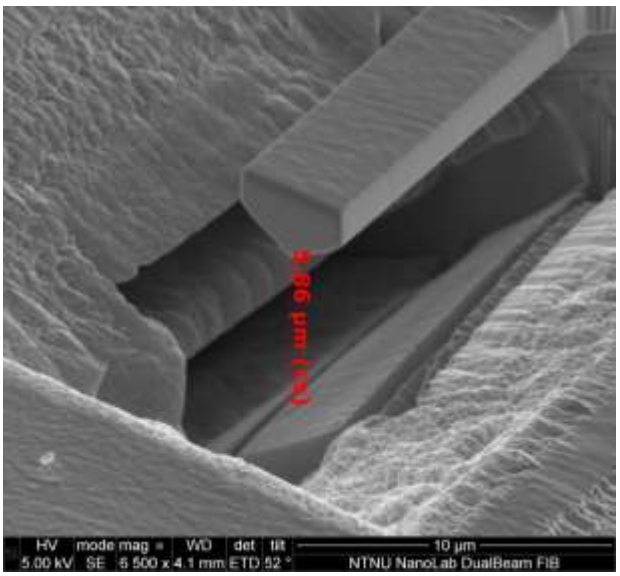

Figure 13 – Height of cantilever after introduction of milling at 7°

2.3.4 Redeposition effect

The redeposition of material on the cantilever during milling has been an unavoidable phenomenon during fabrication. The effect stems from the ion-solid interactions during cutting.. The redepeosited material causes numerous problems, including: wrong cross-section dimensions (Figure 15), roughness on sides of the cantilever, incorrect cantilever height (lowest point on cross-section to ground level) and uneven material distribution (e.g. material deposited on the sides of the cantilever). All of these can lead to the cantilever not being useful for testing. It has therefore been quite a challenge to find ways to control the material redeposition and at the same time produce a cantilever of correct dimensions and minimum FIB damage.

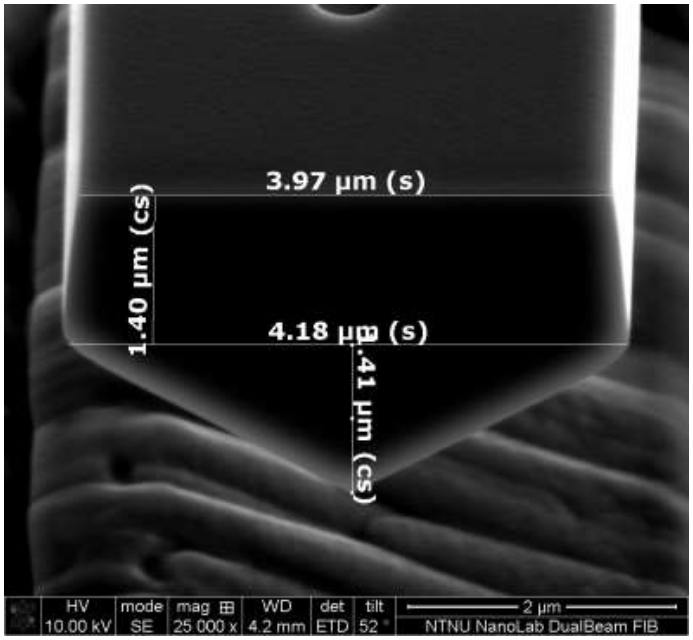

Figure 14 – An example of the redeposited material on a cantilever after fabrication. Material has redeposited on the sides of the cantilever, making a difference of about 20 µm in the final cross-section. This is however considered an acceptable redeposition effect

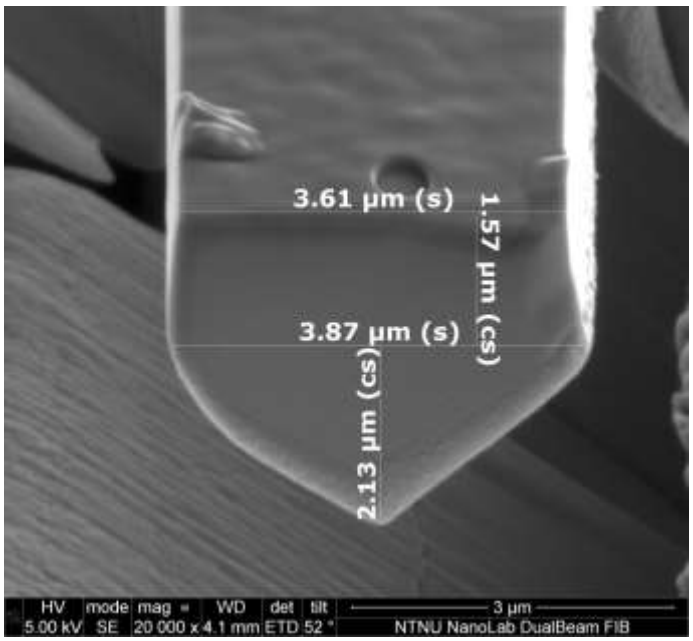

Figure 15 – Another example of redeposited material on a cantilever after fabrication. This is not considered an acceptable redeposition effect

As seen in Table 1, some of the steps have had to be repeated in order to get rid of redeposited material. During the cuts at -9° and 7°, it has been necessary to portion the milling into multiple steps, as to lessen the impact of the redeposition. During each milling, a large chunk of the material removed will be "pushed" over to the other side, thereby increasing the time required for fabrication and causing complications. By milling a large amount at the start and then incrementally lessen the amount of material milled at a time, a satisfactory control of redeposited material was achieved.

2.3.5 FIB damage

Various currents were tested during the experimental part of the thesis. Generally, a smaller current yields a more concentrated beam profile, and thus impacts the area surrounding the milled area less. Time however, has been of significant importance in this project, as the FIB is in high demand and is often booked. Higher currents than would be preferable was chosen as a result.

9.3 nA was the highest current chosen for the rough millings, as it made the machining of the cantilevers swift and did not show signs of FIB damage unless taking multiple images due to bad focus. 21 nA was tried for the first rough milling, but was promptly booted as it showed significant FIB damage both on the cantilever and the surrounding area (milled noticeably into the surface).

For the delicate steps requiring precision, a current of 0,92 nA was chosen. This current was low enough to give a clear image of the cantilever, as well as yielding satisfactory results for its cross-section.

2.3.6 Ion Beam Shift

Due to the high currents used by the FIB, the sample experienced a lot of current build-up during imaging and milling. This caused a shift in the ion beam on the order of a few micrometers when placing the milling patterns on the FIB image. As such, it was often required to take multiple pictures in FIB to make sure the milling patterns were placed correctly. Since this would be a serious problem at higher currents (9.3 nA), instead, a larger safety margin was chosen (5,25 μm instead if 5 μm) to make up for this beam shift.

2.3.7 Inclusion of notch on grain boundary

A notch was milled on the grain boundary to lessen the time needed for testing and to make sure the bend would originate in the grain boundary. This however required that the notch would need to be accurately placed on the grain boundary. To make sure all of it was covered by the notch, the milling was exaggerated, so the sides of the cantilever were also milled. It was therefore very important that the height of the notch on the sides of the cantilever were of similar magnitude, as the bending would experience torsion otherwise (see Figure 16).

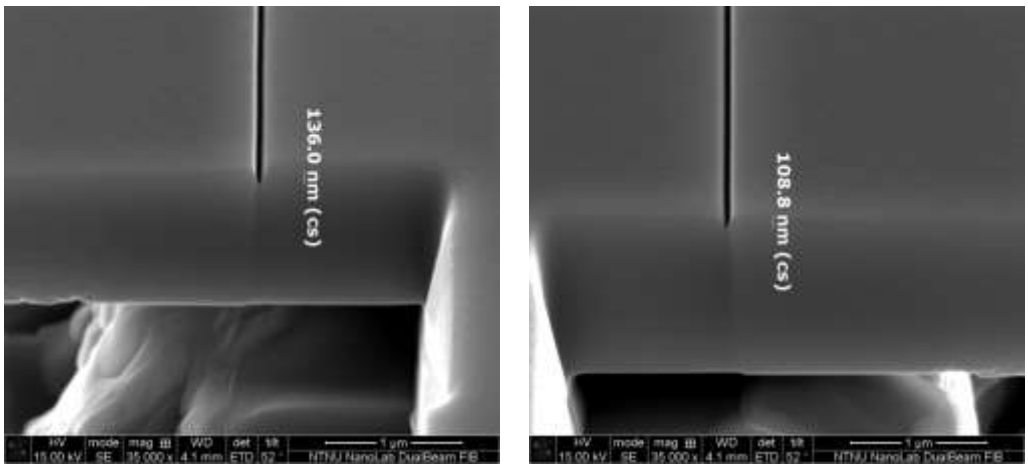

Figure 16 - Side view of notch on grain boundary

The required force needed to bend the cantilever were also lessened due to the notch, so one or more additional cantilevers without a notch were included as references in each sample to determine the difference in force requirements

2.3.8 Cyclic loading of cantilevers

The cantilevers were bent in a hysitron ti 950 triboindenter both under atmospheric conditions (without hydrogen) and under the influence of hydrogen (acidic solution). They were loaded to a depth of 3 μm at the start of the project, and to a depth of 5 μm nearing the end .A rectangle milled in the directions of the cantilevers served as a reference to angle the samples correctly using the triboindenter's optical microscope. The cross above the roman numerals, milled with the same distance from the hole on the cantilever for a batch of cantilevers, saved time when using the triboindenter's AFM to locate the hole for placement of the needle.

.

3. Results and discussion

Overall, a large amount of cantilevers have been fabricated in order to further the understanding of hydrogen embrittlement at the microscale. A few notable examples will be presented in this part of the report. The total of the cantilevers fabricated during the experimental period of the thesis can be viewed in Appendix D.

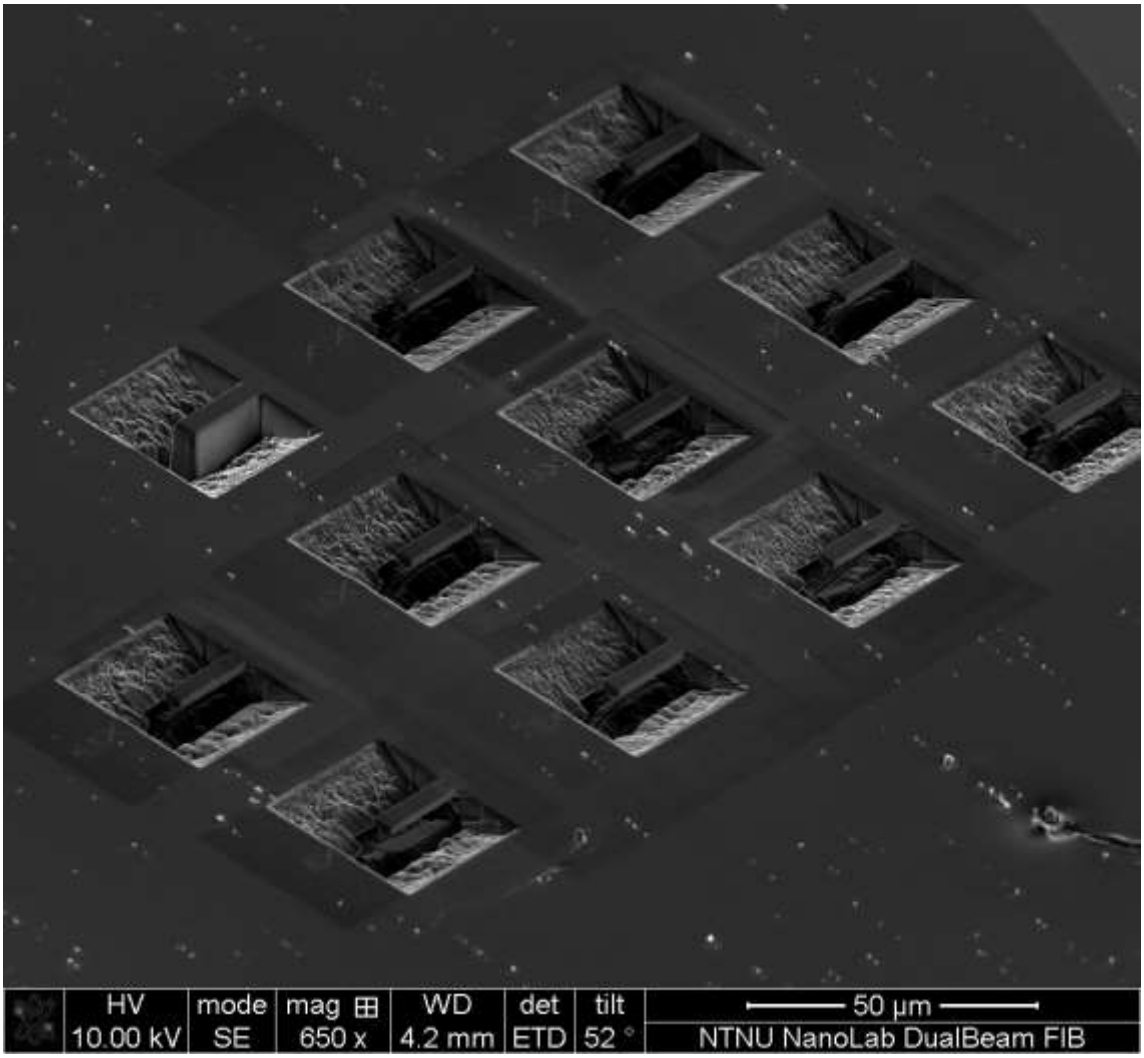

Figure 17 – SEM image of finished cantilevers from a single crystal FeSi sample

Table 3 – Cantilevers from FeSi-alloy (sample 1)

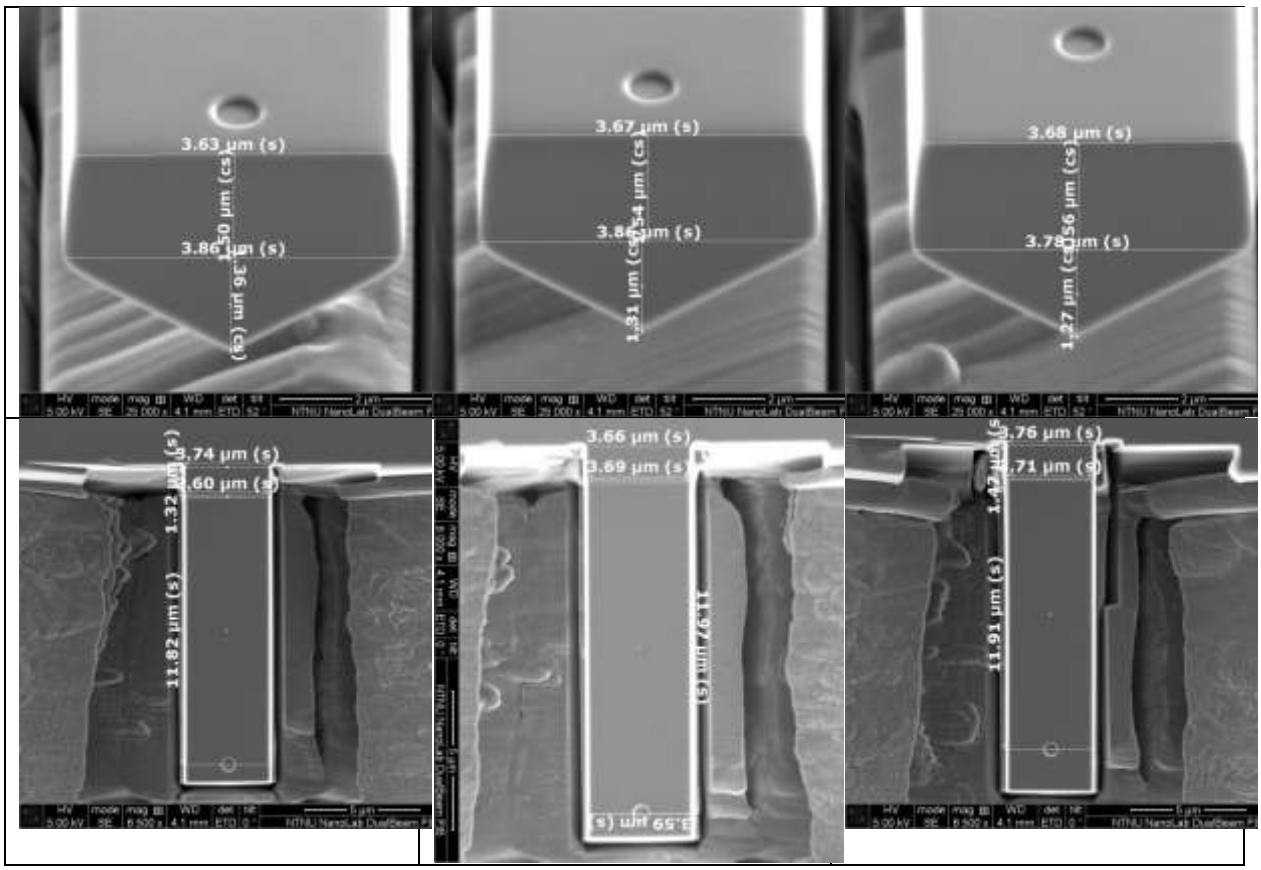

Table 4 - Cantilevers from FeSi-alloy (sample 2)

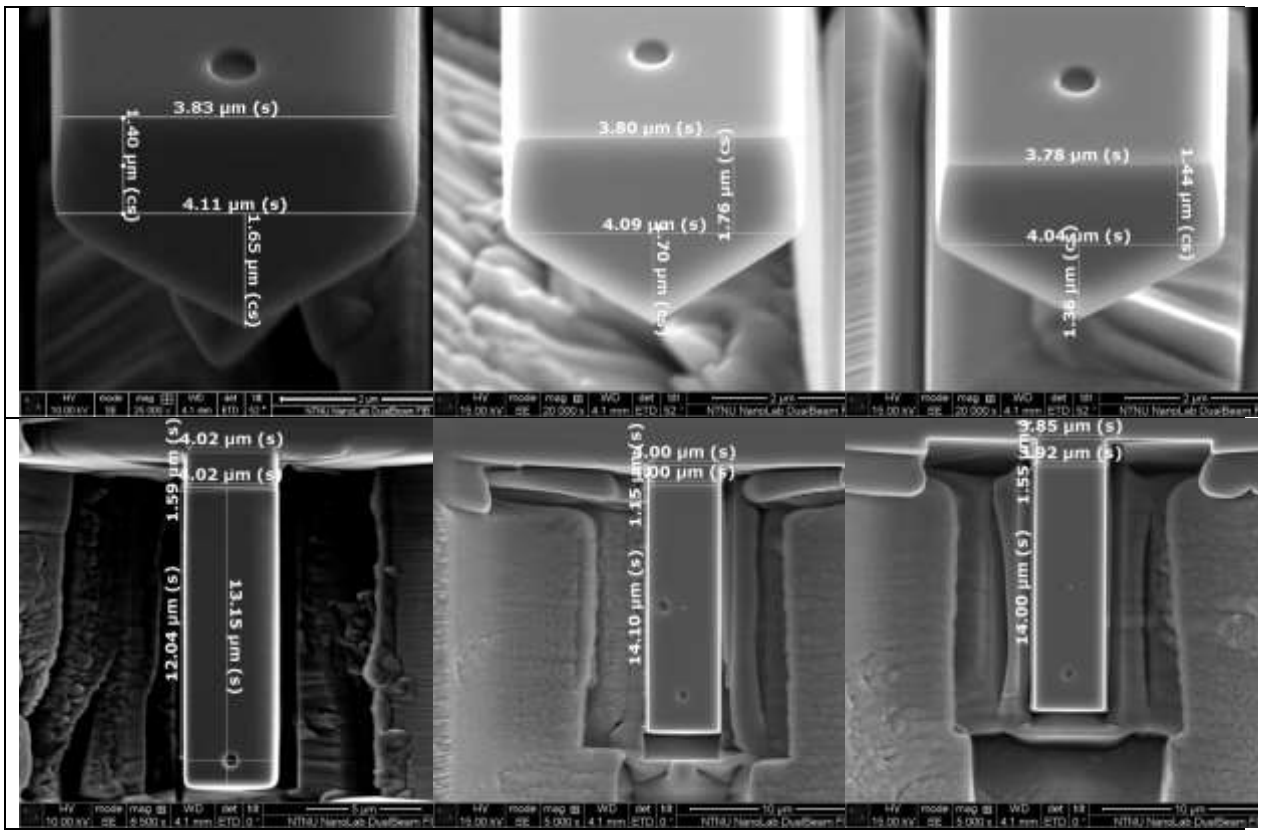

Table 5 – Cantilevers from FeSi single crystal (sample 3)

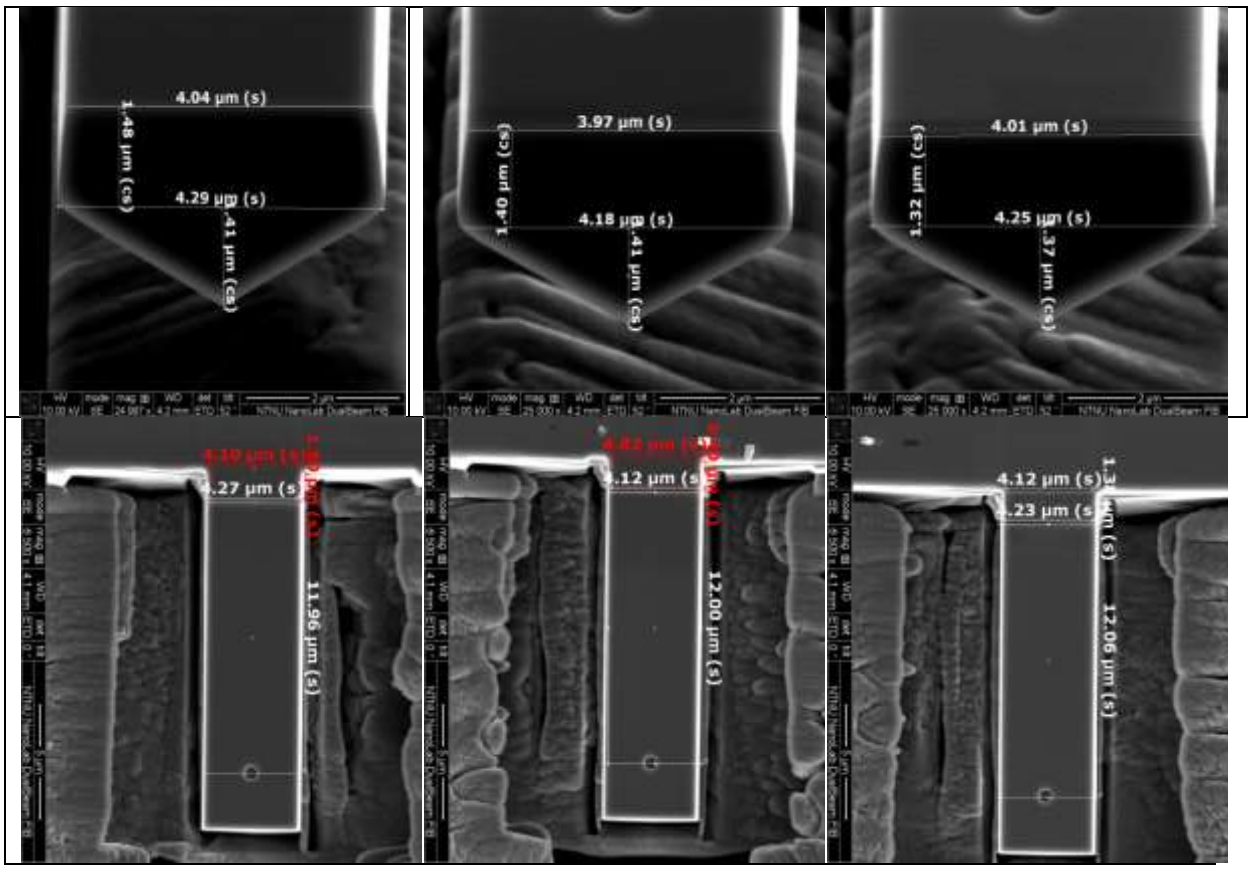

Table 6 – Cantilevers from FeSi sample with carbide precipitate on grain boundary (sample 4)

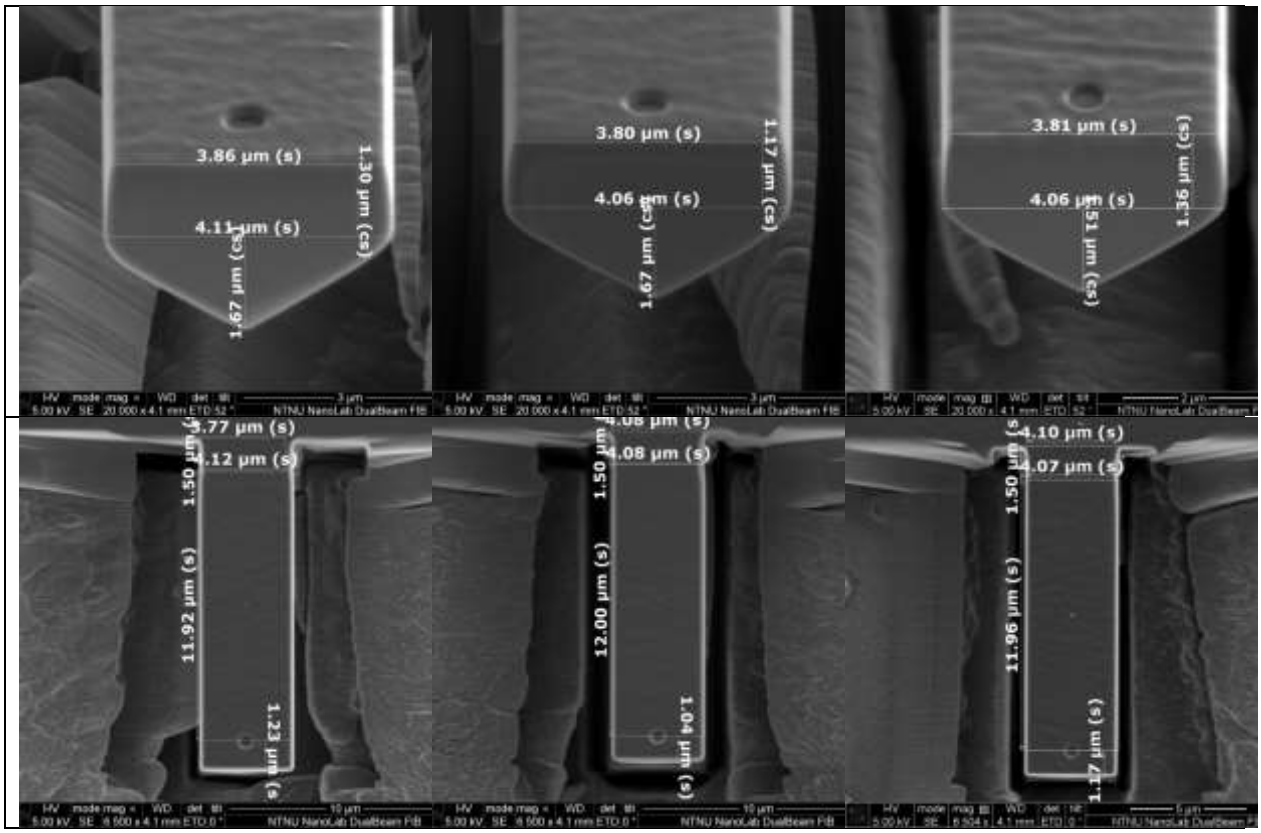

As can be seen from the images, generally the top-down meassurements corresponds more with the width of the redeposition on the cross-section. The cross-sectional size without the redeposition is generally lower by about 20 µm. The redeposition stems from the material being pushed from one side to the other during the final defining of the cross-section profile at -9°. This redeposition can be removed by having an additional milling at 52 °. However, it was found that the dangers of ruining the cross-section symmetry were high, so the redeposition were left as it was considered minute.

Table 7 - Results of bend tests for 2 cantilevers without introducing hydrogen (air) and with the introduction of hydrogen (H)

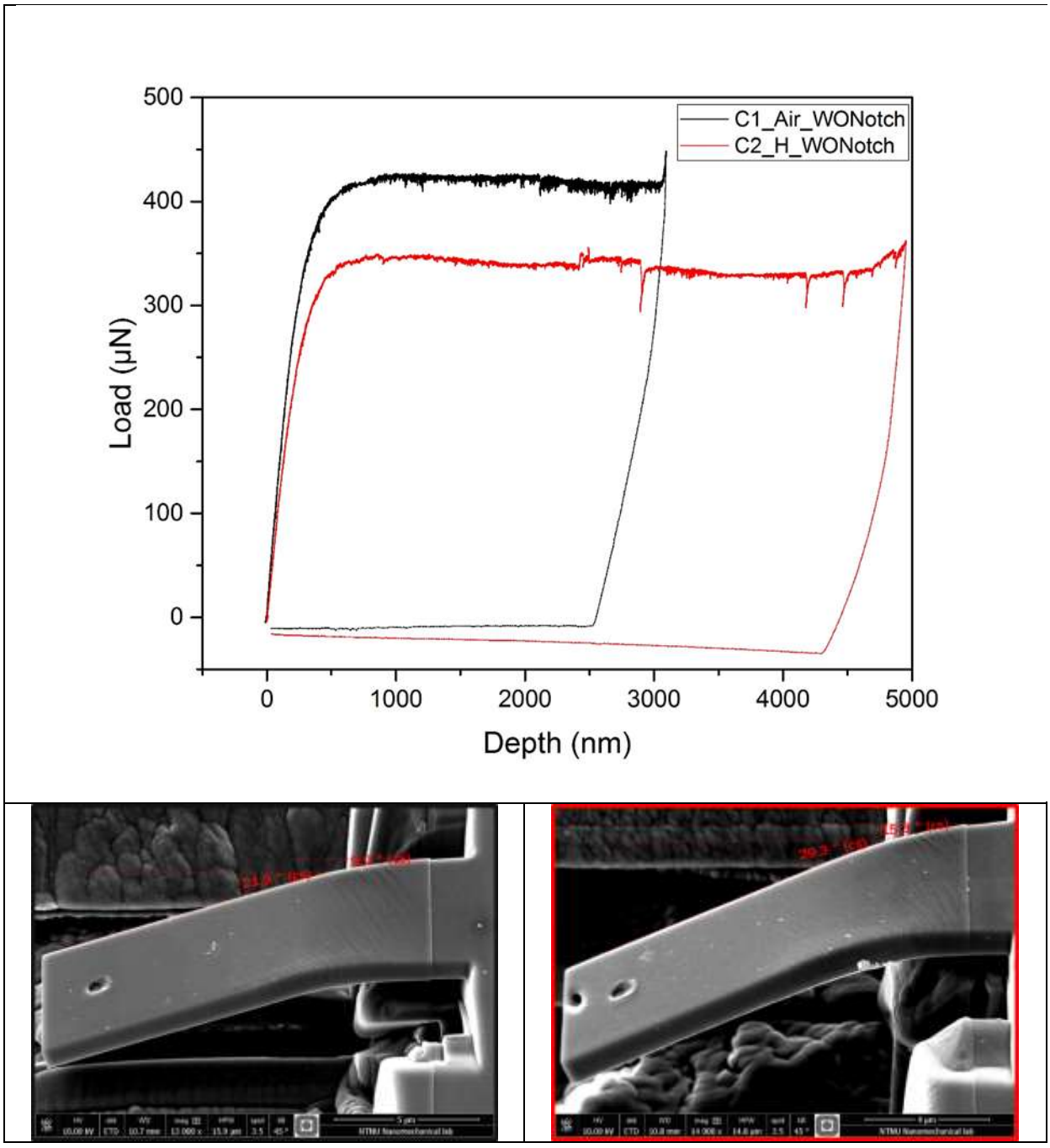

In Table 7 are the results of the cyclic loading of two cantilevers from sample 2 (see appendix D). The introduction of hydrogen to the FeSi-alloy significantly lowered the needed stress to bend the

cantilever to a depth of 5 μm. This is consistent with the theory, where an concentration of hydrogen on the grain boundary causes increased dislocation motion. From the experiment, a stress reduction of 80 μN was shown in the hydrogen charged sample.

The stress propagation during the loading of cantilever 2 (hydrogen induced) can be seen in Figure 18. As can be seen, the stress originates in the grain boundary as expected and a further stress is seen spreading towards the end of the cantilever as it is deformed. This could be a sign of the hydrogen thinning effect. A slight torsion effect is also noticed however, which might have impacted the resulting load curve. The torsion does not come from difference in notch depth, as the cantilevers did not have a notch milled on their grain boundaries. It might stem from a slight misplacement of the needle in the triboindenter during bending, a non-centric placement of the hole on the cantilever, the «hole» defect at the edge of the cantilever, a slip effect during the bending, or a non-uniform weight distribution of the cantilever.

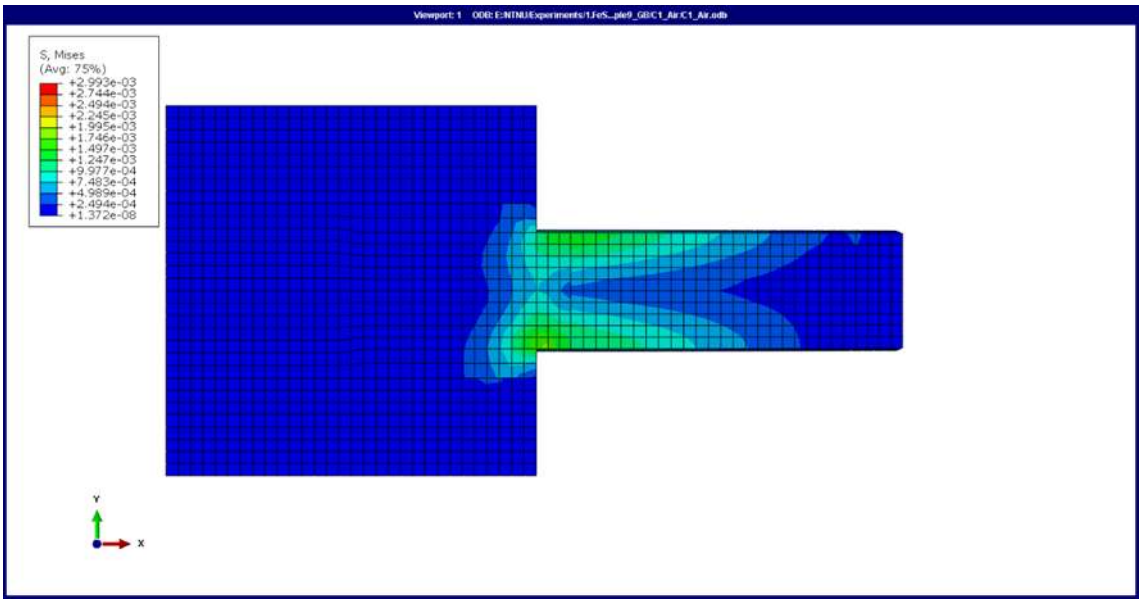

Figure 18 – Stress distribution in cantilever 1 in Table 7

4. Conclusions

A large number of cantilevers has been produced during the completion of this thesis. The cantilevers were made to be tested through cyclic loading in a triboindenter to determine the hydrogen effect on the grain boundary of FeSi-alloys. Tests were done in air and acidic solution. The focus of this report has been on the production of the cantilevers. In the first part of the experimental section, the obtained procedure for cantilever fabrication is presented.

Throughout the fabrication process, a multitude of problems presented themselves and needed to be overcome. This report has presented a milling process which will produce cantilevers of good quality for bend tests.

The problems of redeposition were controlled by gradually decreasing the amount of material milled, changing the incident beam angle, and repeating certain steps in the milling process.

An increase in current gave the needed fabrication speed to produce cantilever at a satisfactory pace. Through experimentation it was found that 9,3 nA and 2,8 nA could be used for the rough millings, while 0,92 nA gave sufficient precision for the fine milling.

Through cyclic loading in a triboindenter, it was found that the introduction of hydrogen to the grain boundary lowered the required force needed to bend the cantilever to a distance of 5 μm, by 80 μN.

5. Further work

Further work will be necessary to fully prove the validity of the results herein.

The fabrication procedure of cantilevers can be further improved to produce cantilevers of better quality, minimizing FIB damage and the effects of redeposition further, and in a swifter fashion.

To fully understand the impact of hydrogen concentrations on the grain boundaries of metals, further testing of different materials and geometries will be required.

Reproduction of the experiments contained in this report will also aid in the understanding of hydrogen embrittlement and help ascertain the numeric differences between hydrogen induced fracture and fracture hydrogen free environments obtained.

I hope that with this report, the fabrication process of the cantilevers will be swift and simple, so the focus can be directed towards the bending of the cantilevers and the analyzation of the obtained results.

.

6. References

[1] Volkert, C.A. et al, Focused Ion Beam Microscopy and Micromaching, MRS Bulletin Vol 32 May 2007 (2007)

[2] Giannuzzi L.A., and Stevie F.A., Introduction to Focused Ion Beams, Springer (2015)

[3]Yao Nan, Focused Ion Beam Systems, Cambridge University Press, (2007)

[4] R. G. Forbes, Understanding how the liquid-metal ion source works, Vacuum Vol 48 no. 1 (1997)

[5] Ian M. Robertson et al, HydrogenEmbrittlement Understood, Edward Demille Campbell Memorial Lecture, Asm International (2014)

Appendix A – Risk Assessment of experimental work

NTNU HMS	Kartlegging av risikofylt aktivitet	Utarbeidet av	Nummer	Dato
		HMS-avd.	HMSRV2601	22.03.2011
		Godkjent av		Erstatter
		Rektor		01.12.2006

Enhet: Institutt for Produktutvikling og Materialer (IPM) **Dato:** 19.01.2016

Linjeleder: Hege Ertzaas Fossland

Deltakere ved kartleggingen (m/ funksjon): Roar Andre Fagerkind (student)
(Ansv. veileder, student, evt. medveiledere, evt. andre m. kompetanse)

Kort beskrivelse av hovedaktivitet/hovedprosess: Milling of micro-sized cantilevers with a FIB microscope at the NTNU nanolab

Er oppgaven rent teoretisk? (JA/NEI): NEI *«JA» betyr at veileder innestår for at oppgaven ikke inneholder noen aktiviteter som krever risikovurdering. Dersom «JA»: Beskriv kort aktiviteteten i kartleggingskjemaet under. Risikovurdering trenger ikke å fylles ut*

Signaturer: *Ansvarlig veileder:* *Student:* Roar Andre Fagerkind

ID nr.	Aktivitet/prosess	Ansvarlig	Eksisterende dokumentasjon	Eksisterende sikringstiltak	Lov, forskrift o.l.	Kommentar
00	Working in cleanroom	Roar A. Fagerkind	Course, Trygg håndtering av nanomaterialer (Arbeidstilsynet)	Alarms and evacuation procedures for dangerous levels of toxic gases or similar hazards. Need training and courses to enter lab and chemical areas. Buddy rule. Recordings of exposure to nanoparticles.	Arbeidsmiljøloven, §3-1, §4-1, §4-5, §5-4. Internkontrollforskriften, §5. Arbeidsmiljøforskriftene, §1-4, §3-1, §2-1. CLP og merkeforskriften. REACH. Forskrift om gjenvinning og behandling av avfall kap. 11 – farlig avfall	
01	Milling of bicrystal cantilevers in specimens using Focused Ion Beam (FIB)	Roar A. Fagerkind	Course, manual (on site), risk assessment (on site), protocol for general usage (on site)	Follow protocol for usage printed on A4-paper on site, users are not allowed to remove covers from the instrument or parts of it,	Law regarding service at and work with electrical constructions and equipment, law regarding ionizing radiation (strålevernloven)	

				maintenance and repair is done by trained engineers only, the instrument will be disconnected from power and the person who will do the work have to wait some minutes prior work that requires the removal of covers, users do not have access to light source, chamber door only allowed to be opened for brief moments for exchange of sample, warning labels for hazardous parts of the equipment		

NTNU HMS	Risikovurdering	Utarbeidet av	Nummer	Dato
		HMS-avd.	HMSRV2601	22.03.2011
		Godkjent av		Erstatter
		Rektor		01.12.2006

Enhet: Institutt for Produktutvikling og Materialer (IPM) **Dato:** 19.01.2016

Linjeleder: Hege Ertzaas Fossland

Deltakere ved kartleggingen (m/ funksjon): Roar Andre Fagerkind (student)
(Ansv. Veileder, student, evt. medveiledere, evt. andre m. kompetanse)

Risikovurderingen gjelder hovedaktivitet: A03-01, 755896, Advanced nano-scale characterization of hydrogen embrittlement.

Signaturer: *Ansvarlig veileder:* *Student:* Roar André Fagerkind

ID nr	Aktivitet fra kartleggings-skjemaet	Mulig uønsket hendelse/ belastning	Vurdering av sannsyn-lighet	Vurdering av konsekvens:				Risiko-Verdi (menn-eske)	Kommentarer/status Forslag til tiltak
			(1-5)	Menneske (A-E)	Ytre miljø (A-E)	Øk/ materiell (A-E)	Om-dømme (A-E)		
00	Working in cleanroom	Discharge/spill of toxic chemicals (HF, PDMS or other toxic substances)	2	C	A	B	B	C2	Chemical spill is mainly a concern for those working in the chemical areas, as the evacuation alarm will initiate as soon as dangerous levels of a gas is detected in the area
00	Working in cleanroom	Spread of nanoparticles	2	B	A	B	B	B2	The effect of nanoparticles on humans is still not fully understood. Can cause inflamation or sickness
01	Milling of bicrystalline cantilevers in specimens using Focused Ion Beam (FIB)	Potential dangerous voltages	1	E	--	--	C	E1	Potentially dangerous electrical currents might be present while power is connected to it. Capacitators might keep high voltage for some minutes after the power is unplugged
01	Milling of bicrystalline cantilevers in specimens using	UV/IR and X-ray hazard	1	A	--	--	B	A1	An optical light source for illuminating the process is contained in the chamber. This

	Focused Ion Beam (FIB)								light source is a UV/IR hazard. The X-ray limit is 1 μS/h at 10 cm distance from the surface
01	Milling of bicrystalline cantilevers in specimens using Focused Ion Beam (FIB)	Failure of cardiac pacemaker	1	E	–	–	B	E1	System uses strong magnets on the ion column. A hazard exists when using magnetizable prosthesis and other metal objects within 5cm of the cold cathode (Penning) gauge. The effect is caused by a permanent magnet, so it affects even if the equipment is not powered. There is however no need for users to go near the ion pump.

Sannsynlighet vurderes etter følgende kriterier:

NTNU HMS	Risikovurdering	Utarbeidet av	Nummer	Dato
		HMS-avd.	HMSRV2601	22.03.2011
		Godkjent av		Erstatter
		Rektor		01.12.2006

Svært liten 1	Liten 2	Middels 3	Stor 4	Svært stor 5
1 gang pr 50 år eller sjeldnere	1 gang pr 10 år eller sjeldnere	1 gang pr år eller sjeldnere	1 gang pr måned eller sjeldnere	Skjer ukentlig

Konsekvens vurderes etter følgende kriterier:

Gradering	Menneske	Ytre miljø Vann, jord og luft	Øk/materiell	Omdømme
E Svært Alvorlig	Død	Svært langvarig og ikke reversibel skade	Drifts- eller aktivitetsstans >1 år.	Troverdighet og respekt betydelig og varig svekket
D Alvorlig	Alvorlig personskade. Mulig uførhet.	Langvarig skade. Lang restitusjonstid	Driftsstans > ½ år Aktivitetsstans i opp til 1 år	Troverdighet og respekt betydelig svekket
C Moderat	Alvorlig personskade.	Mindre skade og lang restitusjonstid	Drifts- eller aktivitetsstans < 1 mnd	Troverdighet og respekt svekket
B Liten	Skade som krever medisinsk behandling	Mindre skade og kort restitusjonstid	Drifts- eller aktivitetsstans < 1uke	Negativ påvirkning på troverdighet og respekt
A Svært liten	Skade som krever førstehjelp	Ubetydelig skade og kort restitusjonstid	Drifts- eller aktivitetsstans < 1dag	Liten påvirkning på troverdighet og respekt

Risikoverdi = Sannsynlighet x Konsekvens
Beregn risikoverdi for Menneske. Enheten vurderer selv om de i tillegg vil beregne risikoverdi for Ytre miljø, Økonomi/materiell og Omdømme. I så fall beregnes disse hver for seg.

Til kolonnen "Kommentarer/status, forslag til forebyggende og korrigerende tiltak":
Tiltak kan påvirke både sannsynlighet og konsekvens. Prioriter tiltak som kan forhindre at hendelsen inntreffer, dvs. sannsynlighetsreduserende tiltak foran skjerpet beredskap, dvs. konsekvensreduserende tiltak.

NTNU	Risikomatrise	utarbeidet av	Nummer	Dato
		HMS-avd.	HMSRV2604	08.03.2010
		godkjent av		Erstatter
HMS/KS		Rektor		09.02.2010

MATRISE FOR RISIKOVURDERINGER ved NTNU

KONSEKVENS						
	Svært alvorlig	E1	E2	E3	E4	E5
	Alvorlig	D1	D2	D3	D4	D5
	Moderat	C1	C2	C3	C4	C5
	Liten	B1	B2	B3	B4	B5
	Svært liten	A1	A2	A3	A4	A5
		Svært liten	Liten	Middels	Stor	Svært stor
		SANNSYNLIGHET				

Prinsipp over akseptkriterium. Forklaring av fargene som er brukt i risikomatrisen.

Farge	Beskrivelse
Rød	Uakseptabel risiko. Tiltak skal gjennomføres for å redusere risikoen.
Gul	Vurderingsområde. Tiltak skal vurderes.
Grønn	Akseptabel risiko. Tiltak kan vurderes ut fra andre hensyn.

Appendix B –Required A3-poster describing the project

Masteroppgave ved

IPM

Våren 2016

Advanced small-scale characterization of hydrogen embrittlement

av

Roar André Fagerkind

Faglærer: Afrooz Barnoush

The work will mostly consist of the same elements as the project work. A large number of cantilevers with pentagonal cross-section will be milled with a FIB/SEM dual-beam microscope at the NTNU nanolab cleanroom. The focus will be on making good cantilevers by optimizing the milling parameters of the microscope. The cantilevers will then be fracture tested by bending in a tribo-indenter at the NTNU nanomechanical lab.

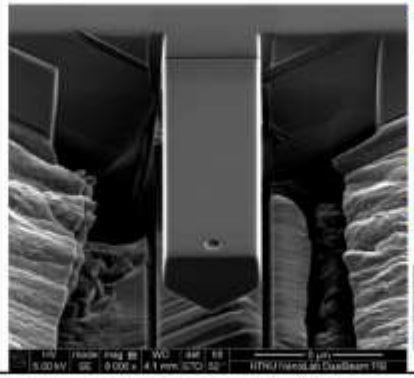

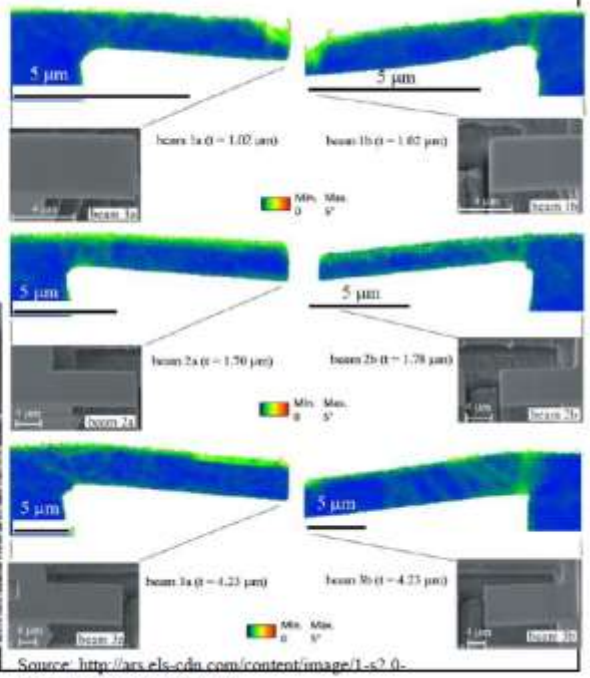

Source: http://ars.els-cdn.com/content/image/1-s2.0-S1359645409008106-gr3.jpg

Appendix C –Required A3-poster describing the achieved results

Masteroppgave ved

IPM

Våren 2016

Advanced small-scale characterization of hydrogen embrittlement

av

Roar André Fagerkind

Faglærer: Afrooz Barnoush

A large amount of micro-cantilevers were fabricated during the experimental period of the master thesis. The cantilevers were of variying dimensions and went through a multitude of changes in their cutting process. Bend tests of the cantilevers in air and acidic solution were conducted to determine the hydrogen effect on the grain boundaries of different FeSi-alloys. The tests were done by co-supervisor Tarlan Hajilou with master student Roar André Fagerkind present. The focus of the Master Thesis has been on the fabrication of the micro-cantilevers.

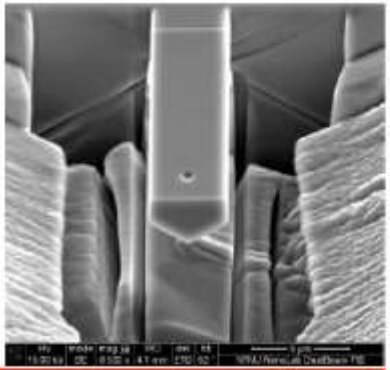

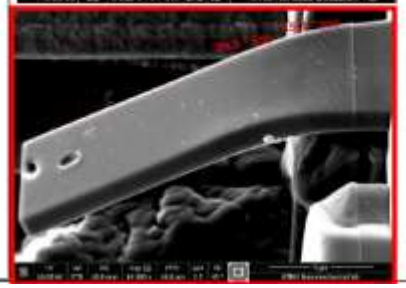

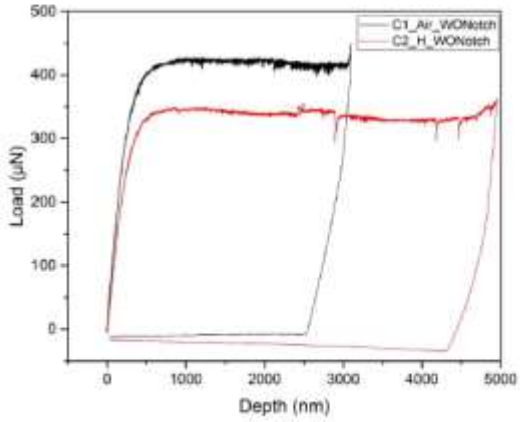

Appendix D – Cantilever images

Sample 1

Cantilever 1

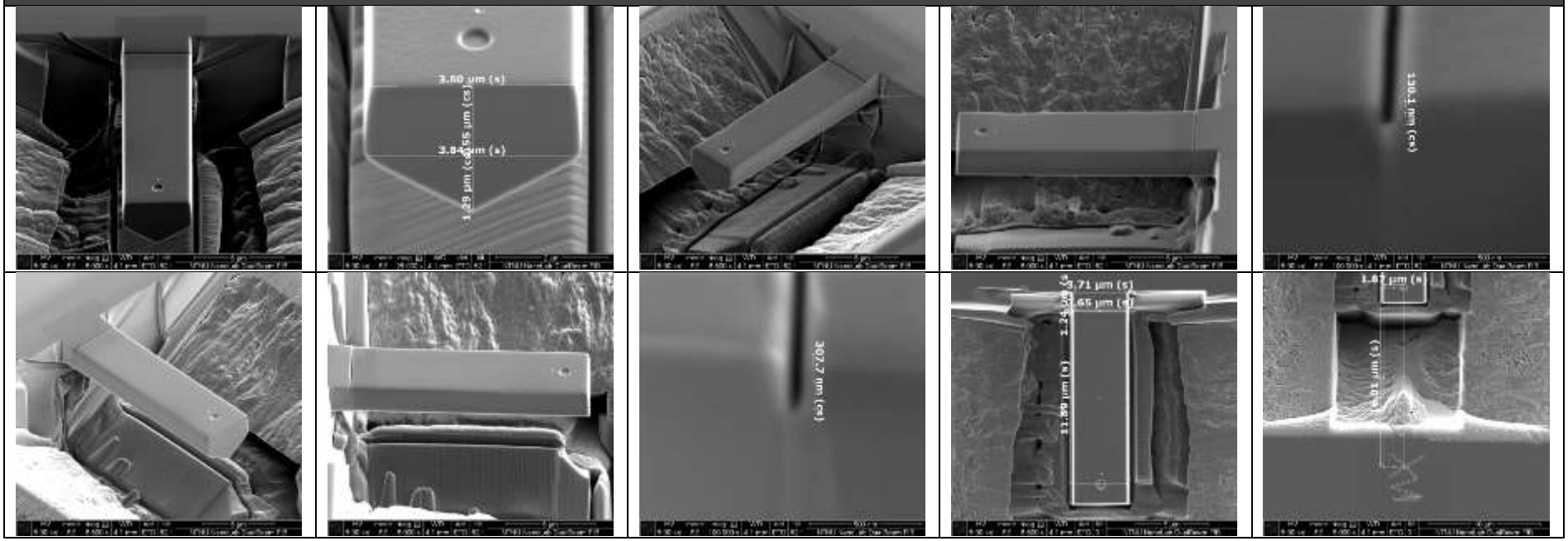

Cantilever 2

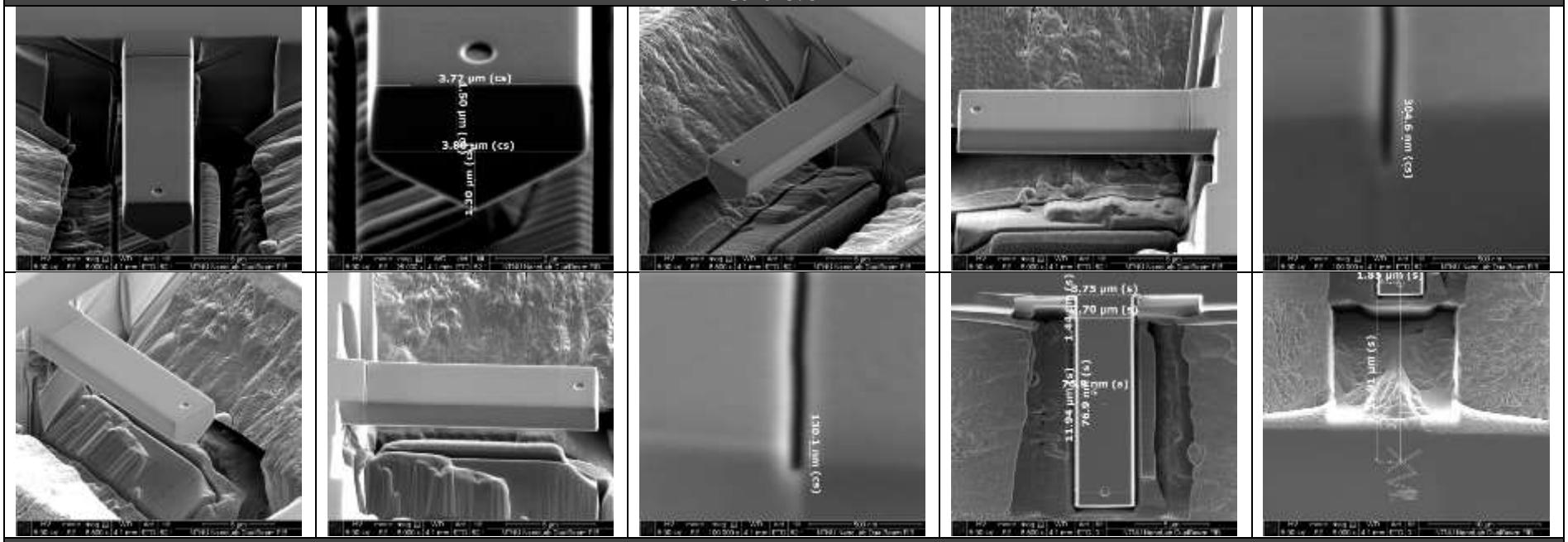

Cantilever 3

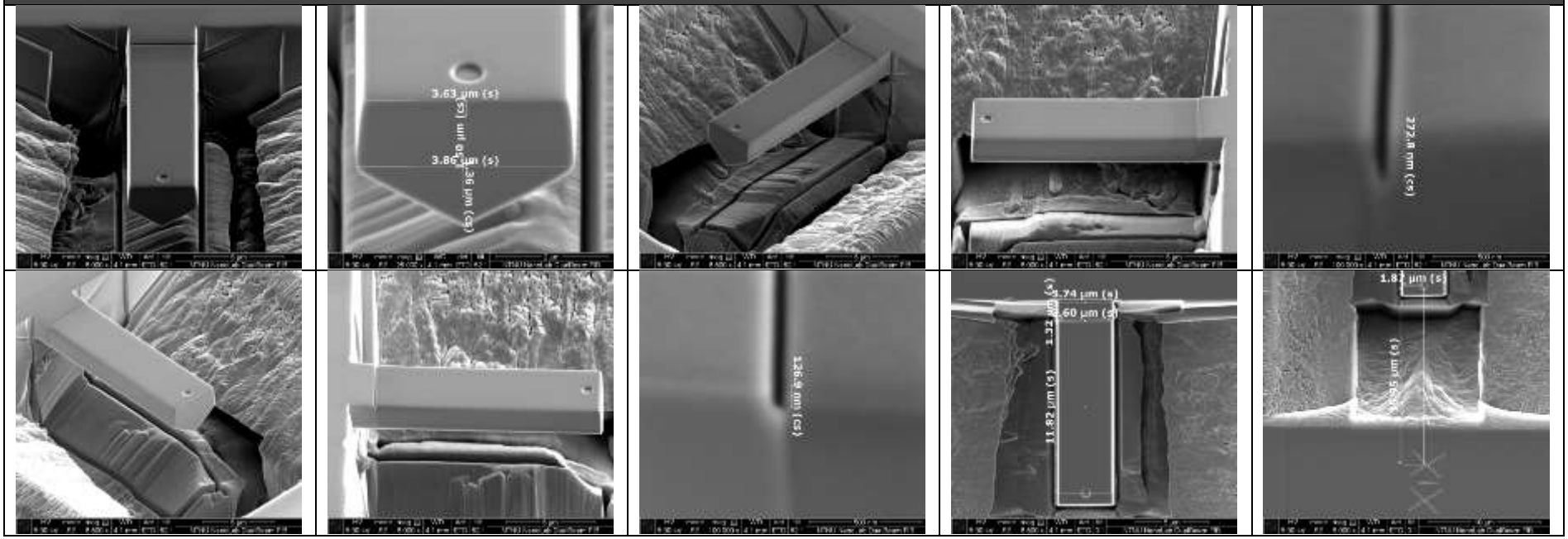

X

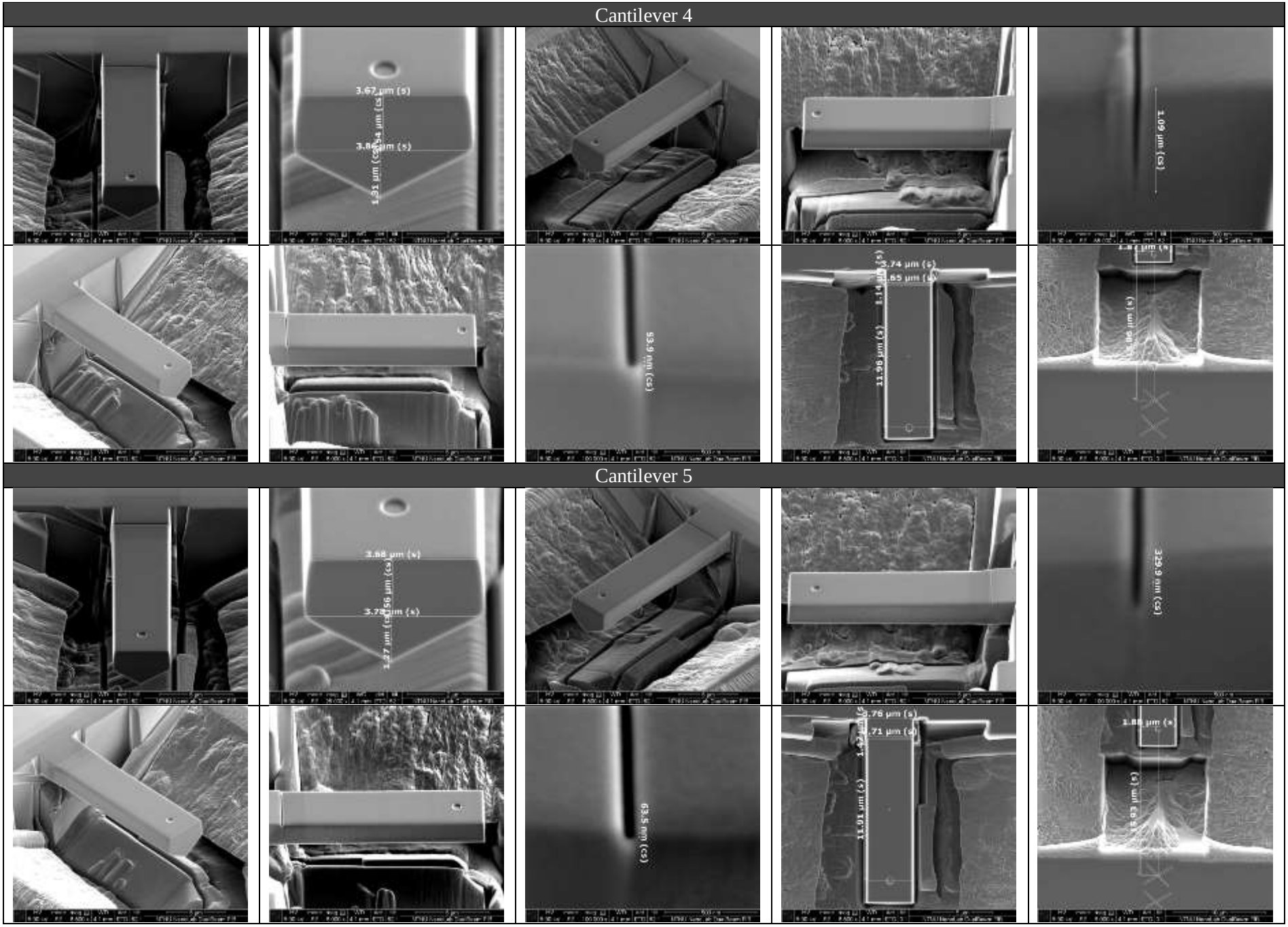
Cantilever 4
3.67 µm (s)
3.86 µm (s)
1.09 µm (cs)
3.74 µm (s)
3.65 µm (s)
11.96 µm (s)
1.14 µm (s)
93.9 nm (cs)
Cantilever 5
3.88 µm (s)
3.78 µm (s)
329.9 nm (cs)
3.76 µm (s)
3.71 µm (s)
11.91 µm (s)
1.88 µm (s)
63.5 nm (cs)

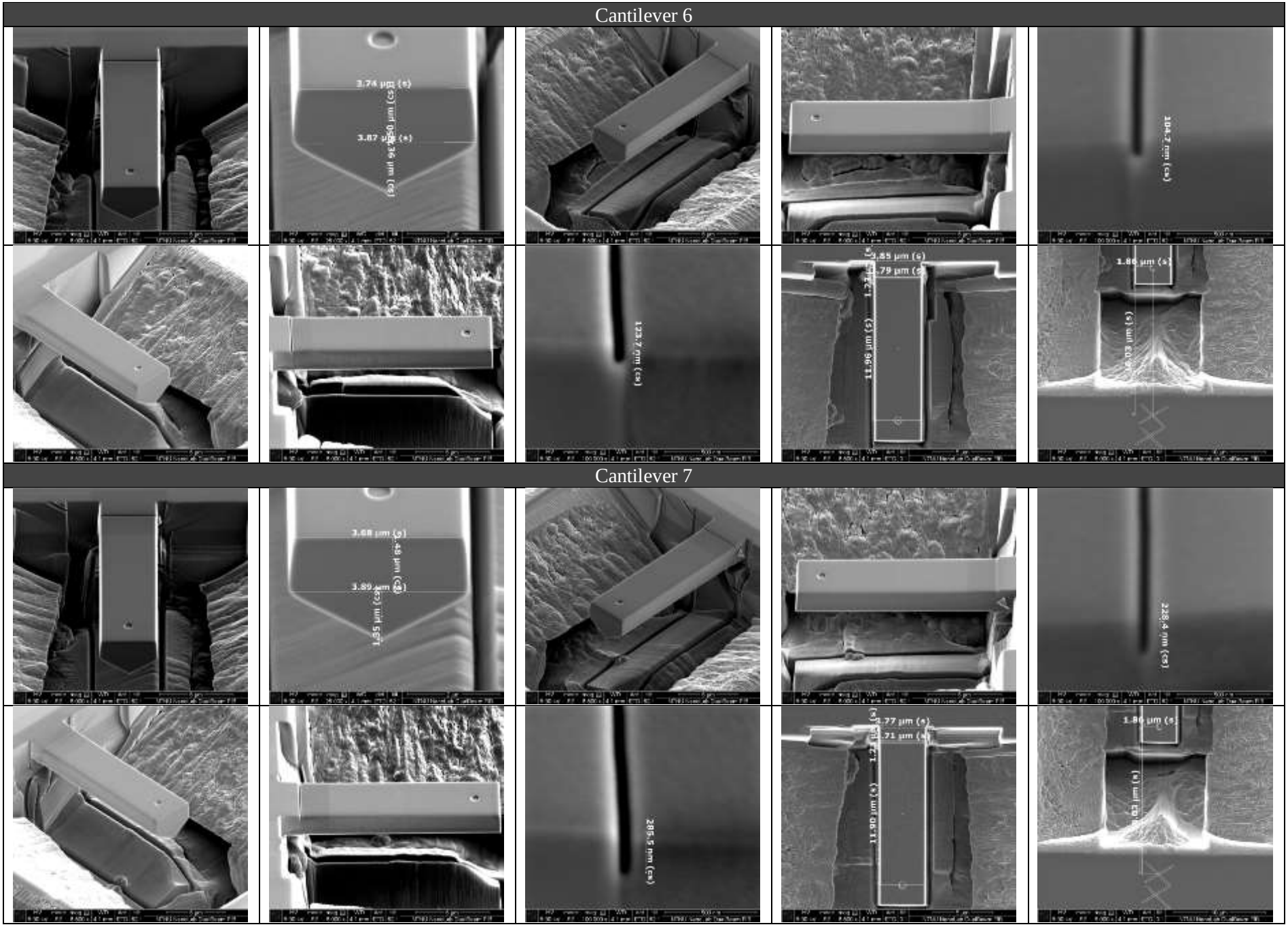
Cantilever 6
Cantilever 7

Cantilever 8				
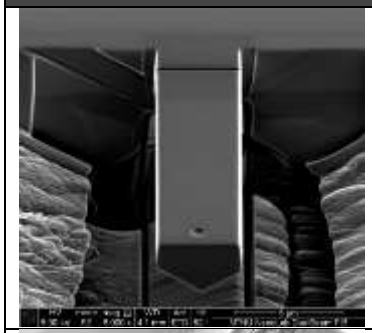	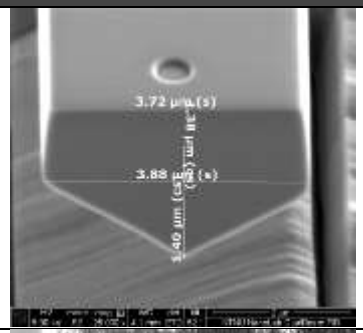	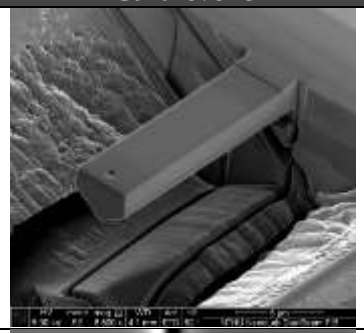	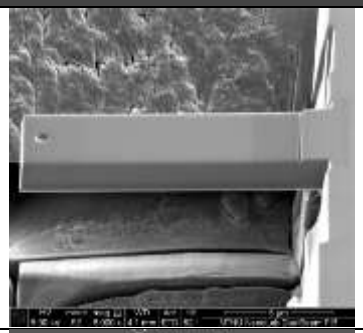	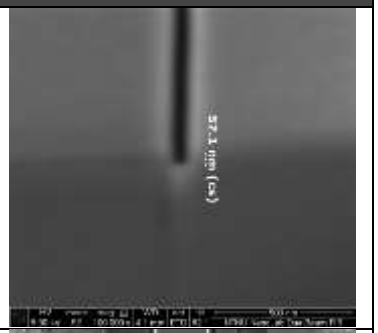
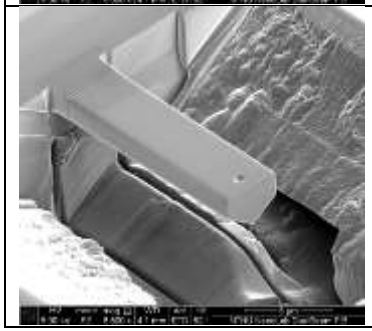	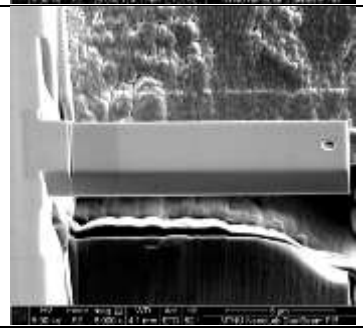	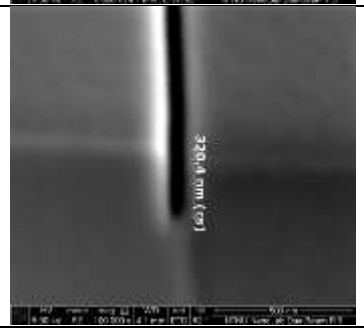	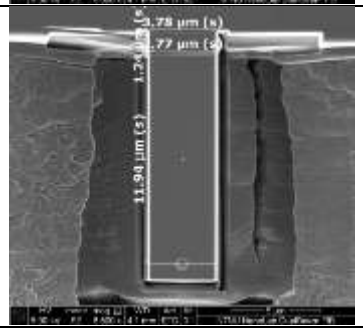	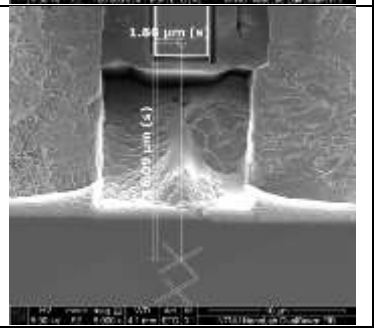

Sample 2

Cantilever 1			
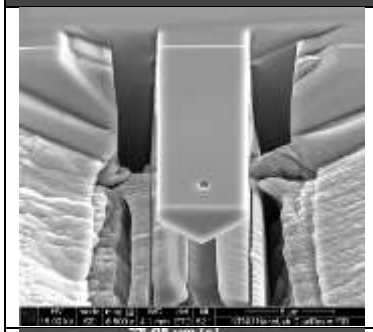	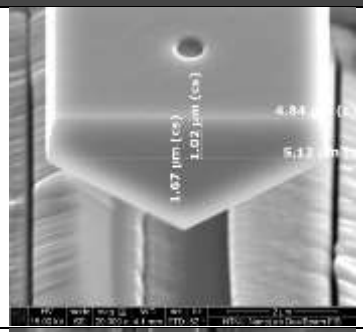	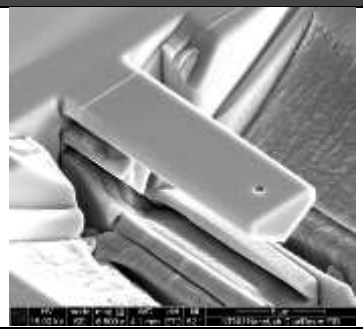	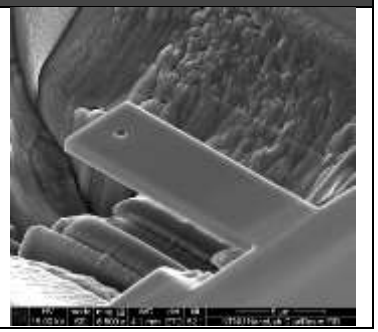
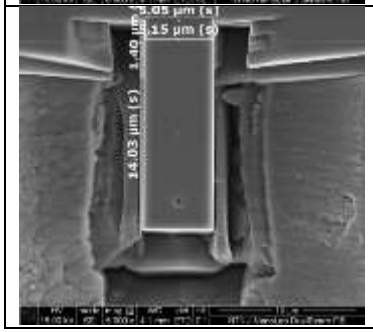			

Cantilever 2

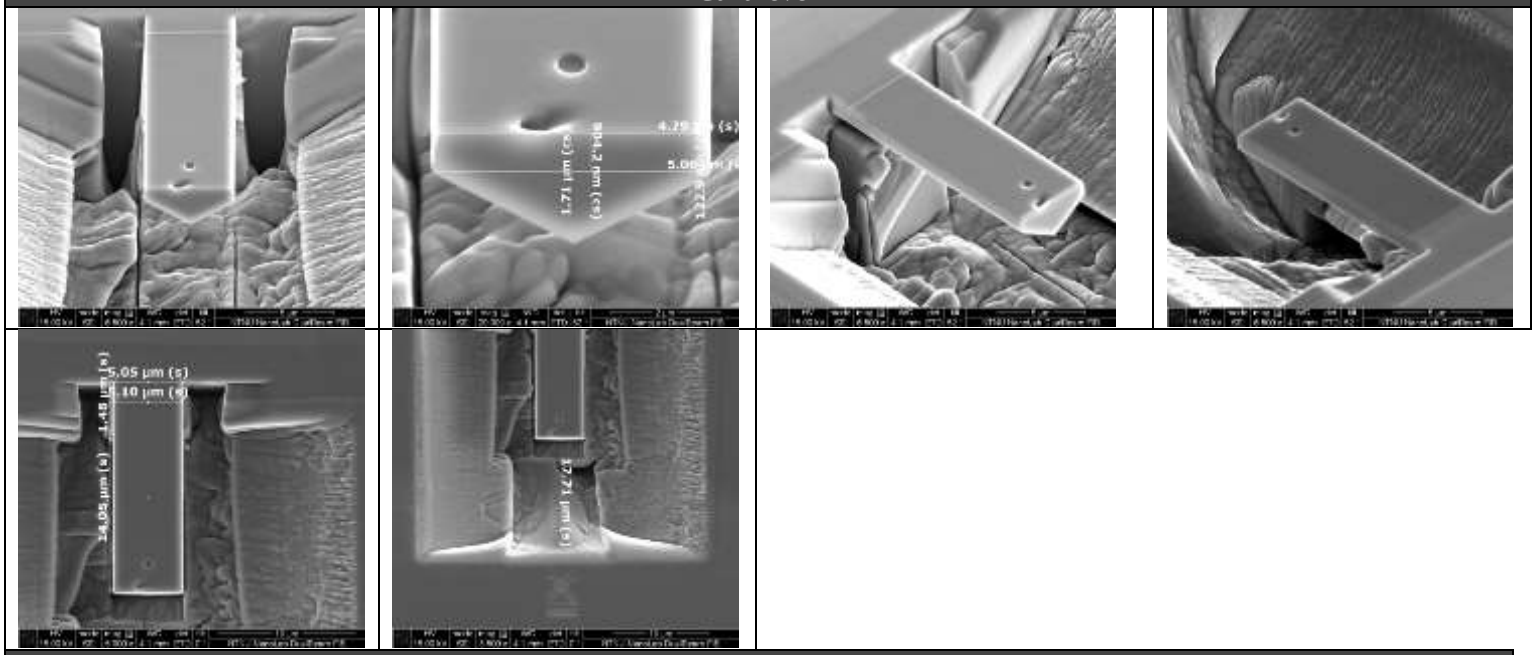

Cantilever 3

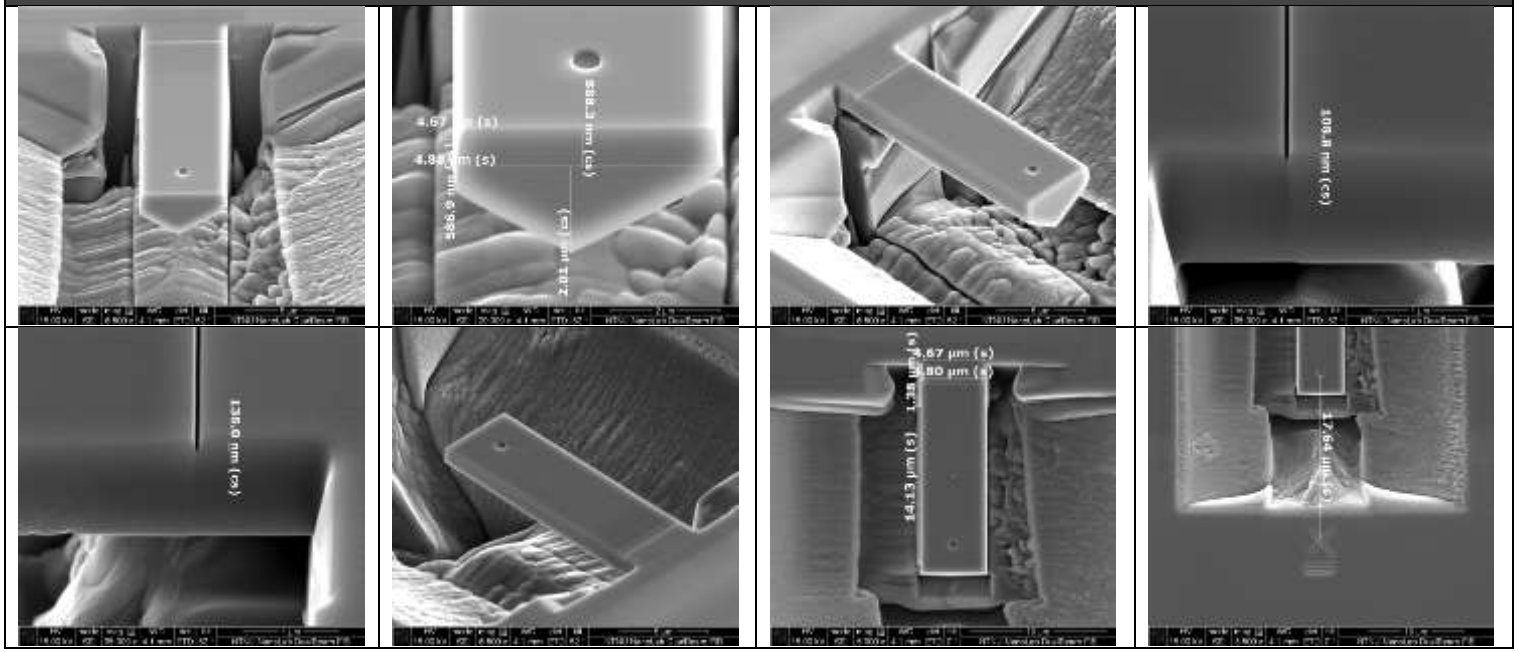

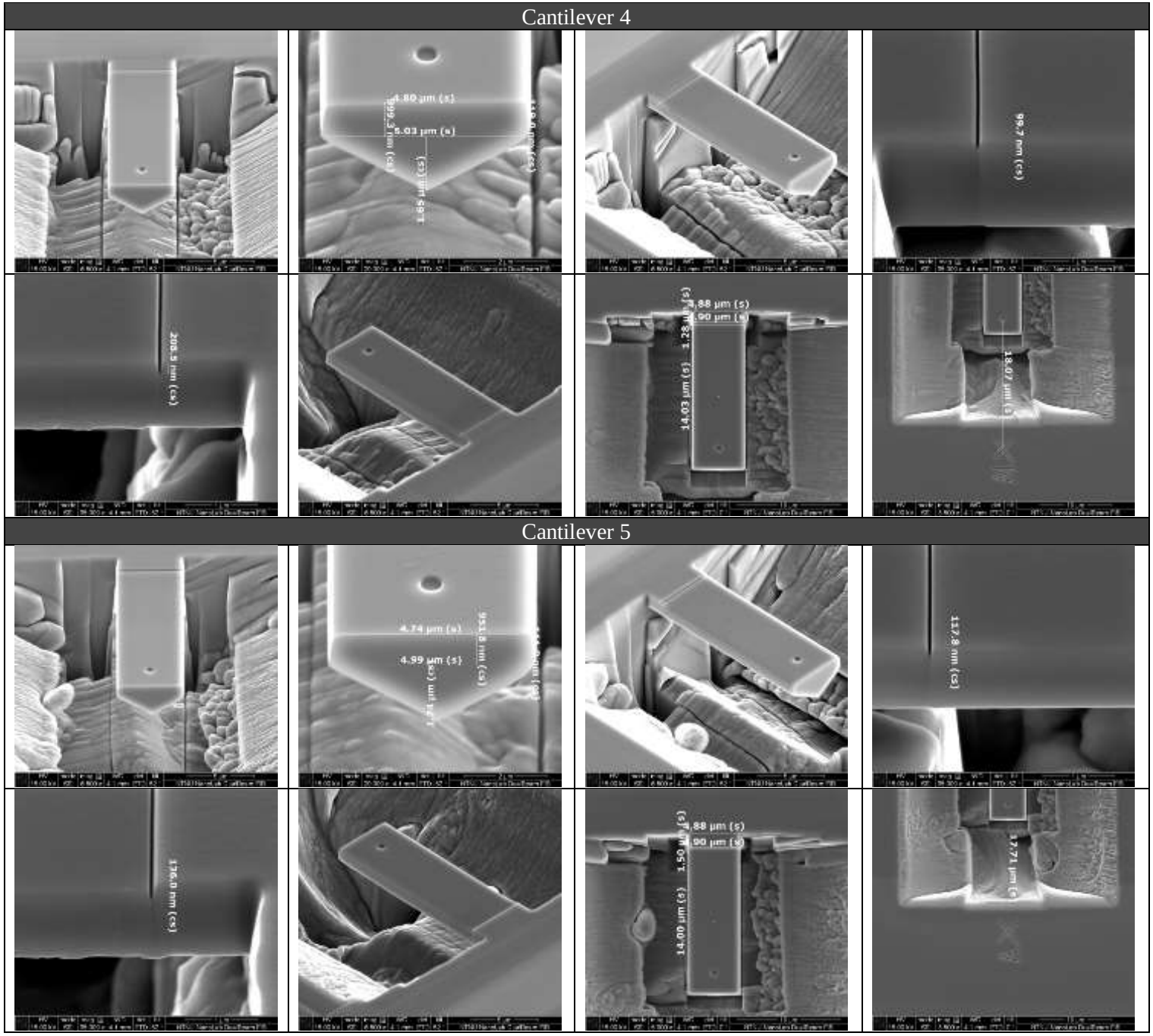
Cantilever 4
4.80 µm (s)
5.03 µm (s)
1.65 µm (cs)
99.7 nm (cs)
208.5 nm (cs)
3.88 µm (s)
3.90 µm (s)
3.28 µm (s)
14.03 µm (s)
18.07 µm (s)
Cantilever 5
4.74 µm (s)
4.99 µm (cs)
951.8 nm (cs)
117.8 nm (cs)
176.0 nm (cs)
3.88 µm (s)
3.90 µm (s)
1.50 µm (s)
14.00 µm (s)
17.71 µm (s)

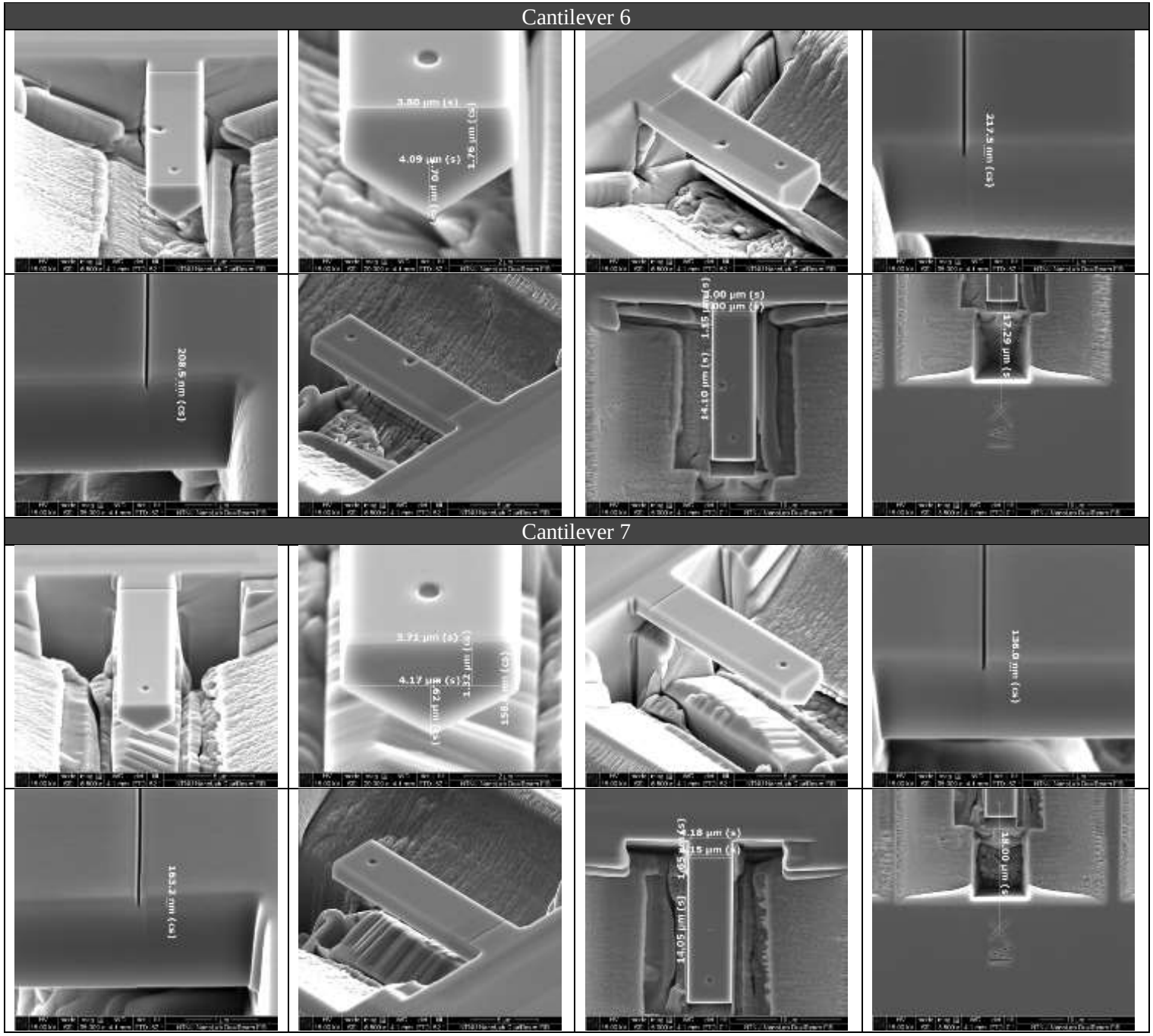
Cantilever 6
3.80 µm (s)
4.09 µm (s)
217.5 nm (cs)
208.5 nm (cs)
14.10 µm (s)
17.29 µm (s)
Cantilever 7
3.71 µm (s)
4.17 µm (s)
138.0 nm (cs)
183.2 nm (cs)
14.05 µm (s)
18.00 µm (s)

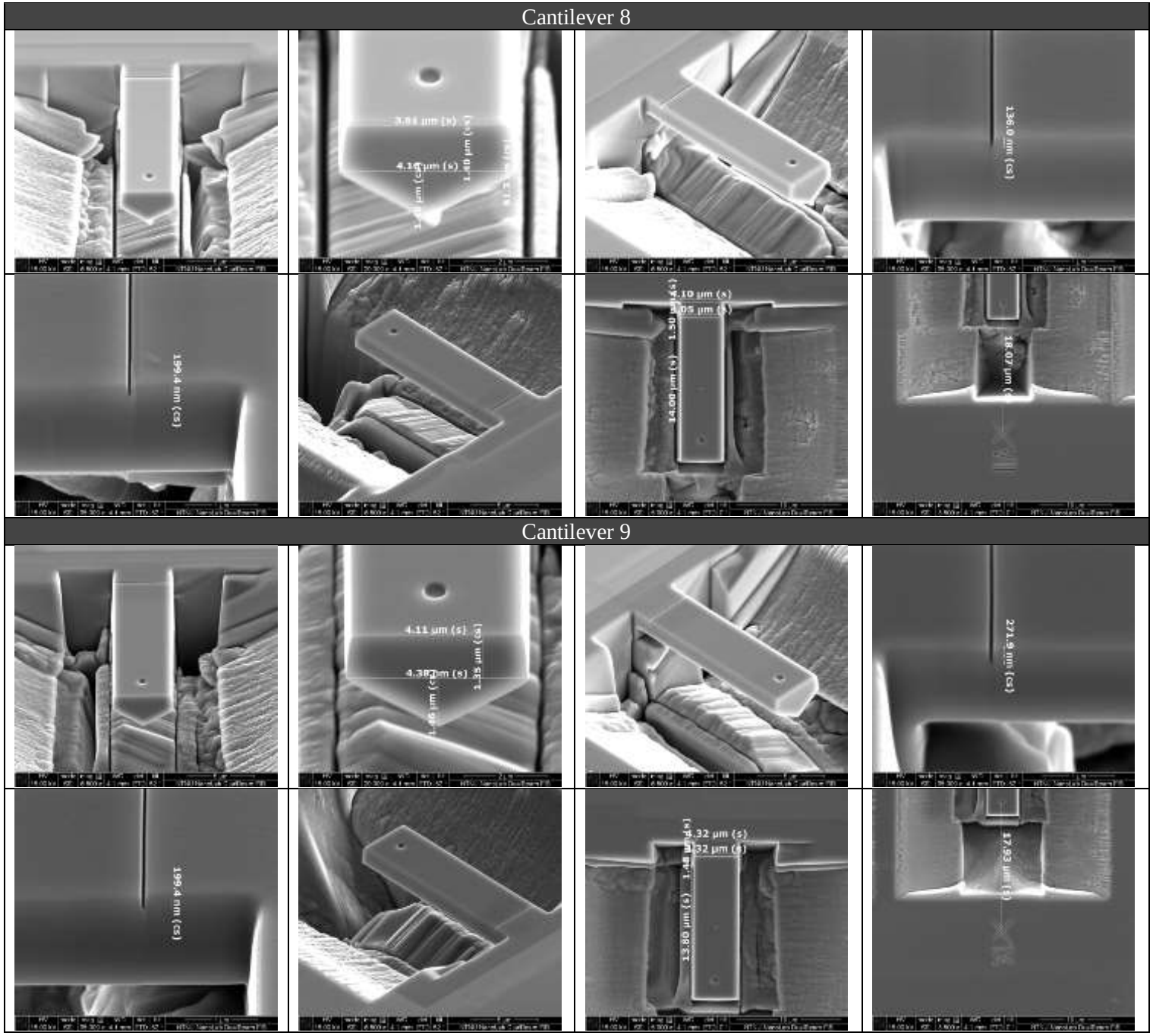
Cantilever 8
138.0 µm (cs)
4.10 µm (s)
5.05 µm (s)
14.00 µm (s)
1.30 µm (s)
18.07 µm (s)
199.4 µm (cs)
Cantilever 9
4.11 µm (s)
4.38 µm (s)
271.9 µm (cs)
4.32 µm (s)
4.32 µm (s)
13.90 µm (s)
17.93 µm (s)
199.4 µm (cs)

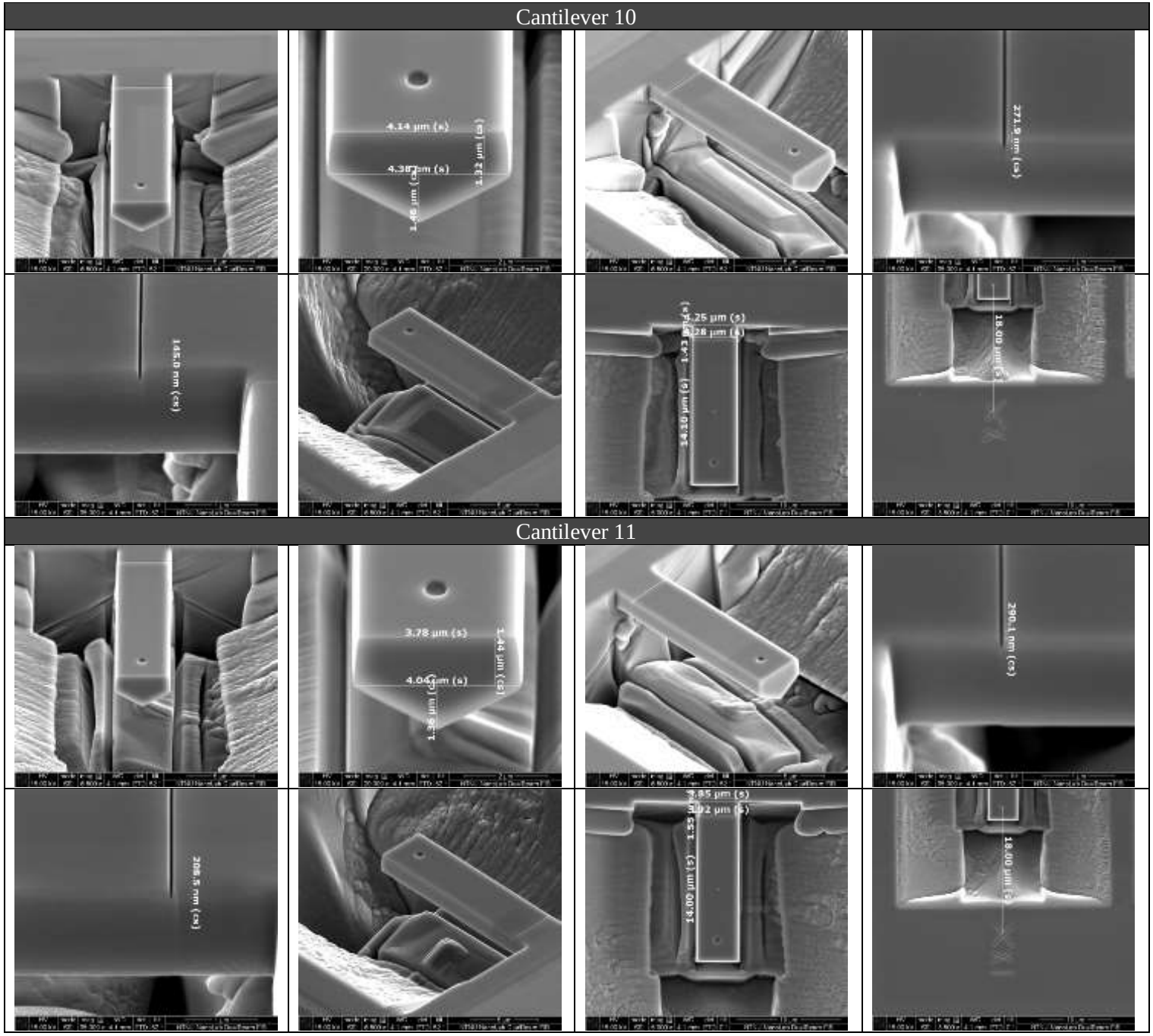
Cantilever 10
4.14 µm (s)
4.38 µm (s)
1.48 µm (s)
271.9 nm (cs)
145.0 nm (cs)
5.25 µm (s)
18.00 µm (s)
Cantilever 11
3.78 µm (s)
1.44 µm (cs)
4.04 µm (s)
290.1 nm (cs)
208.5 nm (cs)
18.00 µm (s)

Cantilever 12

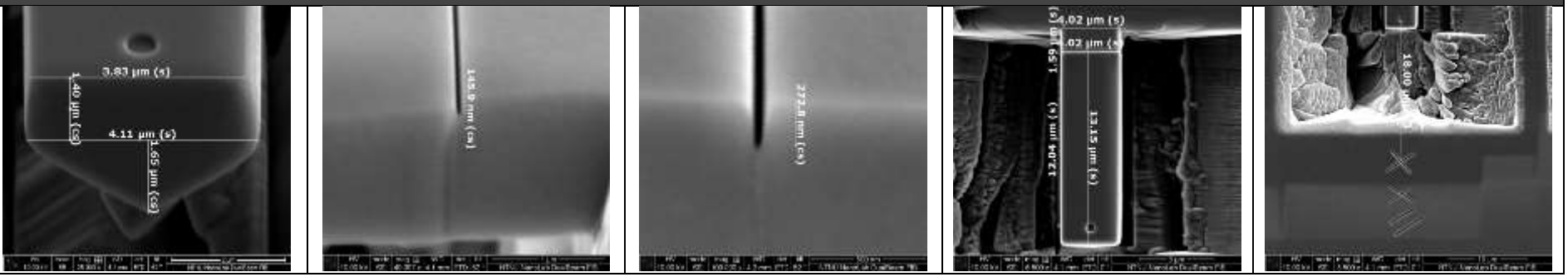

Cantilever 13

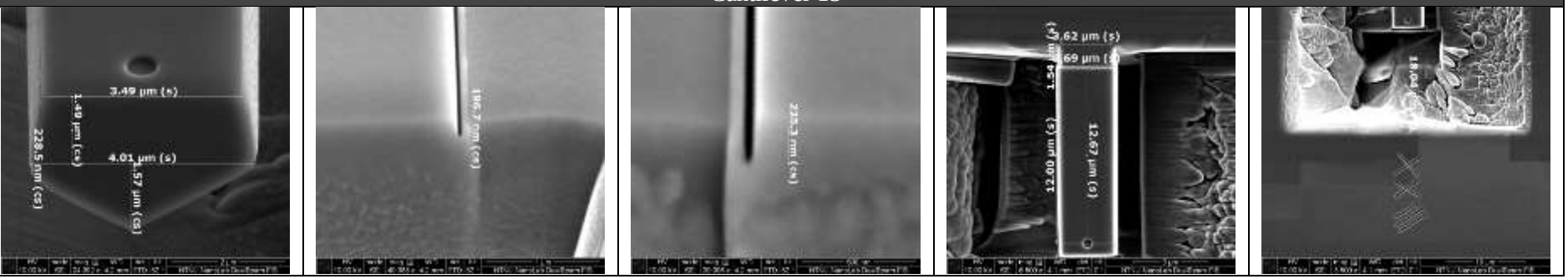

Sample 3

Cantilever 1			
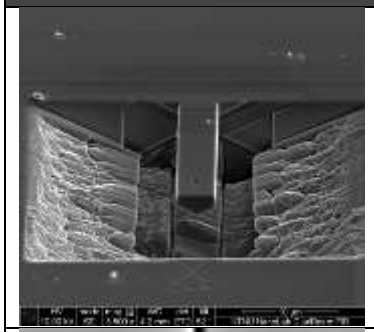	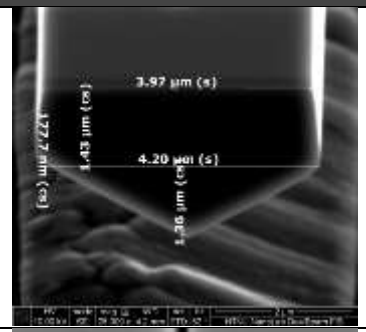	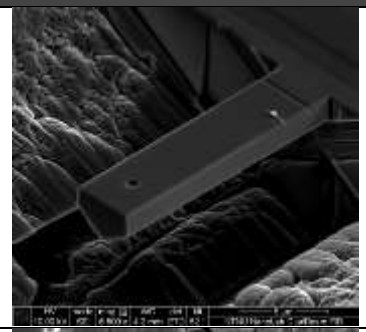	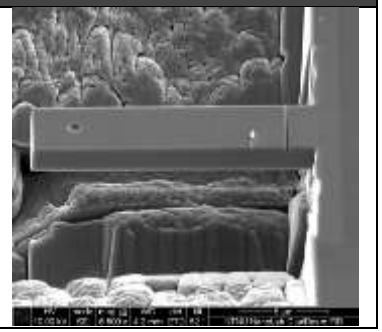
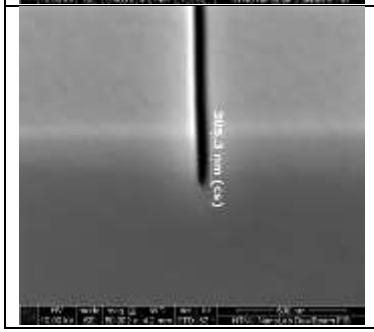	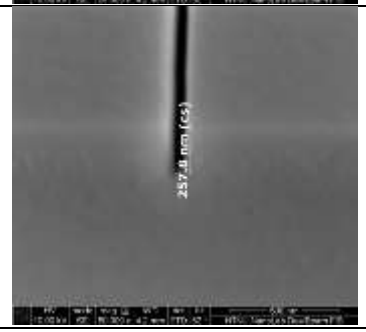	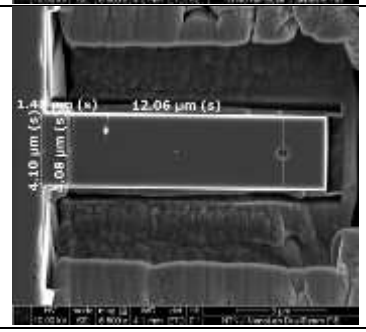	

Cantilever 2

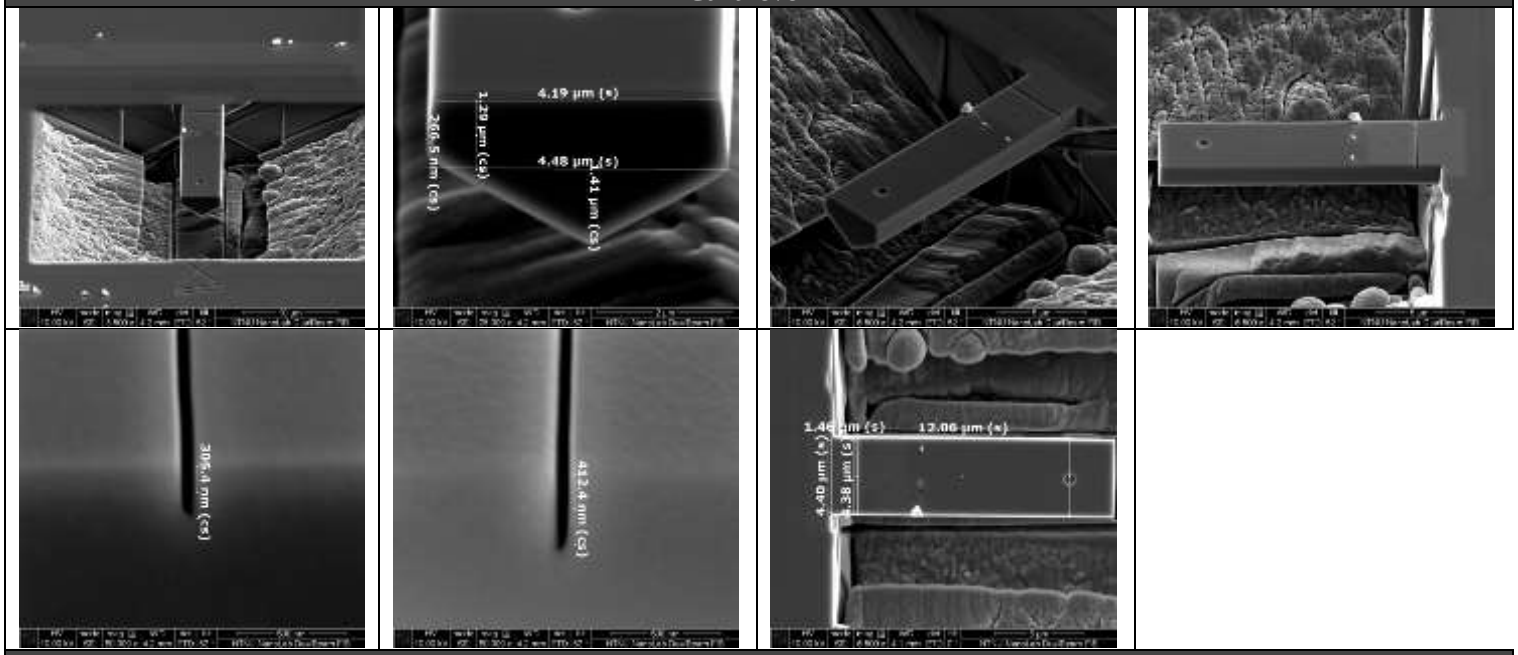

Cantilever 3

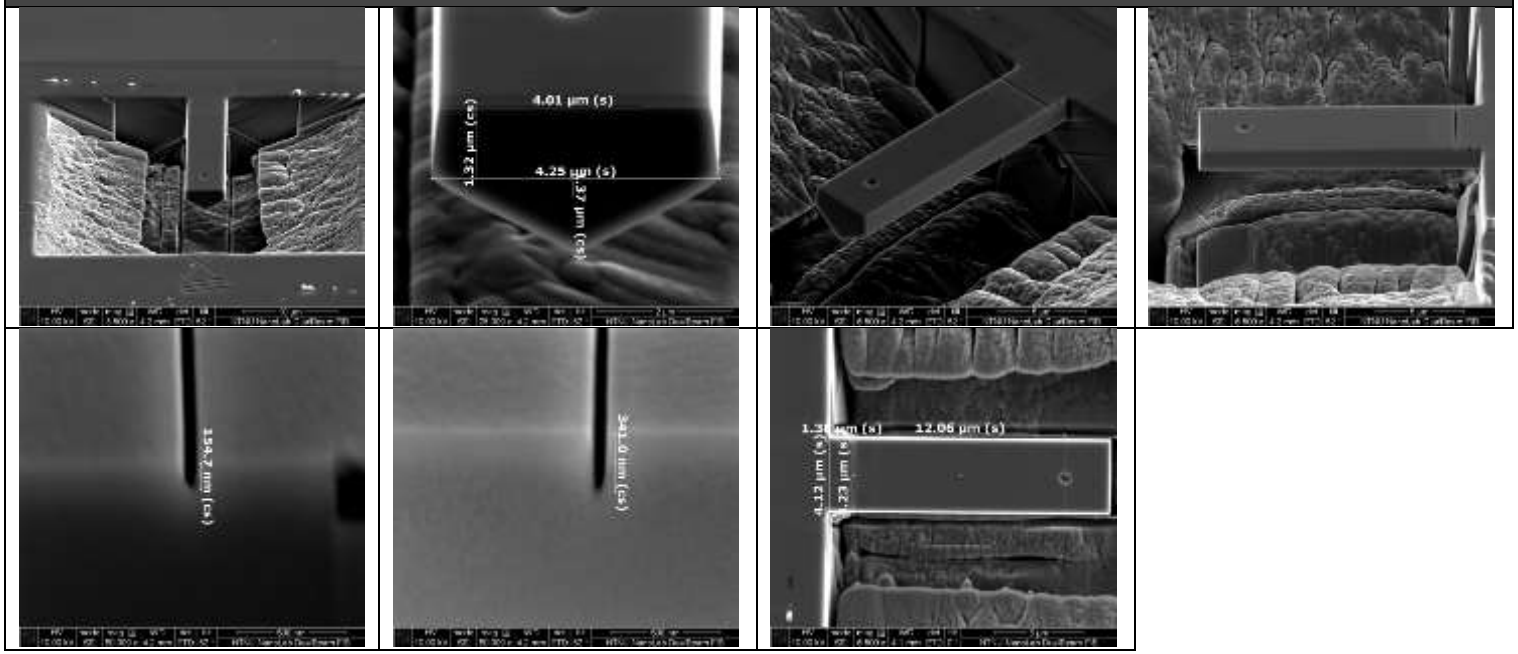

Cantilever 4

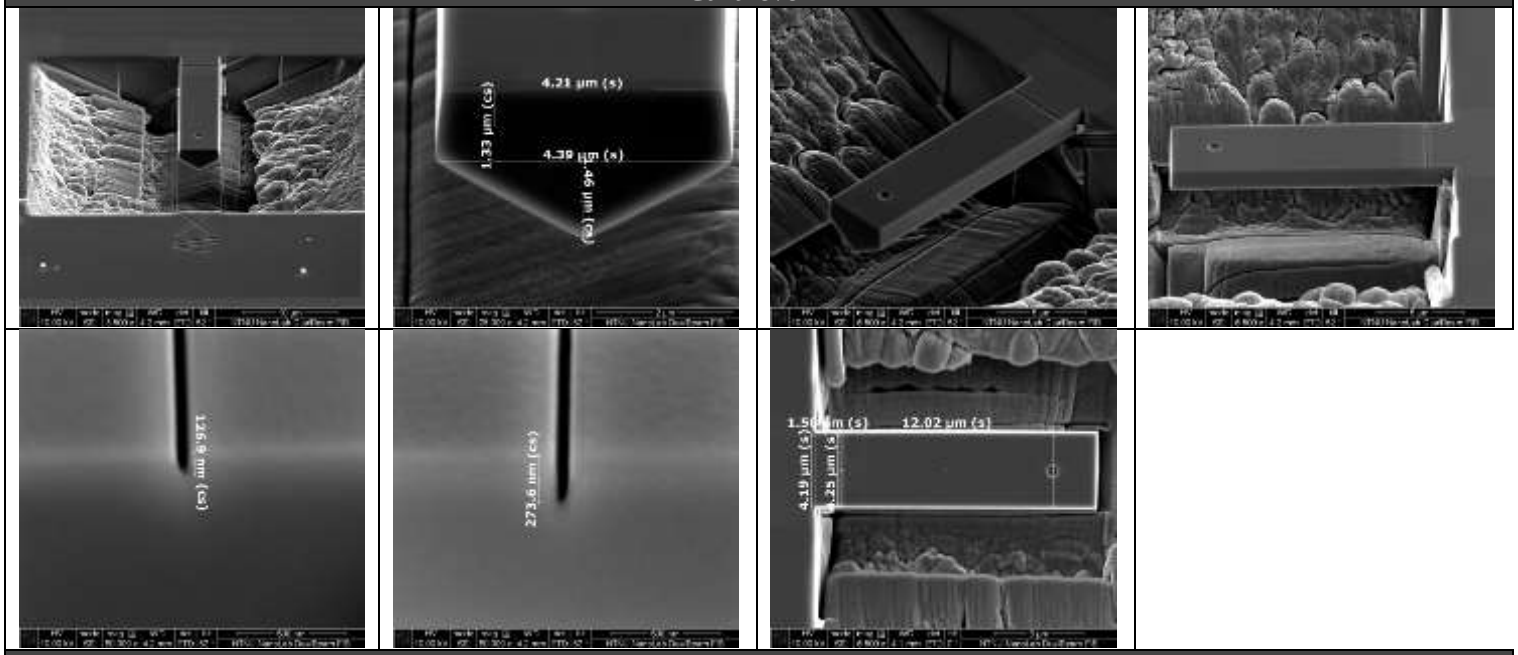

Cantilever 5

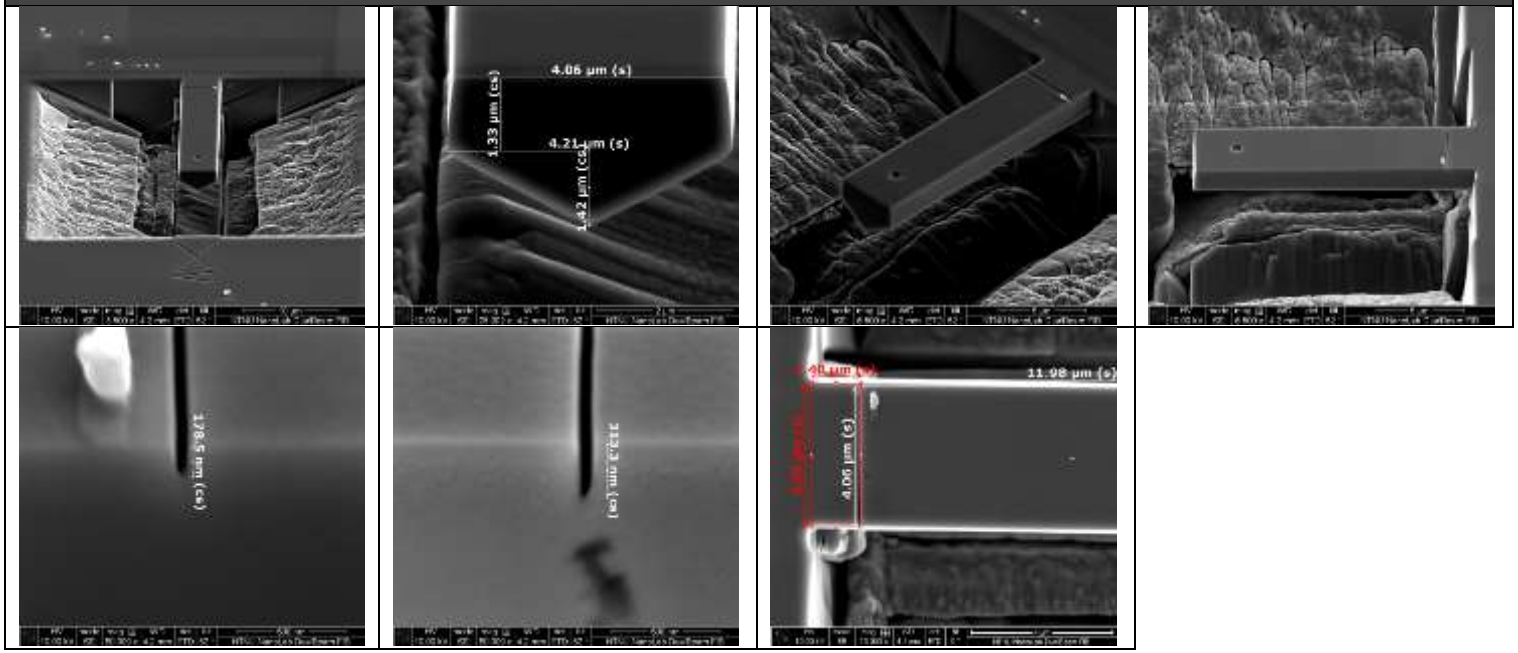

Cantilever 6

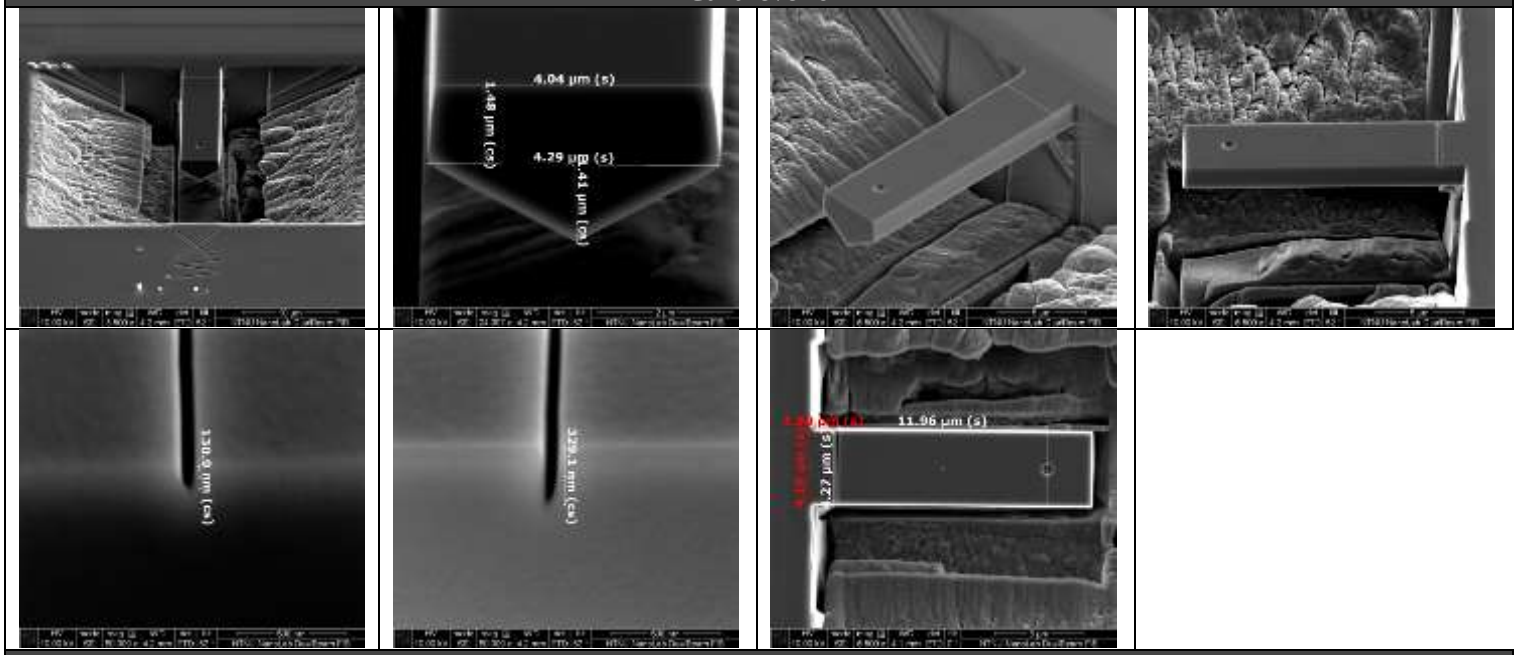

Cantilever 7

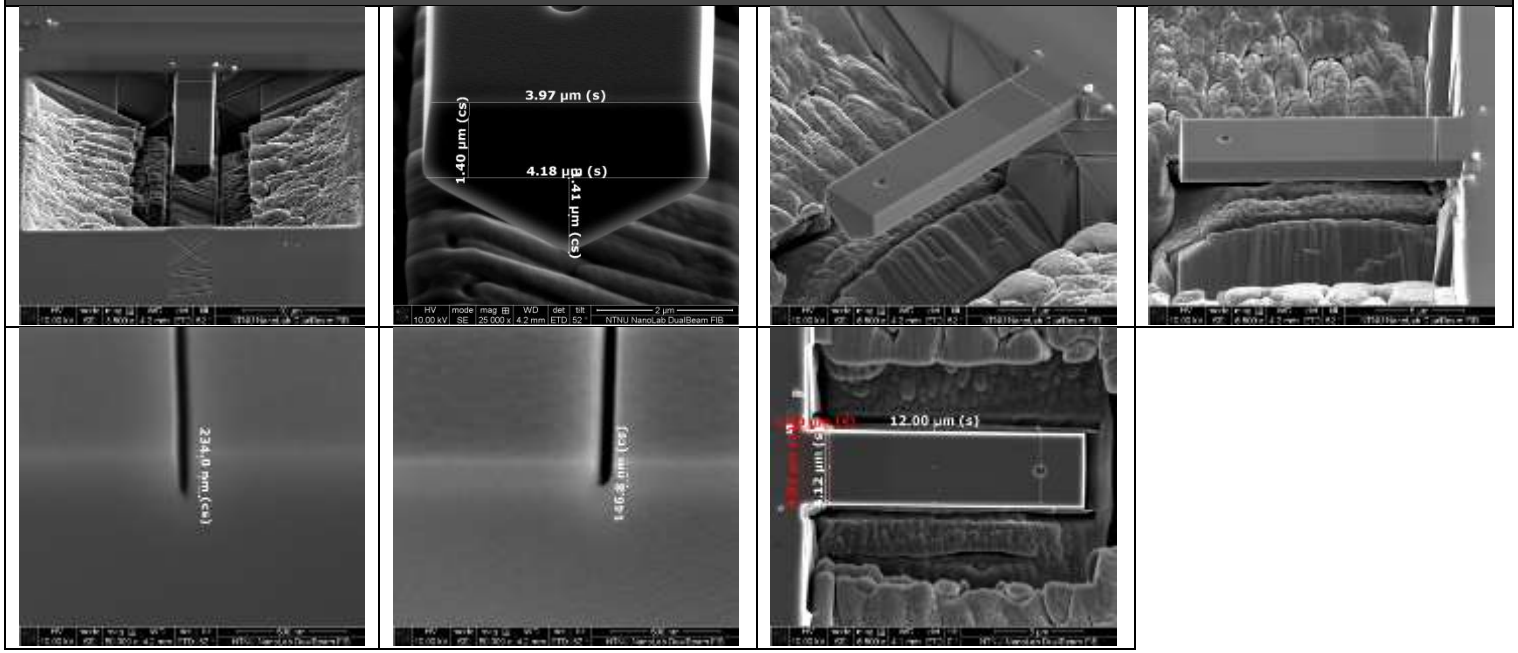

Cantilever 8

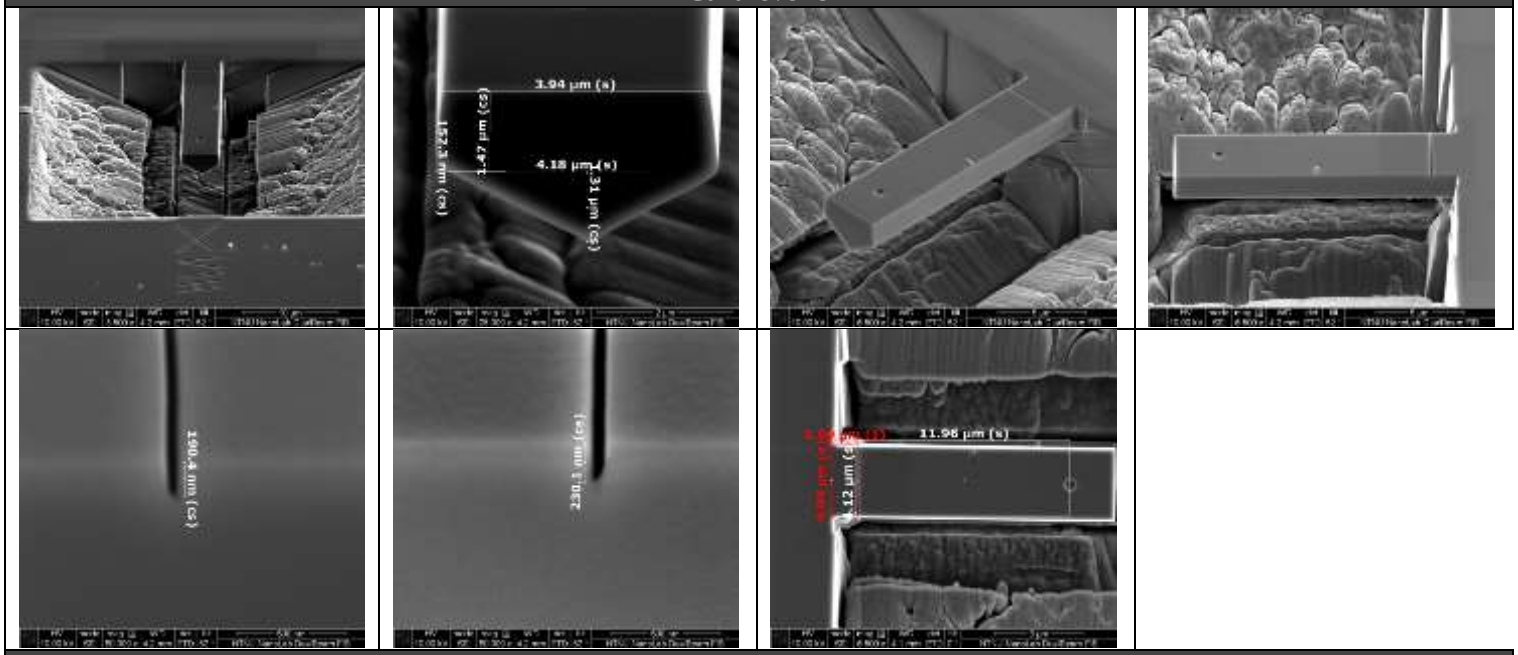

Cantilever 9

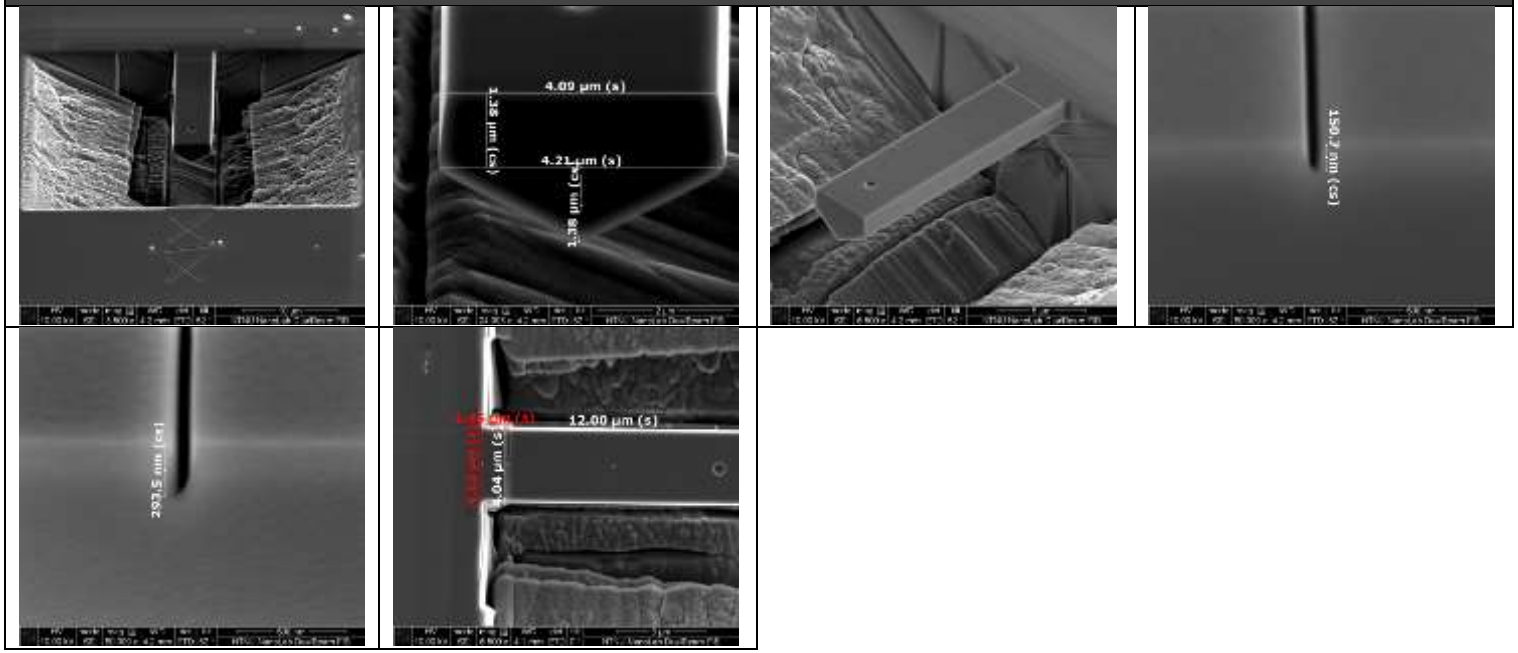

Cantilever 10

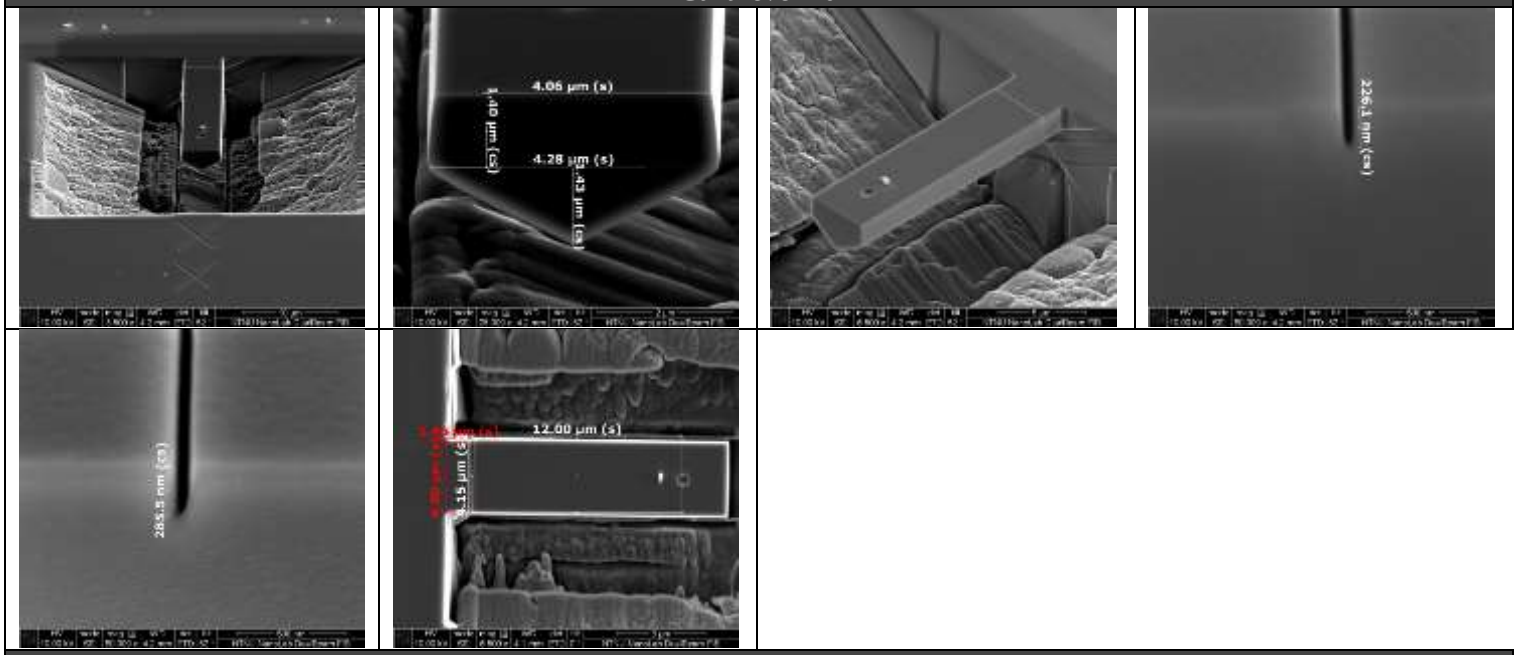

Cantilever 11

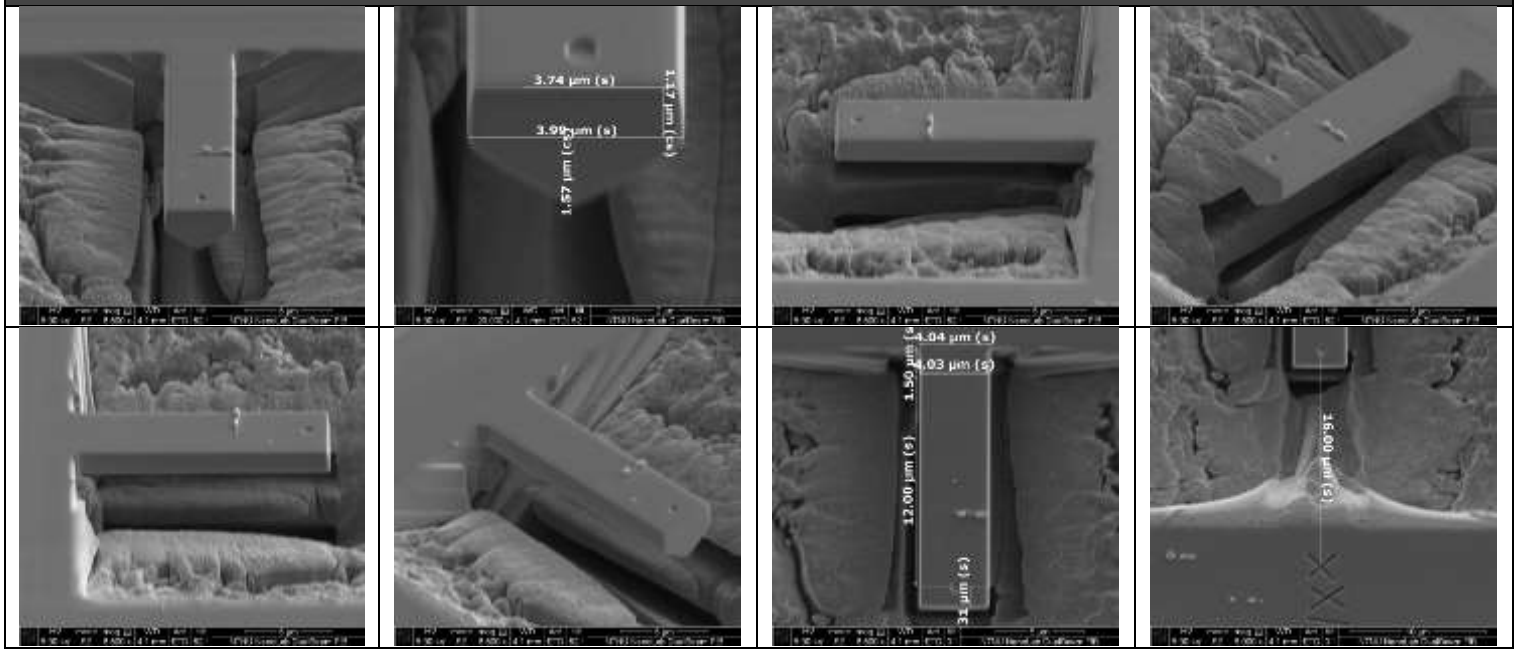

Sample 4

Cantilever 1			
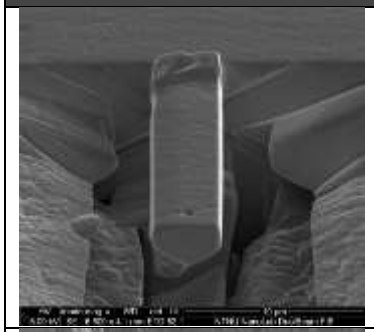	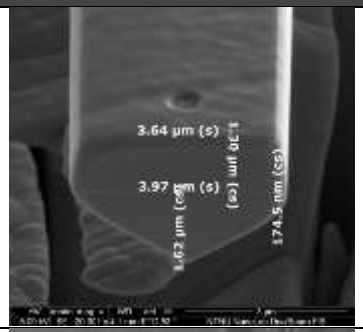	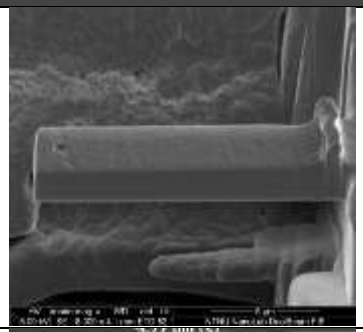	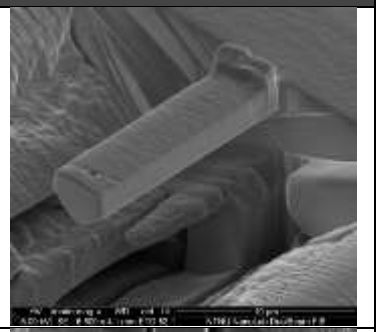
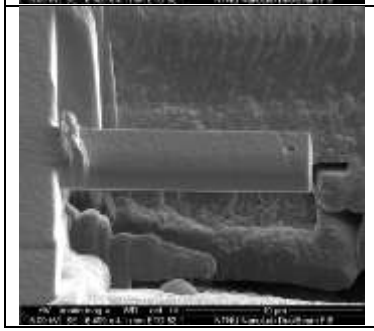	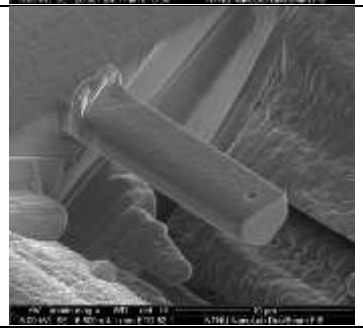	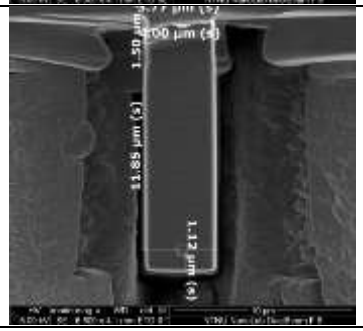	

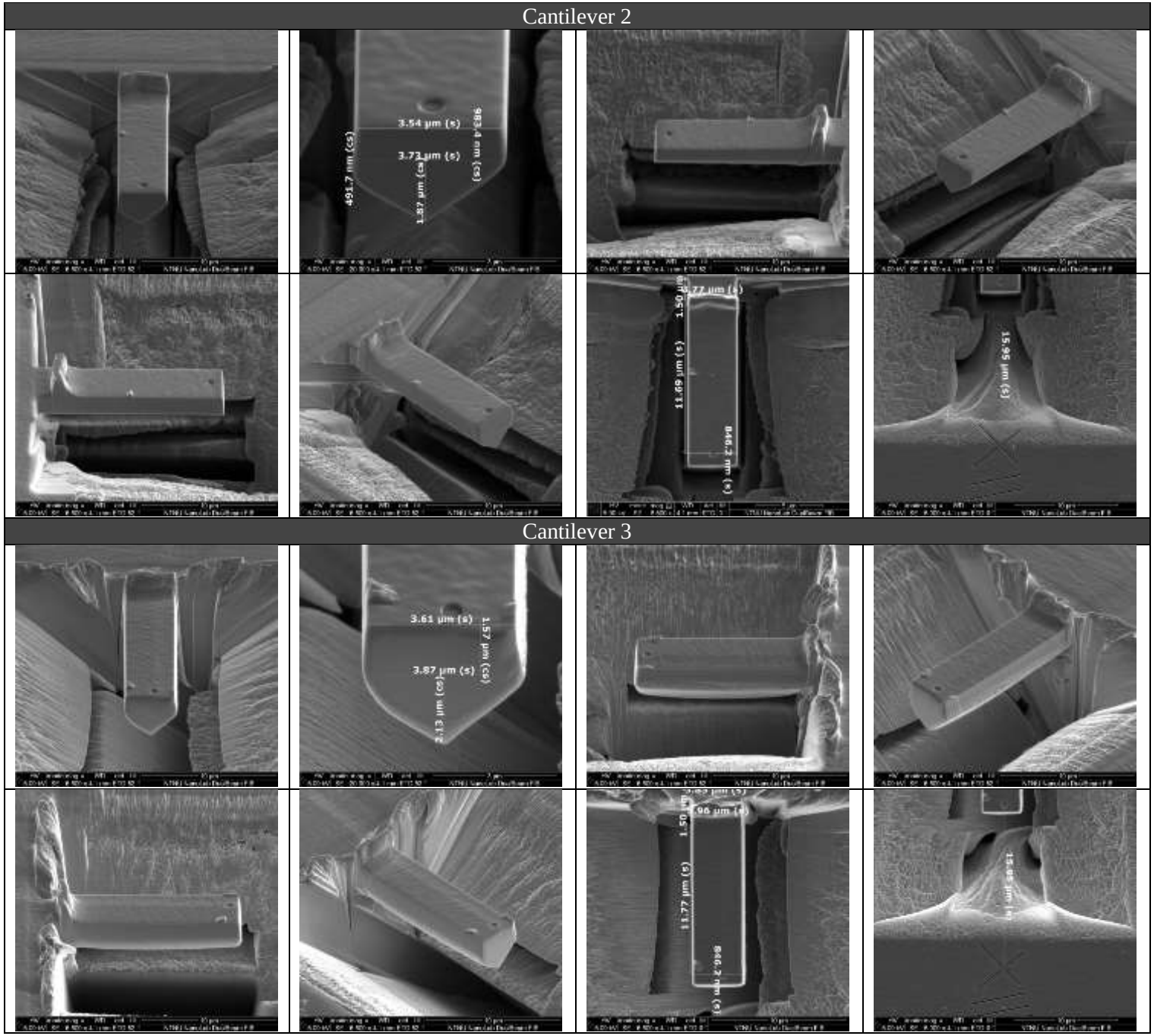
Cantilever 2
3.54 µm (s)
3.71 µm (s)
491.7 nm (cs)
1.87 µm (cs)
983.4 nm (s)
1.50 µm
11.69 µm (s)
848.2 nm (s)
15.95 nm (s)
Cantilever 3
3.61 µm (s)
3.87 µm (s)
2.13 µm (cs)
1.57 µm (cs)
1.50 µm
11.77 µm (s)
868.2 nm (s)
15.68 nm (s)

Cantilever 4

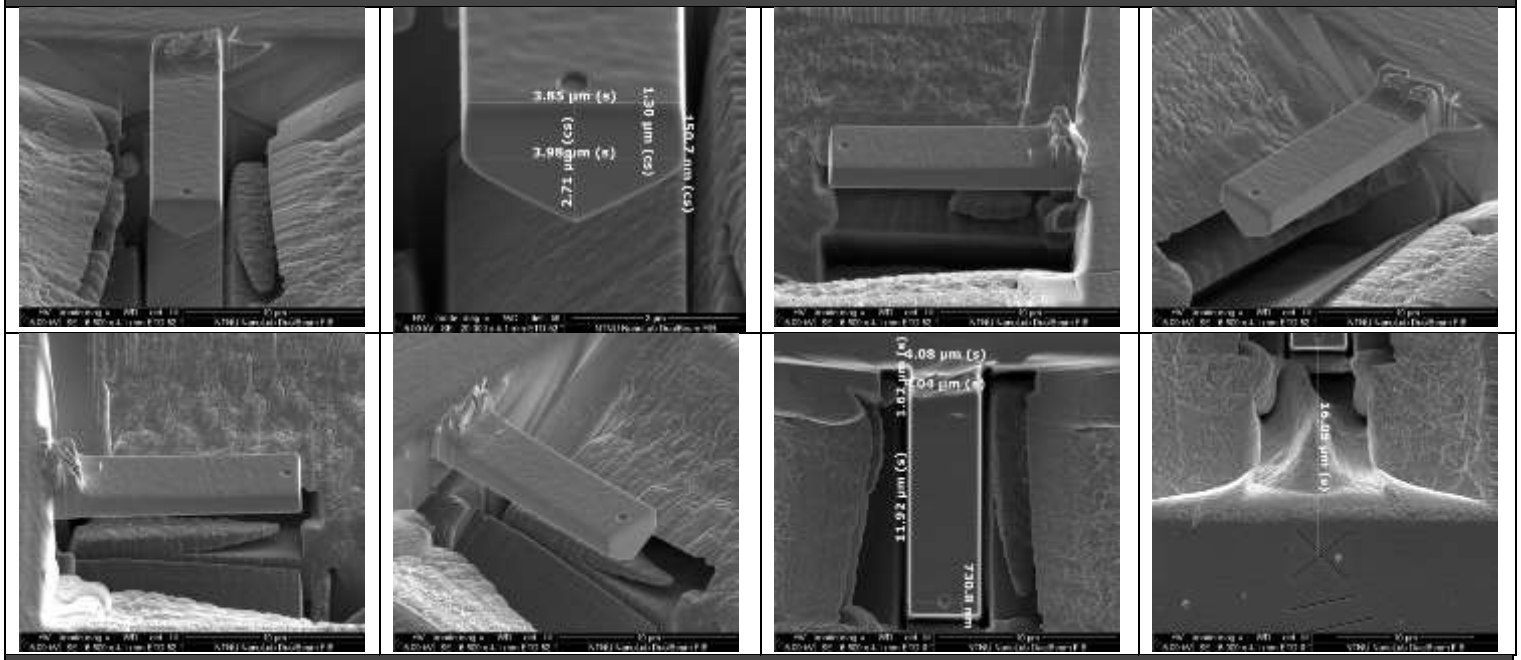

Cantilever 5

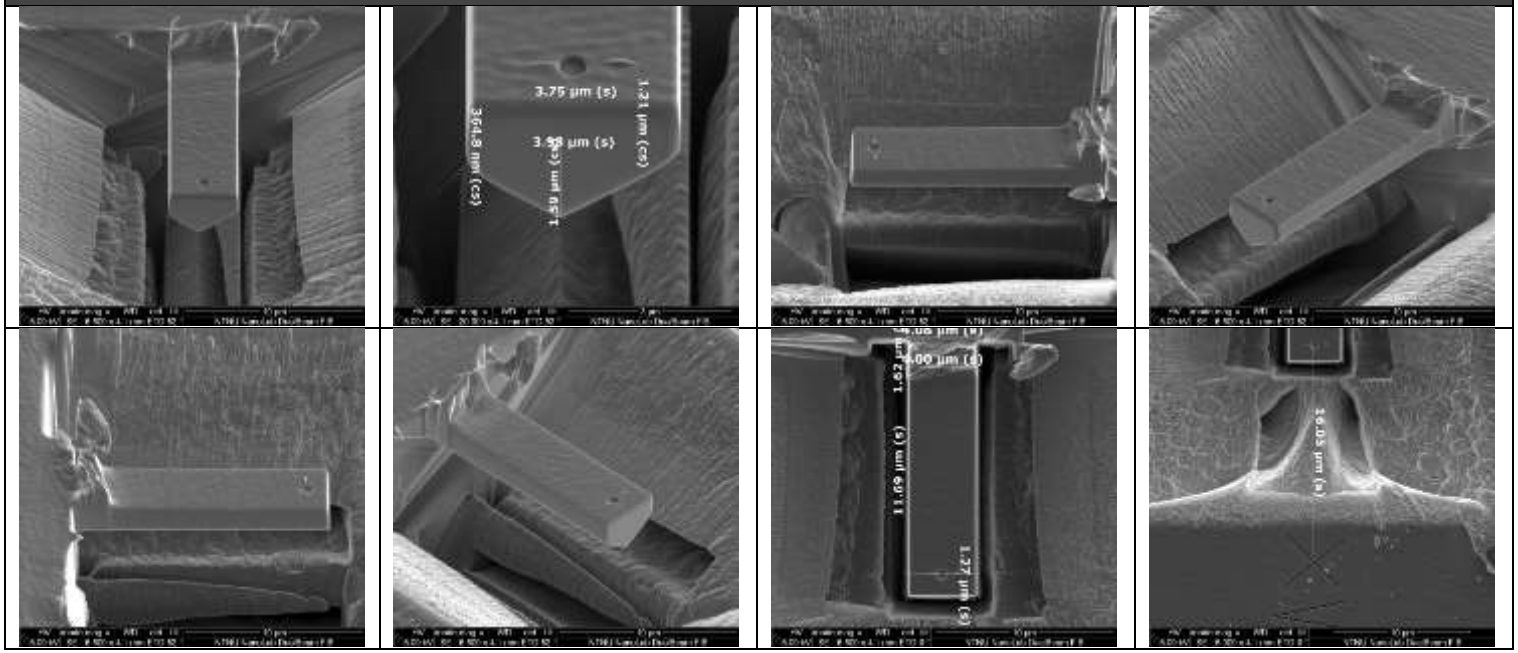

Cantilever 6

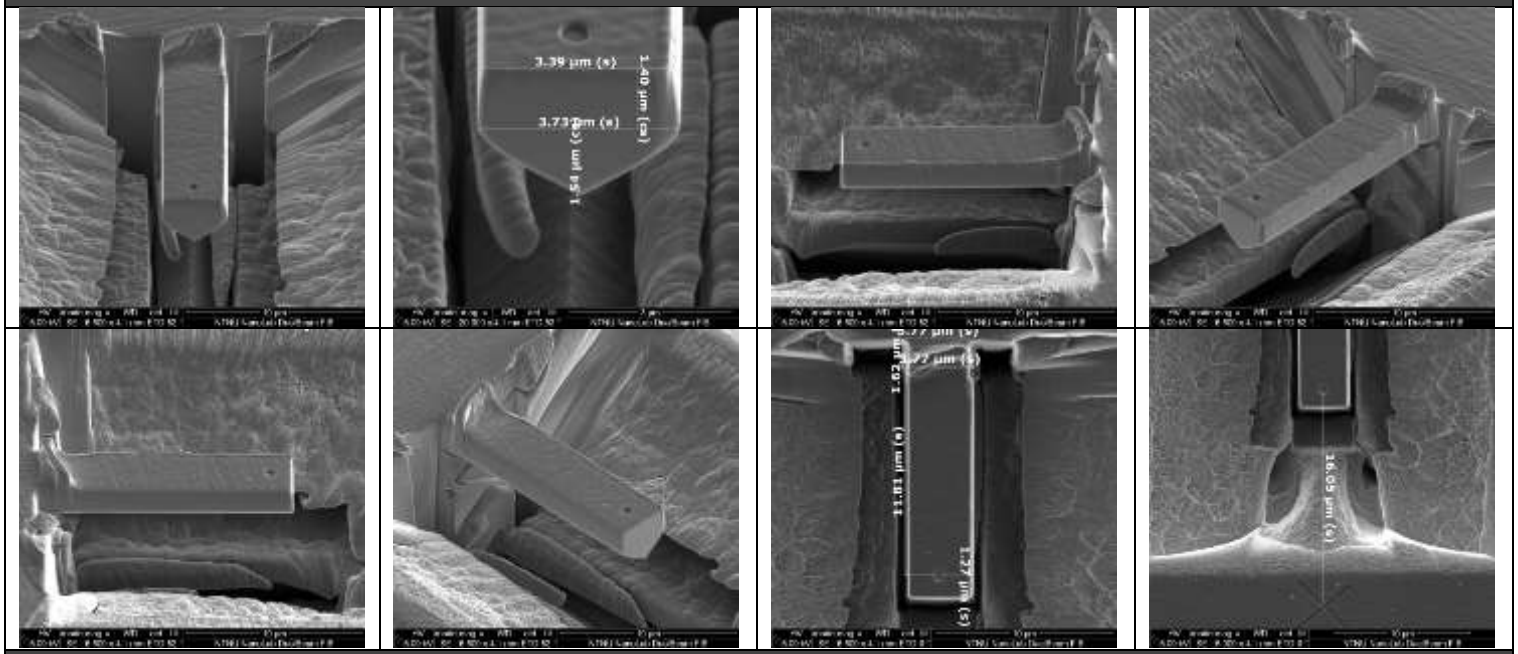

Cantilever 7

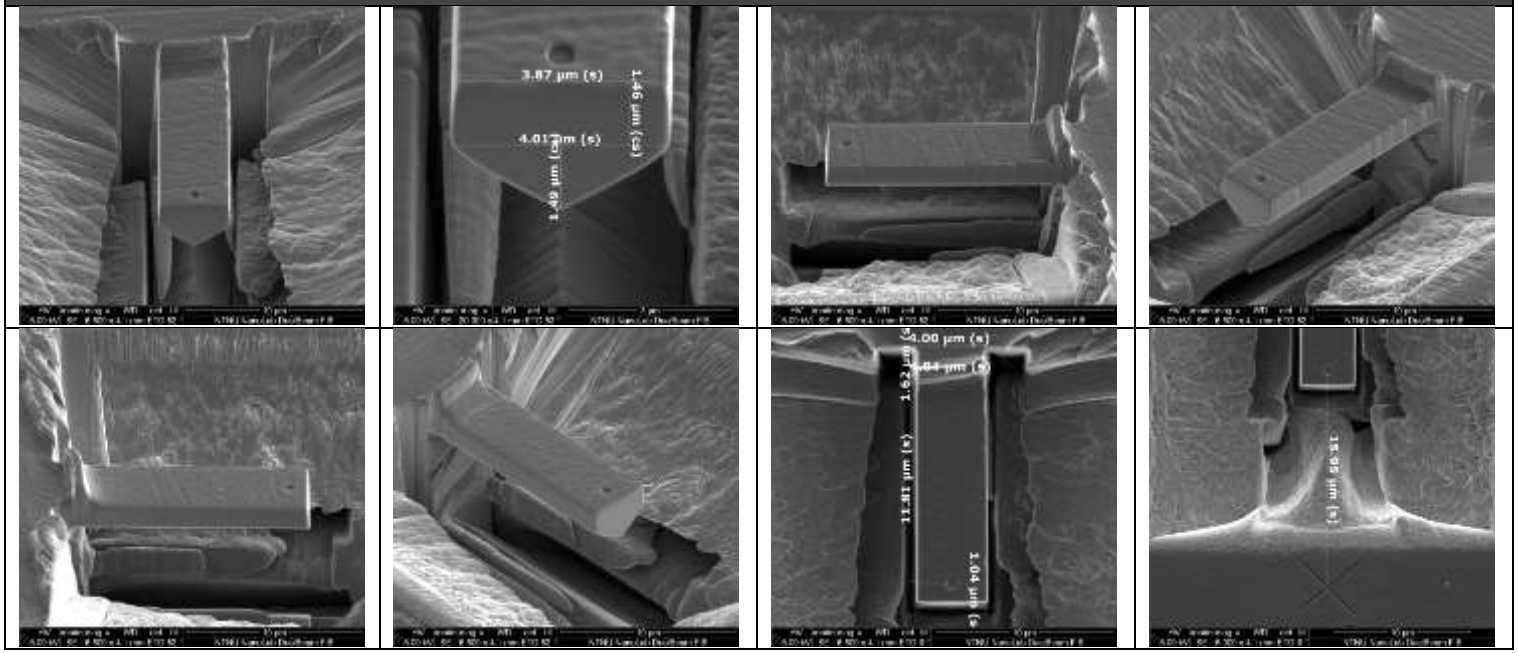

XXX

Cantilever 8

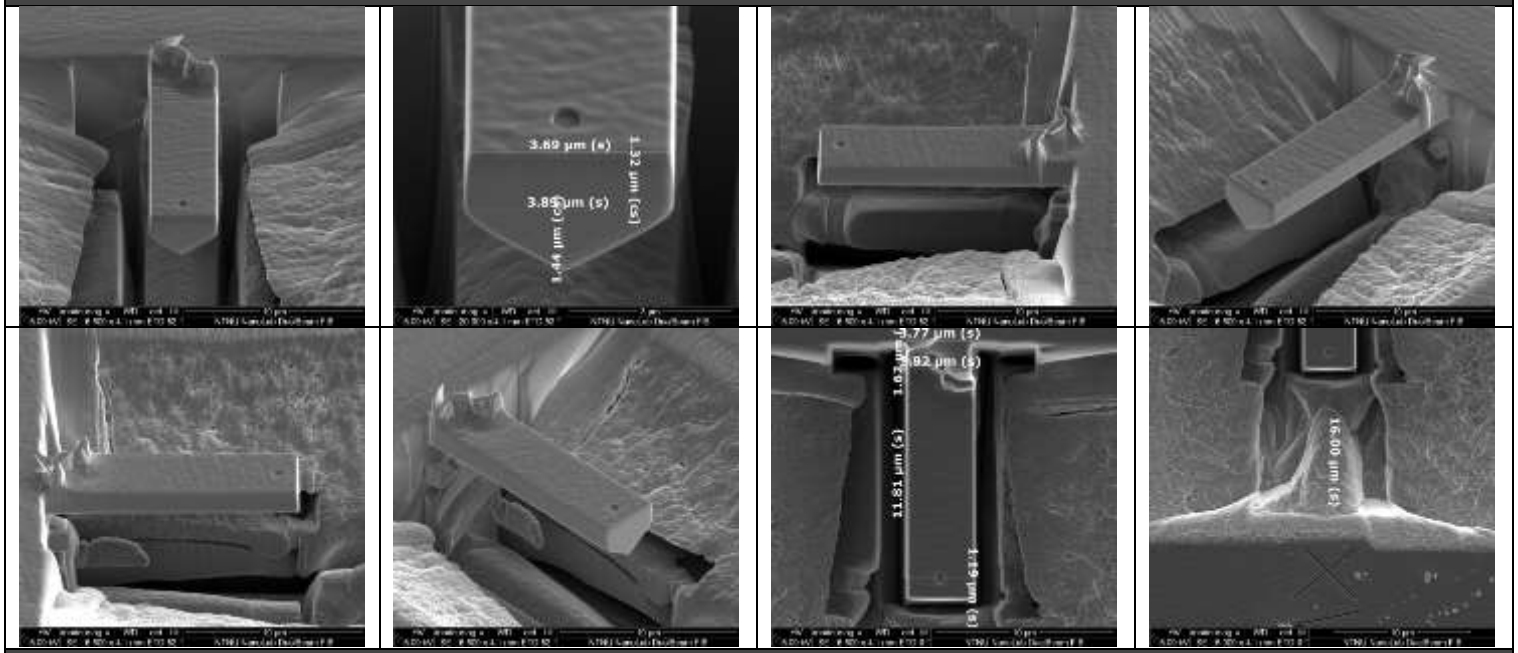

Cantilever 9

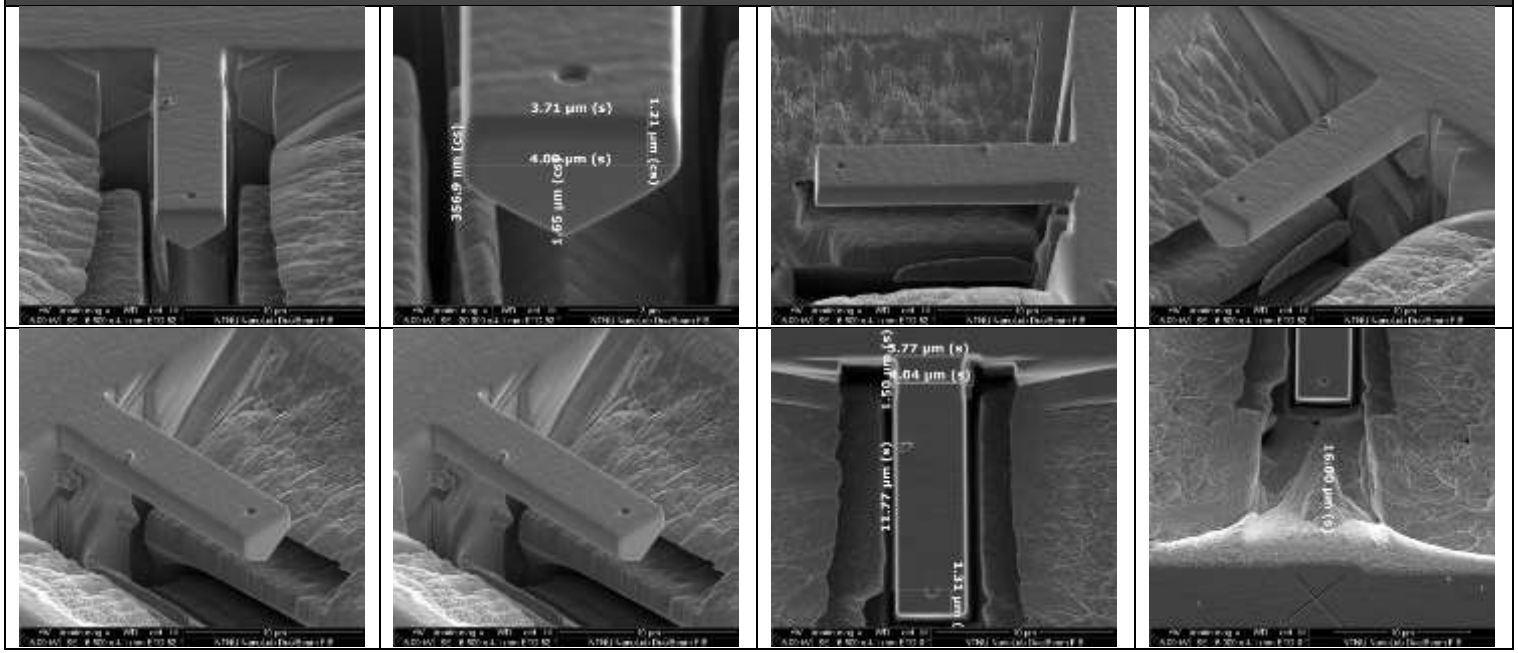

Cantilever 10

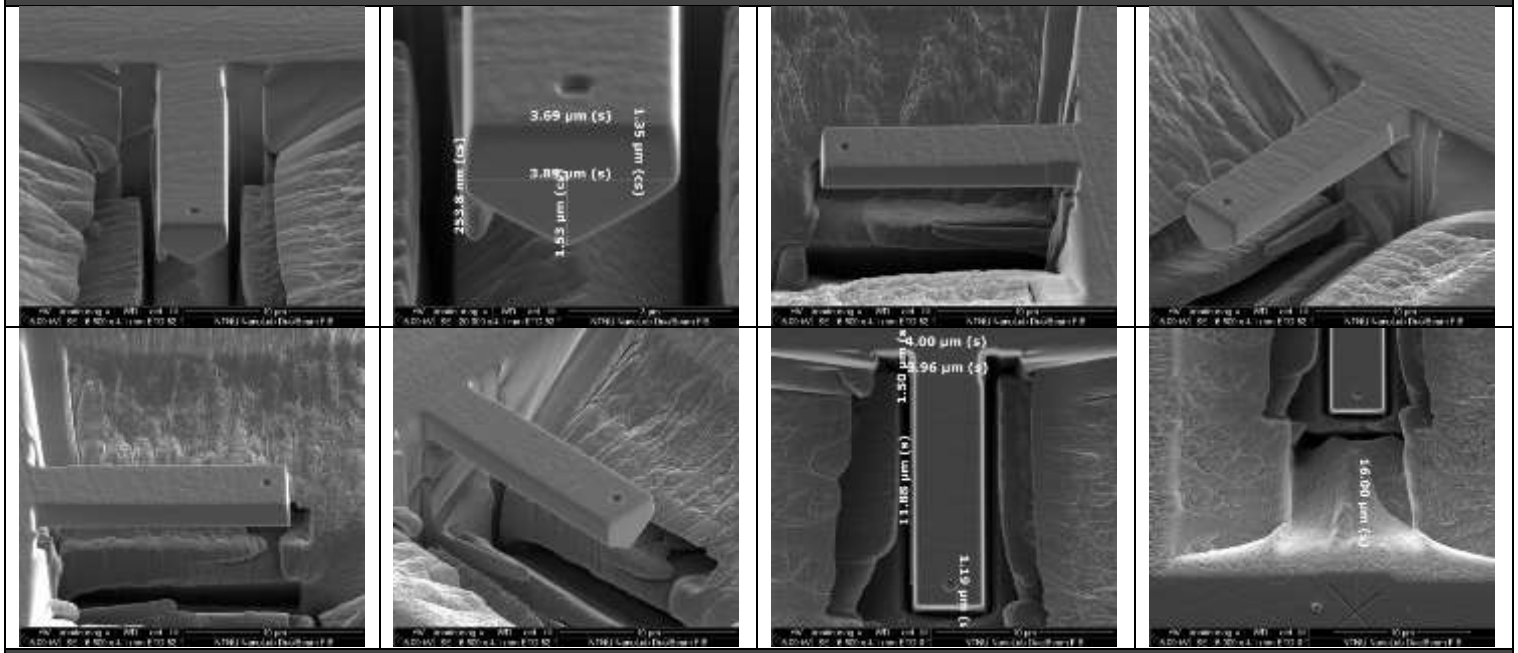

Cantilever 11

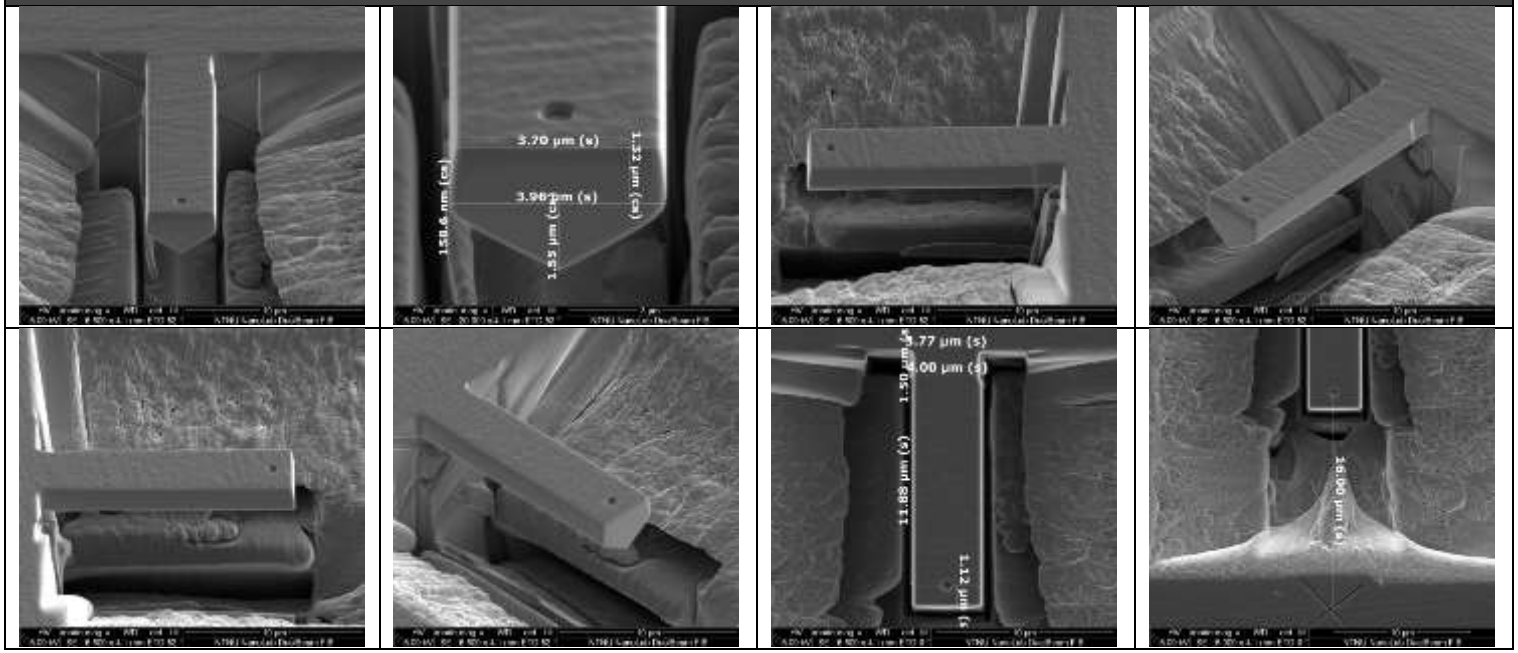

Cantilever 12

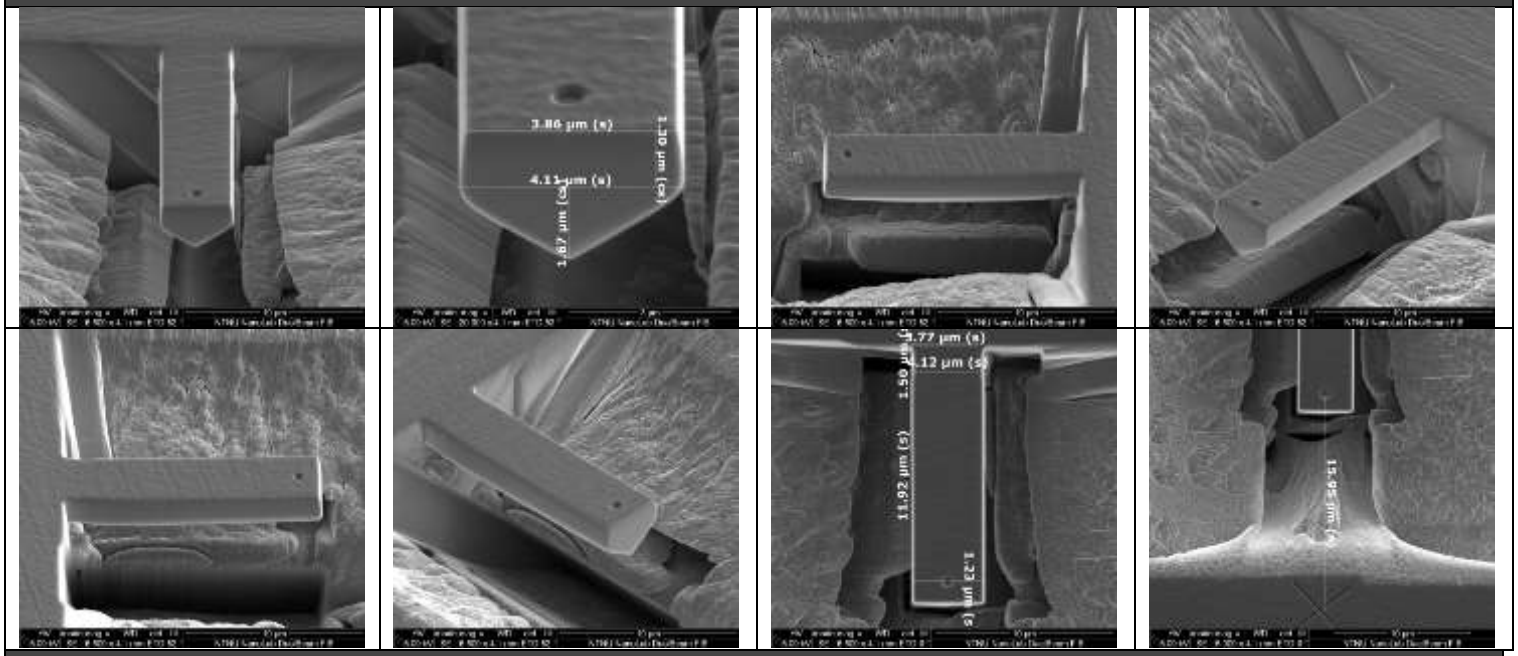

Cantilever 13

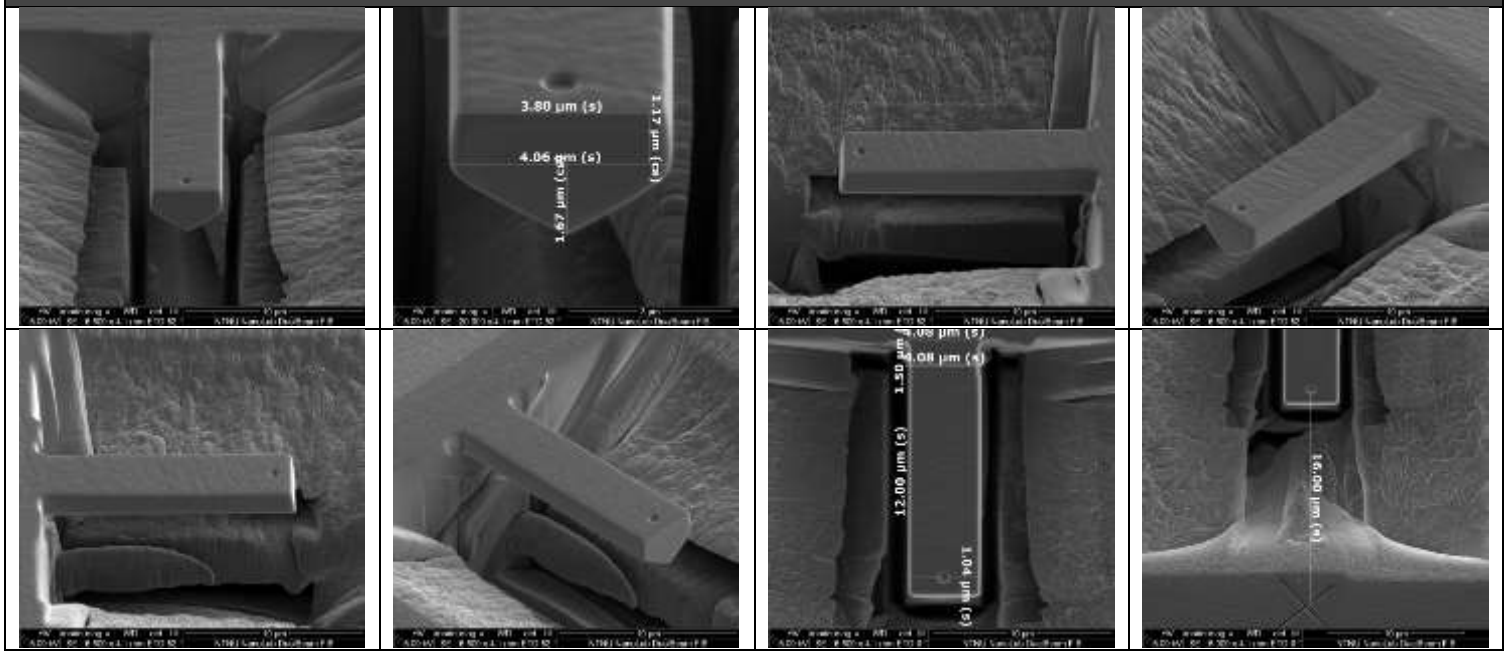

Cantielver 14

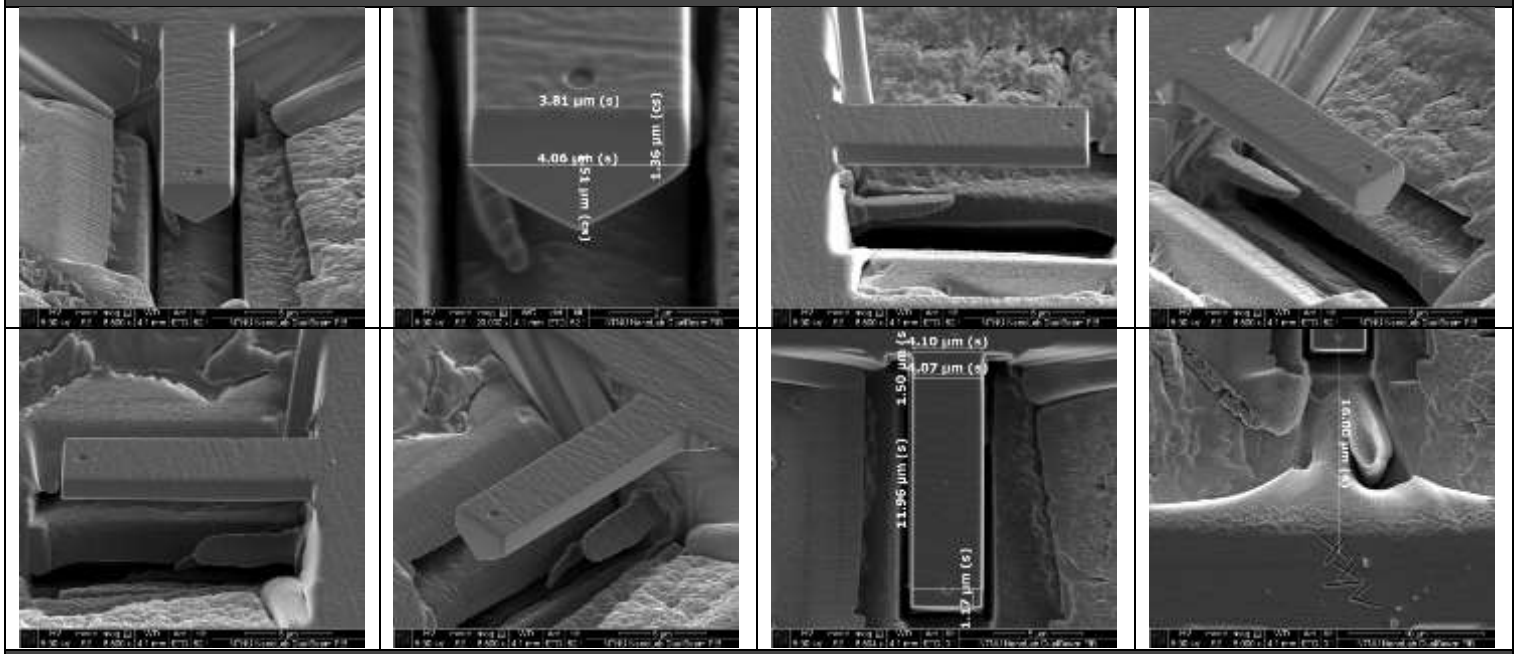

Cantilever 15

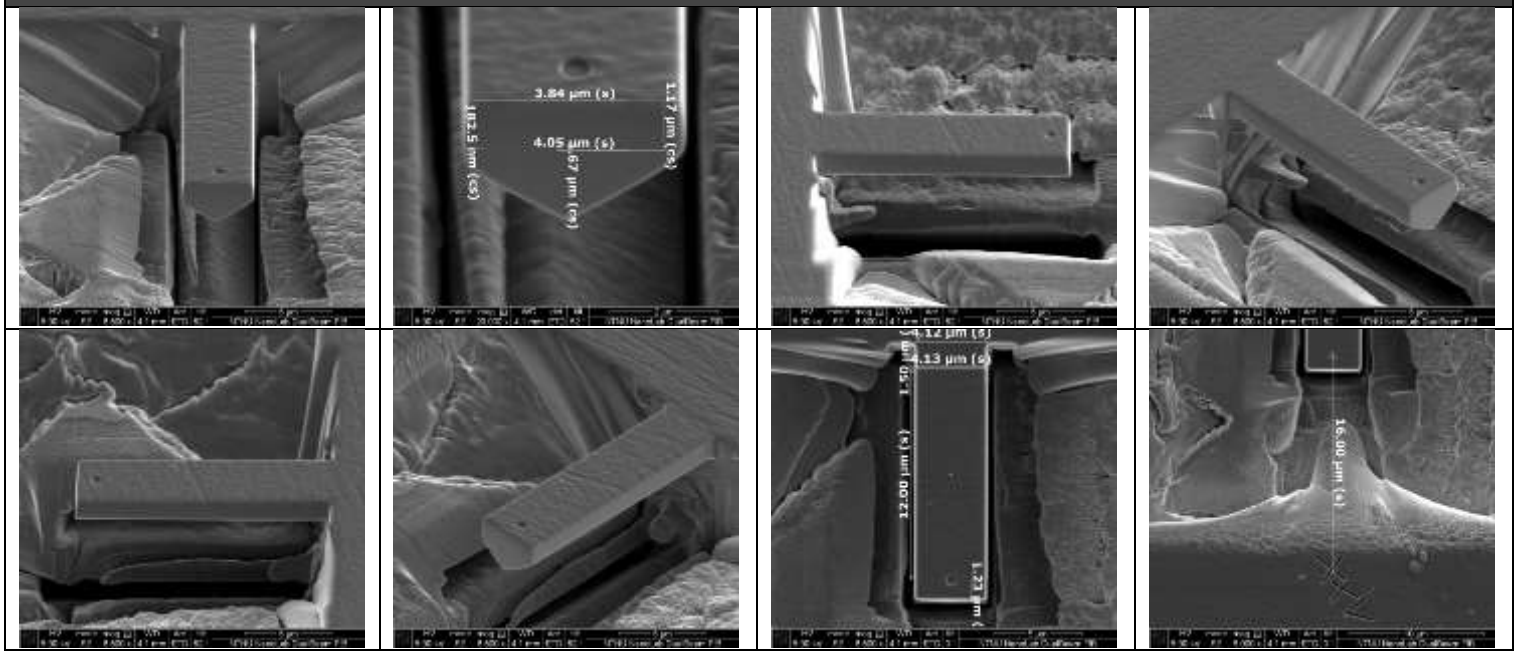

Cantilever 16

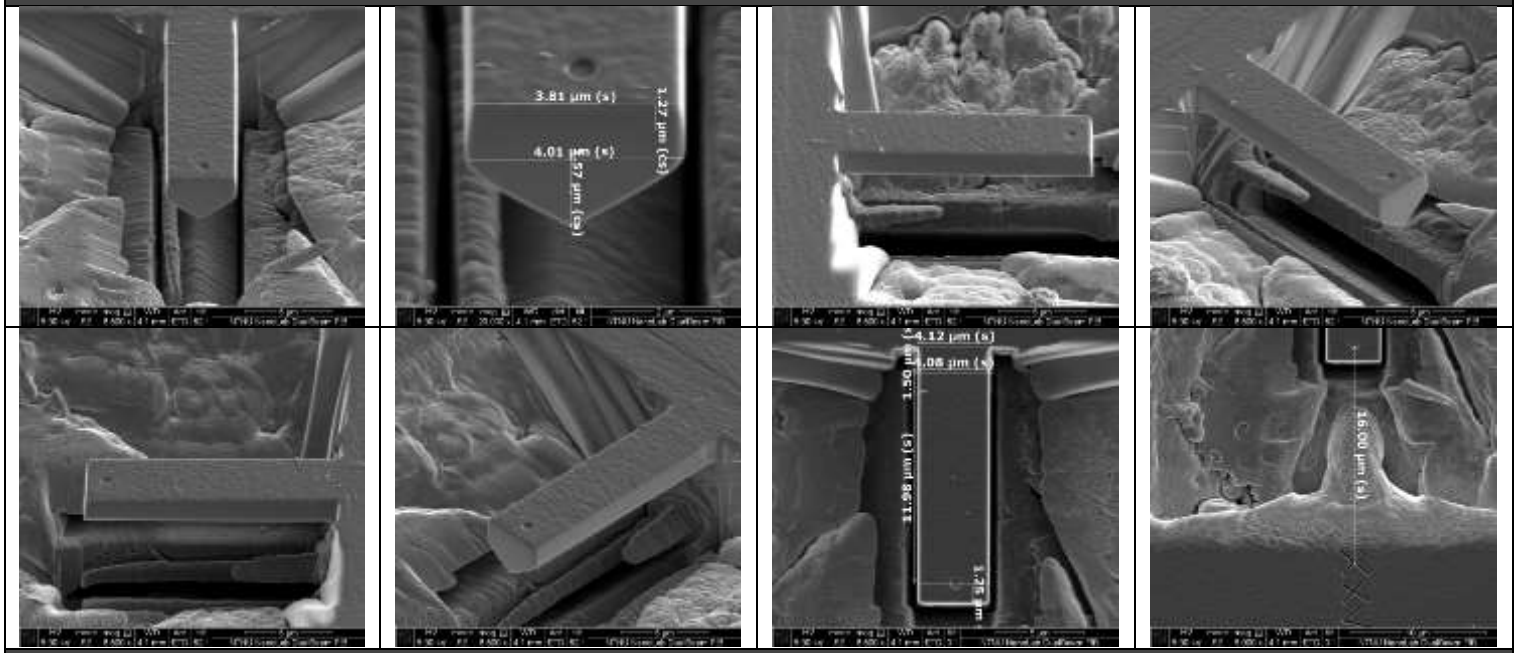

Cantilever 17

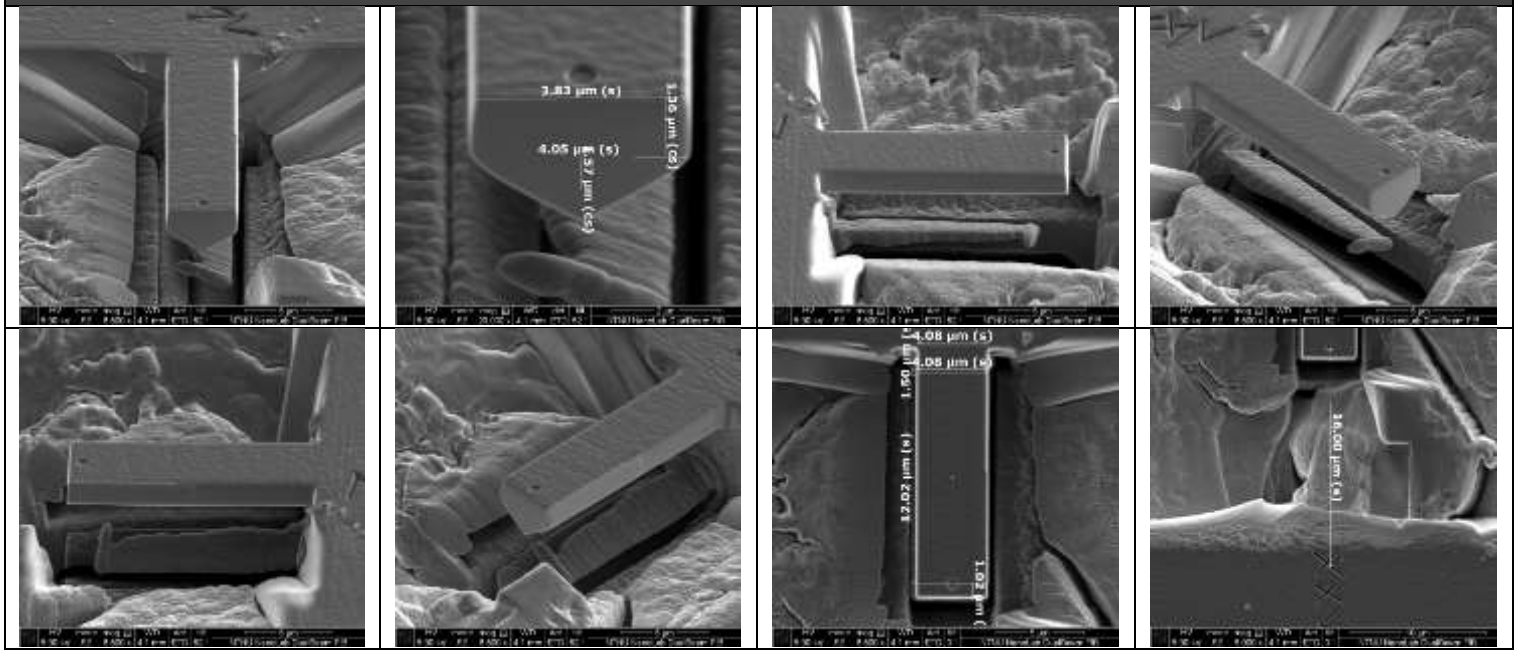

Cantilever 18

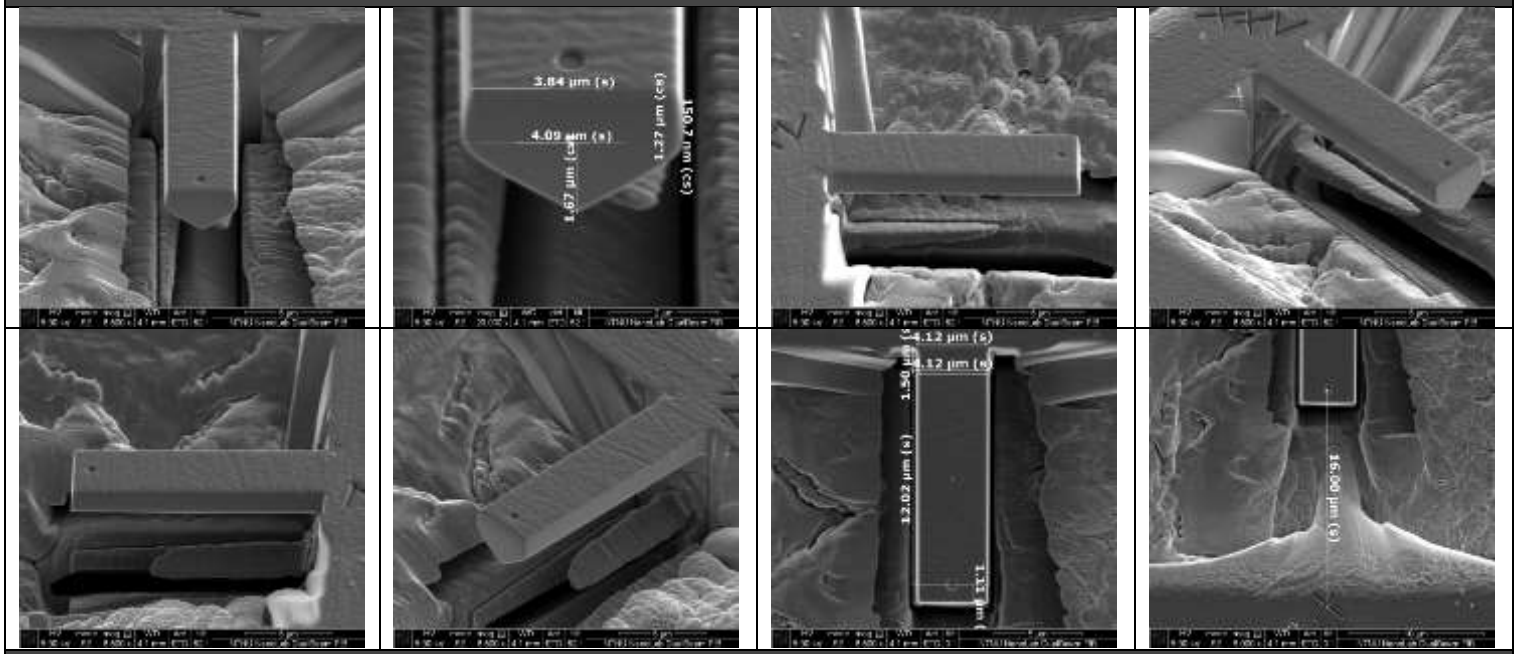

Cantilever 19

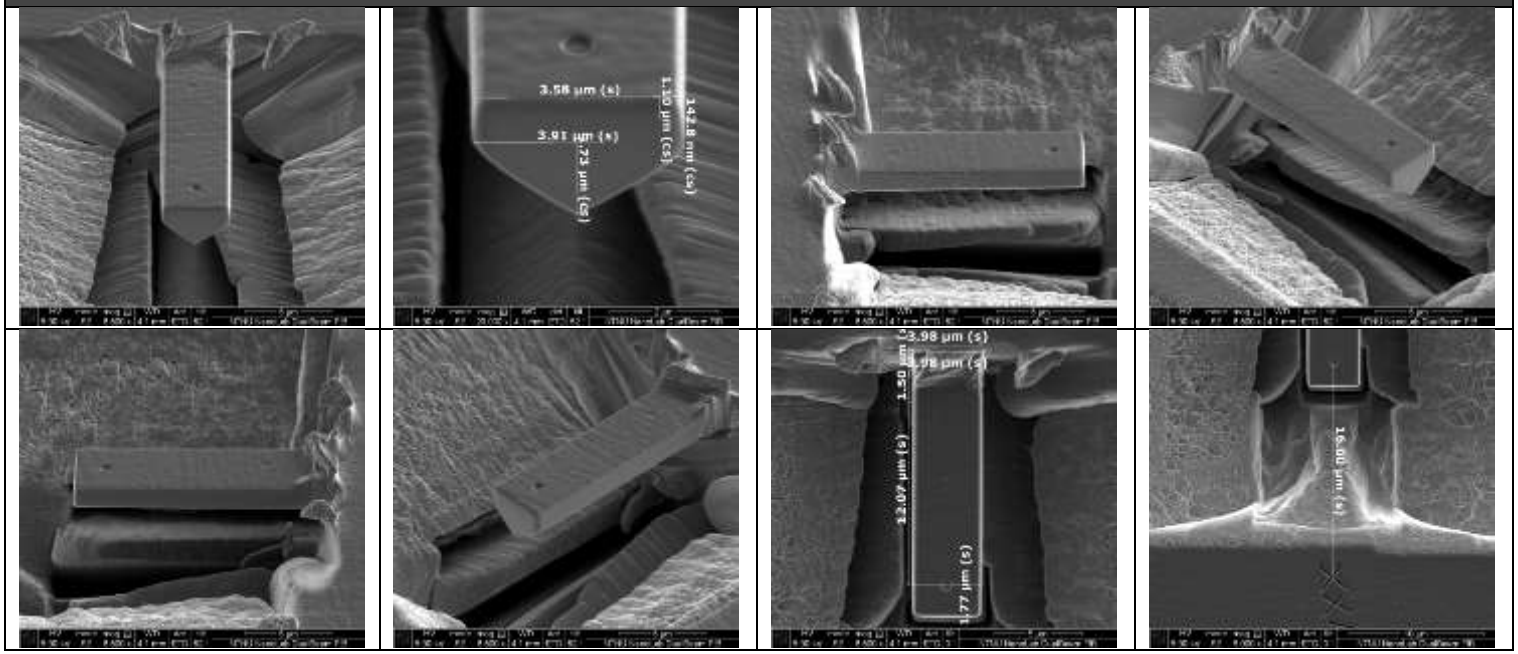

Cantilever 20

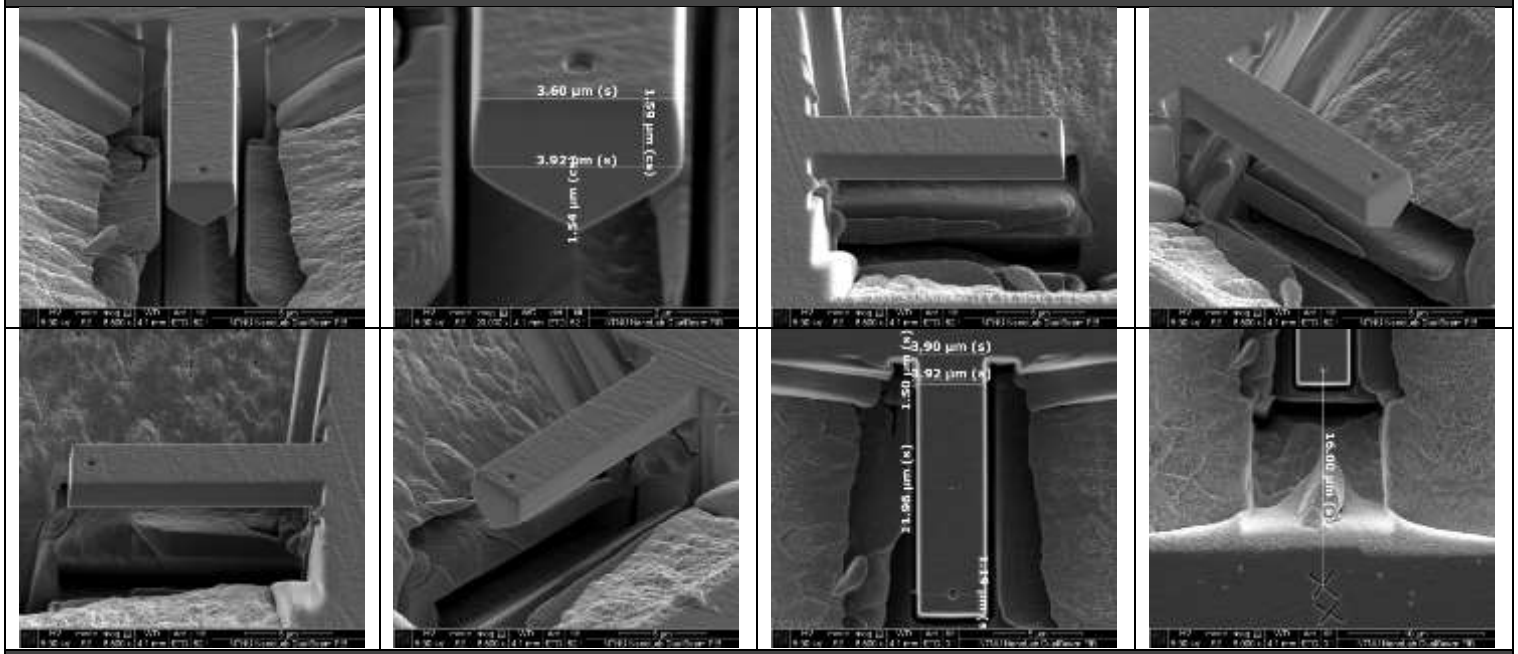

Cantilever 21